European Journal of Medicinal Chemistry 163 (2019) 453–480

Contents lists available at ScienceDirect

European Journal of Medicinal Chemistry

journal homepage: http://www.elsevier.com/locate/ejmech

Research paper

=cmarkid_^{11502}}"Chemistry-oriented synthesis (ChOS) and target deconvolution on neuroprotective effect of a novel scaffold, oxaza spiroquinone

Arramshetti Venkanna [a, 1], Kyo Hee Cho [a, 1], Lama Prema Dhorma [a], Duddukuri Nandan Kumar [a], Jung Mi Hah [b], Hyeung-geun Park [c], Sun Yeou Kim [a, **], Mi-hyun Kim [a, *]

[a] Gachon Institute of Pharmaceutical Science, Department of Pharmacy, College of Pharmacy, Gachon University, Yeonsu-gu, Incheon, Republic of Korea
[b] College of Pharmacy & Institute of Pharmaceutical Science and Technology, Hanyang University, Asan, Republic of Korea
[c] Research Institute of Pharmaceutical Science and College of Pharmacy, Seoul National University, Seoul, Republic of Korea

ARTICLE INFO

Article history:
Received 11 June 2018
Received in revised form
13 November 2018
Accepted 16 November 2018
Available online 29 November 2018

Keywords:
1,5-oxaza spiroquinone
Chemistry-oriented synthesis
Neurodegenerative
NO inhibitory effect
JNK
DAPK
Molecular docking simulation
Y-maze test

ABSTRACT

Here we first time report an unprecedented and unnatural six-membered 1,5-oxaza spiroquinone scaffold with structural novelty, a convenient and efficient synthetic route was developed for the synthesis of new 1,5-oxaza spiroquinone derivatives (**1a-1r)** in high yields from readily available starting materials. The logic of the present work consists of (1) the identification of a promising unprecedented scaffold from privileged scaffolds of biological active molecules through our 'Chemistry-oriented Synthesis' (ChOS) approach, a compensatory strategy for target-based drug discovery, (2) the positioning of the identified 1,5-oxaza spiroquinone scaffold on neuroinflammation and neurodegenerative disease through nitric oxide (NO) inhibitory activity without cytotoxicity in hyper-activated microglia (IC_{50} of NO production: 0.07–1.82 μM) to establish structure–activity relationship (SAR), (3) the investigation on the possibility as a selective kinase inhibitor related to neurodegenerative diseases (eg. JNK1, CDK2, DAPK1) through kinase full panel screening of the most potent compound **1n**, and (4) the evaluation on *in vivo* efficacy of the compound **1n** through Y-maze test.

1. Introduction

Nitric oxide (NO) is an unorthodox messenger molecule and free radical produced by nitric oxide synthase. It has numerous molecular targets and plays an important role in several physiological and pathological processes such as the regulation of neurotransmission, neurovascular coupling to control neocortical blood flow, mediation of immunoresponse, mediated cytotoxicity in microbes and tumour cells, cell–host response, cell-to-cell communication, insulin secretion, airway tone, peristalsis, and angiogenesis, as well as in sexual function [1–9]. However, over-production of NO in humans causes several diseases such as inflammation, rheumatoid arthritis, asthma, chronic inflammation, inflammatory bowel disease, immune-type diabetes, thrombosis stroke, septic shock, cancer, and infection susceptibilities. Over-production is also linked to neurodegenerative disorders such as Parkinson's disease (PD), multiple sclerosis (MS), and Alzheimer's disease (AD) [10–14]. Therefore, inhibition of NO represents an effective and attractive

Abbreviations: ChOS, chemistry-oriented Synthesis; NO, Nitric oxide; NOS, Nitic Oxide Synthase; PD, Parkinson's disease; CNS, Central nervous system; MS, Multiple sclerosis; AD, Alzheimer's disease; LPS, lipopolysaccharide; POC, proof of concept; PTC, Phase-transfer catalysed; MOM, Methoxymethyl ethers; SAR, structure–activity relationship; MTT, 3-(4, 5-dimethylthiazol-2-yl)-2,5-diphenyltetrazolium bromide; PDB, Protein Data Bank; JNK, c-Jun NH2-terminal kinases; BBB, Blood brain barrier; HERG, Ether-a-go-go-Related Gene; MDCK, Madin–Darby canine kidney; Caco-2, colorectal adenocarcinoma; DMPK, Drug metabolism and pharmacokinetics; CYP, Cytochrome P450; PIFA, Bis (trifluoroacetoxy) iodo] benzene; THF, Tetrahydrofuran; EDCI, 1-Ethyl-3-(3 dimethylaminopropyl)carbodiimide; DMAP, 4-Dimethylaminopyridine; $Li(O^tBu)_3H$, Lithium aluminum-tri-tert-butoxyhydride; TMSCl, Trimethylsilyl chloride; BF_3Et_2O, Boron trifluoride-diethyl etherate; TBAI, Tetra-n-butylammonium iodide; $NaHB_4$, Sodium borohydride; KOH, Potassium hydroxide; NaI, Sodium Iodide; ACN, Acetonitrile; DMS, Dimethyl sulfoxide; DCM, Dichloromethane; THF, Tetrahydrofuran.

* Corresponding author.
** Corresponding author.
E-mail addresses: sunnykim@gachon.ac.kr (S.Y. Kim), kmh0515@gachon.ac.kr (M.-h. Kim).
[1] These authors are co-first authors.

https://doi.org/10.1016/j.ejmech.2018.11.037
0223-5234/

therapeutic strategy for the treatment of neurodegenerative diseases.

Several classes of Nitic Oxide Synthase (NOS) inhibitors have been reported in the literature [15–23]. Effective NOS inhibitors have been evaluated in animals, but very few clinical trials have been performed in humans [24,25]. However, NOS is an imperfect target for CNS diseases. Because CNS diseases and their pathologies are neither simple nor understood clearly, further understanding the pathologies and continuous development of diverse therapeutic targets and diagnostic markers are essential for robust clinical POC (proof of concept). In the last five decades, few novel classes except for NOS have been reported for direct regulation of NO levels and prevention of neurodegenerative disorders [5–7]. It is challenging to develop new therapeutic points (novel targets) and tool compounds for regulating targets with novel actions to prevent NO overproduction and side effects [26–30]. Therefore, it is important task to investigate new neuro protective small molecules for treating and managing neurodegenerative diseases. For this purpose, we used our modified 'Chemistry-oriented Synthesis (ChOS)' approach in this study to identify a promising novel scaffold from the privileged scaffolds of biologically active molecules [31]. In particular, we designed for the first time a novel new six membered 1,5-oxaza spiroquinone skeleton by the hybridisation of spiro and quinone as a structural subunits (Fig. 2). The designed core skeleton and our developed strategy is helpful for the rapid and efficient assembly of functionalities with diversification at N-5 and C-3, and on the quinone moiety for synthesis of novel scaffolds.

Spiro moieties are an important class of natural products [32–35] and spiro containing molecules exhibit a wide range of biological activities and play important roles in the pharmaceutical industry (Fig. 1) [36–41]. These molecules easily occupy greater three-dimensional space than planar aromatic, hetero-aromatic compounds, because of their structural novelty. Spiro containing compounds can project functionality into three axes in space because their unique shapes facilitate the occupation of binding sites. Furthermore, spiro containing molecules have high water solubilities, logP, and metabolic stabilities. All these special properties of spiro containing molecules or a spiro frameworks has been used as a privileged scaffolds in many drug synthesis projects. Quinones and their derivatives are also widely distributed in natural products [42–46], play an important roles in biological processes because of their applicability in redox processes. They have also been used in a wide variety of clinical and industrial applications (Fig. 1) [47–53]. In drug discovery and development, the development of new therapeutic agents extends the chemical space for artificial drugs. Therefore, after carefully investigation of the

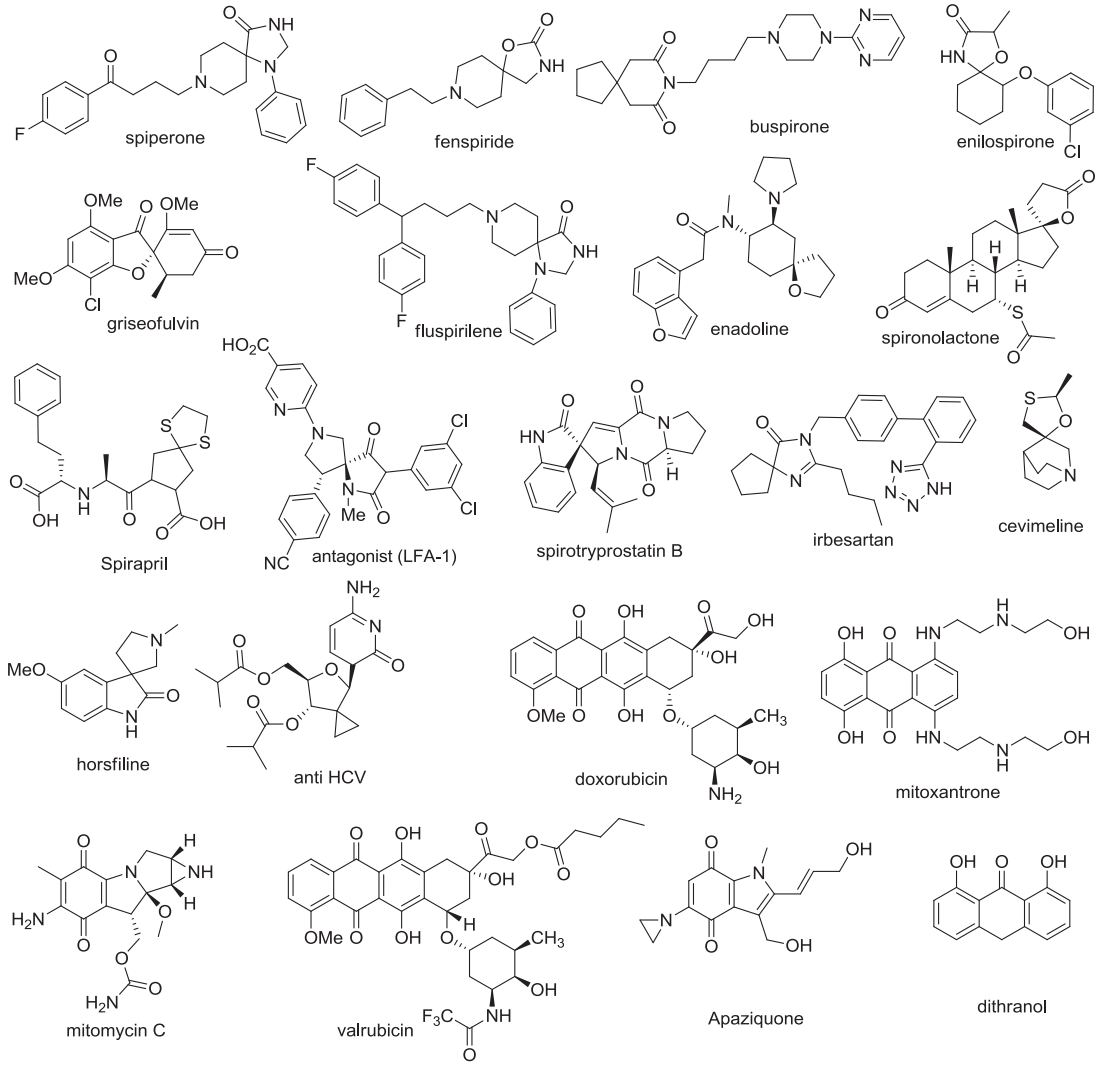

Fig. 1. Some examples of spiro and quinone containing drugs.

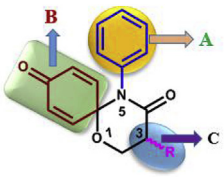

A, B, C = easily accessible positions with different diversification at N-5, C-3 and on Quinone.

Fig. 2. Proposed, designed a new core of sex membered 1,5 oxaza spiroquinone skeleton (**1**)
A, B, C = easily accessible positions with different diversification at N-5, C-3 and on Quinone.

importance of spiro and quinone basic structures, we combined the attractive features of these two structural subunits to design a new core of six-membered 1,5-oxaza spiroquinone skeleton. (Fig. 2). The introduction of spiro and quinone structures as a core skeleton is a novel patentable strategy. As per our knowledge, the designed core has not been reported for the biological evaluation of neuroprotective small molecules. Our group has been involved in the synthesis and biological evaluation of small molecule inhibitors that would help treat and manage CNS diseases [54–59]. Continuing our study in medicinal chemistry, the aim of the present work is to investigate the utility of the proposed unprecedented 1,5-oxaza spiroquinone via diversification at C-3 position with a racemic version, by retaining aryl compound at the N-5 position and unsubstituted quinone.

In this study, we synthesised a series of 1,5-oxaza spiroquinone derivatives with diversification at the C-3 position and all synthesised derivatives were investigated NO inhibition BV-2 cell lines and their cytotoxicities were also estimated by using 3-(4, 5-dimethylthiazol-2-yl)-2,5-diphenyltetrazolium bromide (MTT) assay. SAR studies were developed for synthesised analogues. Further, full panel kinase screening, molecular docking studies and *in vivo* level Y-maze test was perfumed with potent compound.

2. Results and discussion

2.1. Chemical synthesis

2.1.1. Retrosynthetic analysis

Our synthetic approach to six-membered 1,5-oxaza spiroquinone involves PIFA-mediated cyclisation (Scheme 1). Cleavage of the C–O bond revealed **2** as a potential key intermediate. The Key fragment **2** was obtained by Phase-transfer catalysed (PTC) alkylation, followed by sequential reactions of reduction and MOM deprotection of common amide fragment **4**; for all derivatives, **4** was obtained by amide coupling of 3-methoxy-3-oxopropanoic acid (**6**) with the 2° amine compound (**5**). Amine compound (**5**) was in turn accessed by using MOM-protected 3-bromo-phenol compound (**7**) with aniline (**8**) through a Pd-mediated Buchwald-Hartwig coupling reaction. Our present synthesis of the six-membered 1,5-oxaza spiroquinone scaffold (**1**) involves Pd-mediated Buchwald-Hartwig coupling, PTC alkylation, and PIFA-mediated oxidative cyclisation as key reactions. Furthermore, the simplicity of the precursors of this route makes it an attractive method for the library synthesis of six-membered 1,5-oxaza spiroquinones with diversification at C-3 and N-5, as well as on the quinone moiety for complete utilisation of the proposed new core and for their biological screening as novel neuroprotective agents for the treatment of neurodegenerative diseases.

2.1.2. Synthesis of common amide fragment (4) for the synthesis of all derivatives

To synthesise common amide fragment (**4**), we have chosen inexpensive, commercially available 4-bromophenol (**9**) as the starting material. As mentioned in Scheme 2, the phenolic group in 4-bromophenol (**9**) was protected in the form of MOM ether [60–63] using MOM-Br and NaH in dry THF. Then, it was subjected to Pd-mediated Buchwald-Hartwig reaction [64–68] with aniline (**8**) to give the coupled compound **5** in 92% yield. To obtain common amide fragment (**4**) for the synthesis of all derivatives, **5** was

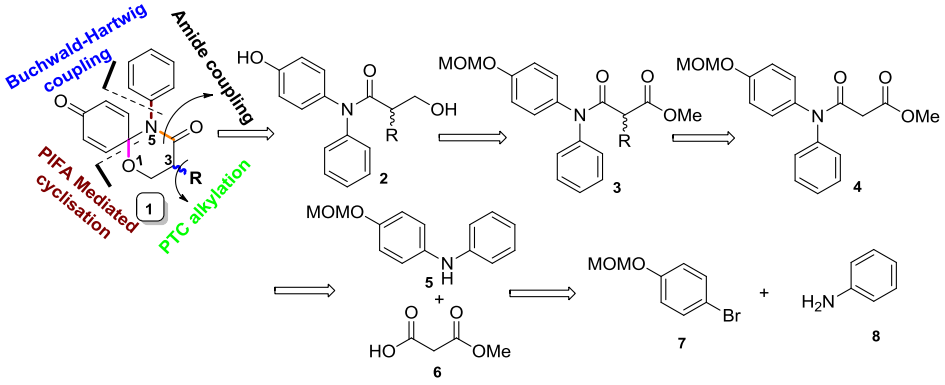

Scheme 1. Retrosynthetic analysis of six membered 1,5 oxaza spiroquinone moiety (1).

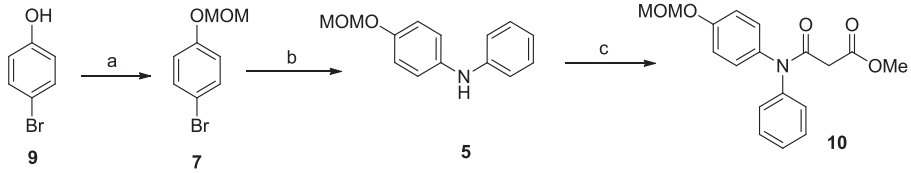

Scheme 2. Reagents and conditions: (a) MOM-Br, NaH, dry THF 0°C-rt, 4 h, 92%; (b) aniline (**8**) Pd_2 (dba)$_3$, BINAP, NaO^{t}Bu, anhydrous toluene, rt- 100 °C, 94%; (c) 3-methoxy-3-oxopropanoic acid (**6**), EDCI, DMAP, 0°C-rt, 6 h, 78%.

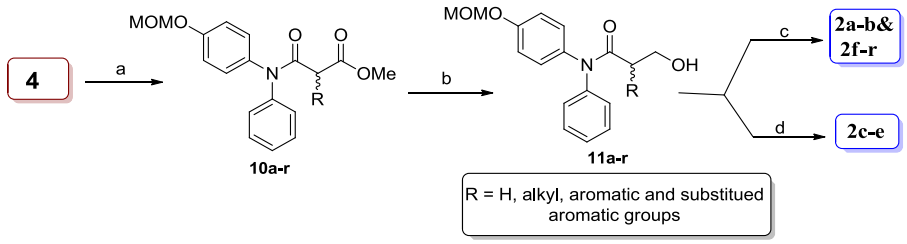

Scheme 3. Reagents and conditions: (a) 50% KOH, TBAI, X-R (different halides), toluene, −10°C-rt, 1 h; (b) $LiAl(O^tBu)_3H$, dry THF, −15 °C- rt, 4 h; (In case of unsubstituted compound $NaBH_4$, dry THF,0°C-rt was used) (c) TMSCl, NaI, ACN, DCM (1:1), 0°C-rt, 1 h; (d) BF_3Et_2O, DMS, 0 °C −15 °C, 10–20 min.

subjected to the EDCI/DMAP-mediated amide coupling reaction with 3-methoxy-3-oxopropanoic acid (**6**) in dry DCM to afford common amide fragment **4** [69,70] in 86% yield.

Table 1
Optimization of reaction conditions for PIFA mediated cyclisation of six membered 1,5 oxaza spiroquinones.

Entry	Reagent	Base	Solvent	Temperature	Time	Yield [f]
1	PIFA[a]	K_2CO_3	TFE[b]	−10 °C – 0 °C	6 h	20%
2	PIFA	K_2CO_3	HFIP[c]	−10 °C – 0 °C	5 h	35%
3	**PIFA**	**K_2CO_3**	**MeCN[d]**	**0°C - rt**	**3–4 h**	**Upto 91**
4	PIFA	K_2CO_3	DCM[e]	0 °C - rt	5–6 h	45%

[a] [Bis (trifluoroacetoxy) iodo] benzene (PIFA).
[b] 2, 2, 2-trifluoroethanol (TFE).
[c] Hexafluoroisopropyl alcohol (HFIP).
[d] Acetonitrile (MeCN).
[e] Dichloromethane (DCM).
[f] Isolated yield.

2.1.3. Synthesis of key fragments (2a-r)

The common amide fragment (**4**) was in our hand, our next target was the synthesis of diversity-oriented key fragments (**2a-r**), as illustrated in Scheme 3. Initially, phase-transfer-catalysed (PTC) mono-α-alkylation of compound **4** with aliphatic, aromatic, and substituted aromatic alkyl halides in the presence of TBAI and 50% aqueous KOH in toluene at −10 °C afforded mono-α-alkylated ester (**10b-r**) [71–73]. To understand the effect of substitution at C-3 position with aliphatic, aromatic, and substituted aromatic alkyl moieties during biological screening, we prepared scaffold **1a** without substitution. Selective reduction [74–76] of the ester moiety in **10a-r** with $Li(O^tBu)_3H$ in dry THF at −15 °C gave selective mono-reduced compounds (**11a-r**) with good yields. To prepare unsubstituted compound (**1a**), **4** was subjected to $NaBH_4$ reduction [77–80] in dry THF to afford **11a** in 78% yield. At this stage, we planned the deprotection of the aromatic MOM group with generalised conditions NaI, TMSCl [81–83] in DCM: ACN (1:1). The reactions progressed smoothly without problems for

Table 2
Synthetic derivatives of six membered 1,5oxaza spiroquinone novel scaffolds (**1a-r**).

Entry	R-group	Time (hr)	%yield	Entry	R-group	Time (hr)	% yield
1	Unsubstituted (H)	3.5	86	10		3.2	74
2		4	85	11		4	75
3		3.5	82	12		4	66
4		4	80	13	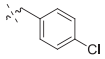	3.9	70
5	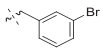	3.5	83	14	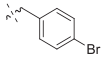	3.6	78
6	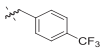	4	80	15	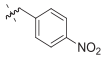	3.2	82
7	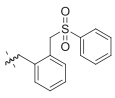	3.8	78	16	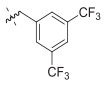	4	64
8	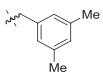	3.7	76	17	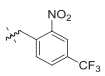	3.7	68
9		3	91	18		3.9	72

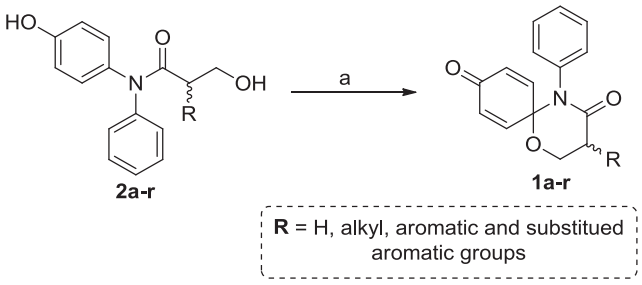

Scheme 4. Reagents and conditions: (a) PIFA, anhydrous K_2CO_3, dry ACN, 0°C- 25 °C, 4 h, upto 91%.

unsubstituted, aromatic, and substituted aromatic compounds (**11a-b** and **11f-r**), and products (**2a-b** and **2f-r**) were obtained in good yields. Under these conditions, **11c-e** produced the required MOM deprotected products (**2c-e**) in low yields, and unwanted by-products were observed. To overcome this problem, we used BF_3Et_2O and DMS conditions [84,85] at 0 °C and −15 °C instead of NaI and TMSCl. With the changed reaction conditions, the required products (**2c-e**) were obtained in good yields.

2.1.4. Synthesis of final oxaza scaffolds (1a-1r)

The key fragments were obtained and the synthesis of six-membered 1,5-oxaza spirocyclic scaffolds (**1a-1r**) was planned (see Table 2, Scheme 4). We first attempted MOM deprotection of key fragments (**2a-r**) for PIFA-mediated oxidative cyclisation transformation [86–93] and cyclised compounds were obtained in good yields (see Table 2). We also optimised the reaction conditions for the cyclisation reaction. (see Table 1), key fragment **2j** was used as the model substrate for optimization of condition, entry **3** in Table 1 was optimised conditions for the cyclisation of the six-membered 1,5-oxaza spirocyclic scaffolds (**1a-1r**).

2.2. Biological activity

2.2.1. Lipopolysaccharide (LPS)-induced NO production and structure-activity relationships

We investigated whether the synthesised six-membered 1,5-oxaza spiroquinone derivatives (**1a-r**) regulate inflammatory response in BV-2 cells. For this, we attempted to evaluate their anti-inflammatory activities, especially focused on the inhibitory effect of NO production in lipopolysaccharide (LPS)-induced BV-2 cell lines [94] as an initial screening study. NO production was measured based on the accumulation of nitrite using the standard Griess method and cell viability was measured using 3-(4,5-dimethylthiazol-2-yl)-2,5-diphenyltetrazolium bromide (MTT)-assay on the same cell lines [95]. The screened assay results are summarised in Table 3 (see Fig. 3).

After carefully analysing the obtained results, we established the SAR of the synthesised 1,5-oxaza spiroquinone derivatives (**1a-r**). All the synthesised derivatives showed moderate to potent NO inhibitory effect with low cytotoxicity. Higher inhibitory activity was observed with compound 1n with IC_{50} value of 0.07 μM and cell viability rate of 92%. Compounds **1d**, **1f**, **1g**, **1h**, **1i**, **1l,** and **1q** also showed potent NO inhibitory effects with low cytotoxic effects. The rest of the compounds also showed moderate NO inhibition effects with moderate cytotoxic effects.

Based on the results, we concluded that substitution at the α position to keto (C-3 position) was mandatory for activity. This observation was confirmed from the unsubstituted compound **1a.** Among all derivatives, the unsubstituted analogue **1a** showed low NO inhibitory effect (expect compounds **1k** and **1o**). Allyl substituted compounds (**1c-e**) showed higher efficiency than alkyl substituted compound **1b**. The aromatic substituted compounds played remarkable roles in NO inhibition, it was concluded based on the result obtained from compound **1n**. Analogues **1b-d** had methyl, ally and isobutylene groups at the α position to keto. Among the three analogues, compound **1d** showed a significant effect NO inhibition with IC_{50} value of 0.45 μM, increase in the carbon chain length of **1b-d** gradually enhanced the activity of compounds. Among the two structural isomers as a substitution at C-3 position in compound **1d** and **1e**, isobutylene substituted compound **1d** was remarkably active against NO production. Among compounds **1f-1r**, substitution on the aromatic ring played an important role for potent activity. Halogen substitution (F, Cl, and Br) on the aromatic ring showed better NO inhibition than unsubstituted aromatic compound **1f.** Among the halogen-containing compounds, the Cl-containing analogue showed the best activity. Our SAR studies suggested that moderately electro-negative atoms played important roles in the activity. A comparison of Br substitution at the meta and para positions, the meta-substituted compound (**1i**) was 50% more potent than the para-substituted compound (**1j**). Strong electron-withdrawing groups at the para-position showed more potency for NO inhibition than weak electron-withdrawing groups, as confirmed by the activities of **1k** and **1l**, and the inhibitory effects were 1.65 and 0.43 μM respectively. The compound having sulfone moiety **1m** showed a moderate effect with an inhibition value of 0.98 μM.

Interesting results were observed for compounds **1n** and **1o.** Compound **1n** had CF_3 groups at positions meta to each other, and compound **1o** had two methyl groups at positions meta to each other, with inhibition rates 0.07 and 1.83 μM respectively. This might be because of the electron-withdrawing nature of the CF_3 groups meta to each other. The combination of two electron-withdrawing groups (NO_2 and CF_3) at ortho and para positions displayed moderate effects with an NO inhibition value of 1.97 μM. Analogues **1q** and **1r** contained both CF_3 and halogen atoms (F, Cl). In **1q,** the CF_3 and F groups were ortho to each other. In **1r**, the CF_3 and Cl groups were para to each other and showed more potency than that of the mono-substituted CF_3 group at the para position in **1k** with inhibitory effect values of 1.55 μM and 1.74 μM respectively.

2.2.2. Analyse the SAR studies

Based on the above observations, the following SAR results can be summarised:

i. For activity, substitution at the α position to keto is mandatory.
ii. Aromatic group at the α position to keto had a remarkable effect on the activity, except in **1d.**
iii. Electron-withdrawing groups on the aromatic ring showed potent activity.
iv. Among the halogen atoms on the aromatic ring, Cl showed the highest potent activity.

Based on the above observations, we concluded that most of the synthesised derivatives showed moderate to potency activity for NO inhibition in the tested BV-2 cell lines. Almost all the synthesised compounds had low to moderate cytotoxicity. Among all the tested derivatives, **1n** was observed most active compound with very low cytotoxicity. In addition, the cytotoxicity of all synthesised analogues in normal BV-2 cell lines were also tested, the results was summarised in Table 3 and Fig. 3. After carefully analysis of the obtained results, all analogues are exhibited very less to moderated cytotoxicity in normal BV-2 cell lines.

Table 3
Nitric oxide inhibition IC_{50} values and cell viability of synthesised derivaties (**1a-r**) in LPS induced BV-2 cells.[a]

Compound No:	R-group	NO inhibition IC_{50} values[b] (μM)	LPS induced cell survival rate (%)	Normal cell survival rate (%)
1a	Unsubstituted (H)	1.30 ± 0.41	79.75 ± 3.68	101.72 ± 8.79
1b		1.22 ± 0.29	72.80 ± 9.59	86.088 ± 3.85
1c	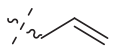	1.03 ± 0.03	84.56 ± 4.84	89.68 ± 3.29
1d		0.45 ± 0.00	80.07 ± 0.22	91.39 ± 5.90
1e	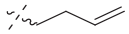	0.73 ± 0.00	80.39 ± 3.65	88.99 ± 8.38
1f	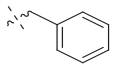	0.57 ± 0.00	76.12 ± 0.30	82.06 ± 4.78
1g	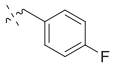	0.40 ± 0.04	85.25 ± 12.42	82.86 ± 2.33
1h	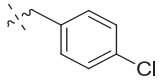	0.54 ± 0.02	78.99 ± 2.61	91.05 ± 5.18
1i	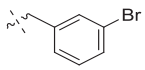	0.54 ± 0.00	73.96 ± 7.09	96.02 ± 10.63
1j		1.38 ± 0.33	72.01 ± 3.47	82.71 ± 3.92
1k	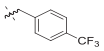	1.65 ± 0.64	84.13 ± 6.71	87.13 ± 1.16
1l	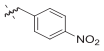	0.43 ± 0.08	82.70 ± 10.27	95.55 ± 4.79
1m		0.98 ± 0.03	84.31 ± 2.94	97.51 ± 8.86
1n		**0.07 ± 0.01**	**92.13 ± 13.37**	**85.43 ± 2.51**
1°	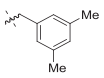	1.82 ± 0.23	78.01 ± 1.99	94.21 ± 0.71
1p	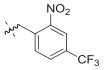	0.97 ± 0.13	80.43 ± 1.73	84.50 ± 1.70
1q		0.60 ± 0.05	71.14 ± 4.42	84.42 ± 8.51
1r		0.77 ± 0.02	64.44 ± 0.08	70.49 ± 0.68
N-NMMA[c]		16.05 ± 0.07	60.54 ± 1.82	–

[a] Cell lines were treated different concentration of compounds for 24 h. Cell viability was measured by MTT assay as described in the experimental section.
[b] IC_{50} values are indicated as the mean ± SD of three independent experiments.
[c] N-Methylarginine used as a positive control.

2.3. Physiochemical and DMPK parameters prediction for compound (*1a-1n*)

Our continuation efforts in CHOS strategy and studies [31] for development of novel lead compounds to Neurodegenerative diseases, various drug like properties such as chemical and physical properties of synthesised derivaties (**1a-1r**) was studied with Qik-Prop. As considering the designed new skeleton [Fig. 2] and synthesised derivaties (**1a-1r**) as a CNS druggable scaffolds, drug properties were predicted from multi conformers of all synthesised derivaties. The prediction showed solubility, polar surface area, BBB penetration, HERG inhibition, cell permeability, Human oral

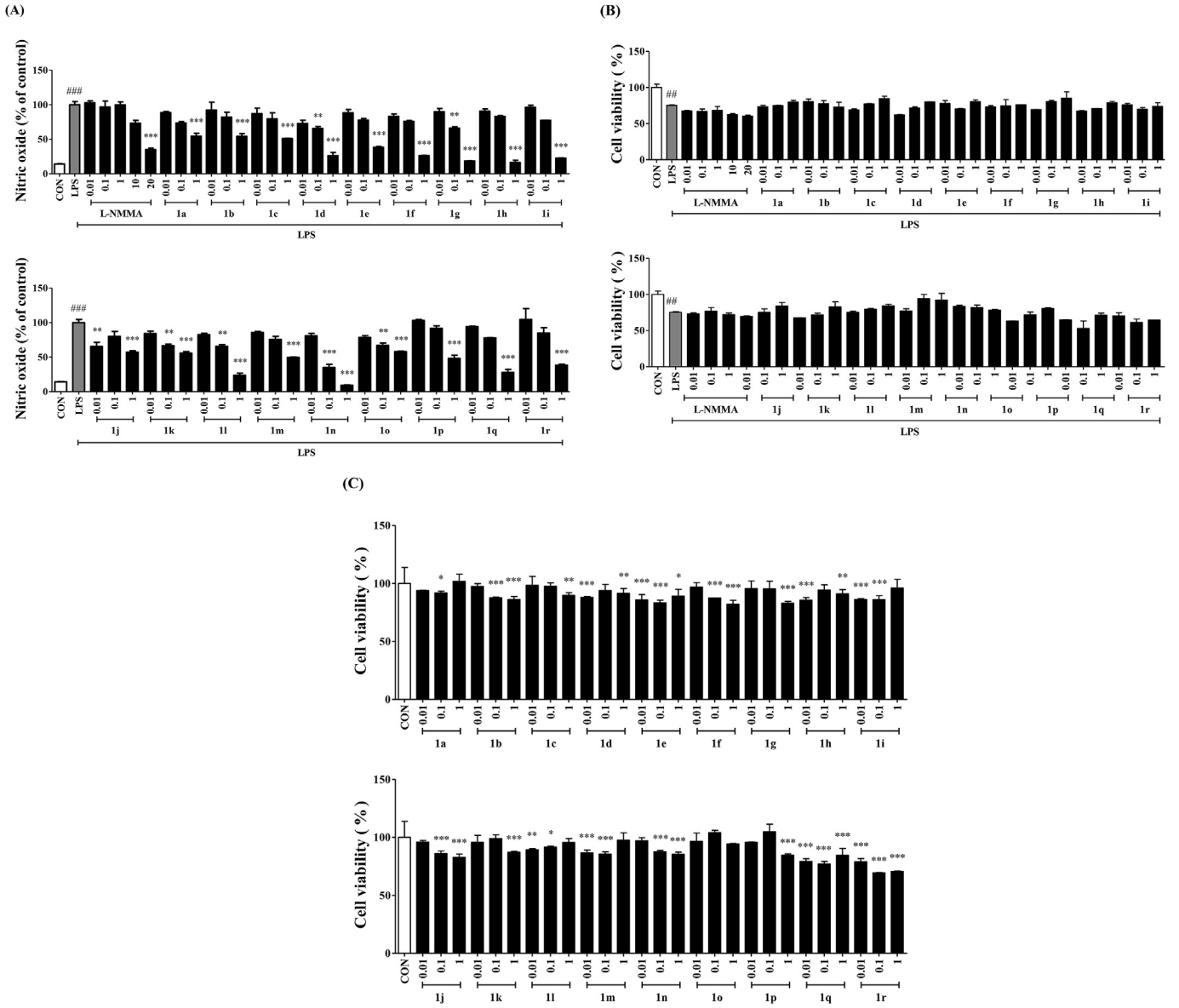

Fig. 3. **(A)** NO Inhibitory effect of compounds **1a-r** at the concentration of 0.01, 0.1, 1 μM in LPS-stimulated BV-2 cells. BV-2 cells were treated with 100 ng/mL of LPS for 30 min and then treated with compounds for 24 h. All the data are presented as the mean ± SEM of three independent experiments. $^{*}p < 0.01$, $^{***}p < 0.001$ vs. LPS control. **(B)** Cell survival rate after treating compounds **1a-r** at the concentration of 0.01, 0.1, 1 μM in LPS-stimulated BV-2 cells. **(C)** Cell survival rate after treating compounds **1a-r** at the concentration of 0.01, 0.1, 1 μM in BV-2 cells.

absorption, permeability (Caco-2 & MDCK), and CNS activity. The analysed results were summarised in Table 4. In addition, CYP metabolism of all compounds (**1a-1r**) was predicted, results were summarised in Supplementary information (see Tables 1 and 2). After carefully analysing the obtained result, all the synthesised derivaties (**1a-1r**) were within the standard values and it is also important to note that the potent compound **1n** was satisfied every standard range.

2.4. Kinase panel screening of compound 1n

After primary screening of the synthesised derivatives against LPS-induced NO inhibition in BV-2 cell lines, and based on the inhibition rates and cell viabilities of compounds, we selected our potent compound **1n** for further studies. We considered the kinase assay is use full to further investigation of our potent compound **1n** in evaluation of its neuroprotective effect. Protein kinases helpful in Phosphorylation, abnormal phosphorylation by kinases in cells, as a result major diseases including cancer, diabetic and chronic inflammation. For that reason protein kinases are occupied second most for drug target.

We screened compound **1n** for 369 wild type kinases [97–99] through a single dose duplicate assay at 30 μM (Reaction Biology Corporation, USA). To visualise the kinase inhibitory spectrum of compound **1n**, a kinome dendrogram was prepared (Fig. 4). The specificity of compound **1n** was represented in a dendrogram view of the human kinome phylogenetic tree. In the kinome dendrogram, the inhibitory activity was classified as high, medium, low, and no compound affinity for kinase activity (with respect to DMSO control) of <50%, 50–60%, 60–75%, and >75%, respectively. The % enzyme activity (relative to DMSO control) of chosen kinases (cut off: >73%) is presented in Table 5.

Table 4
Physiochemical and DMPK parameters prediction for compound (**1a-1r**) QikProp**.

No.	No.of Conf.	PSA	log S[a]	log BB[b]	CNS activity[c]	log HERG[d]	Apparent Caco-2 permeability (nm/s)	Apparent MDCK permeability (nm/s)	% Human Oral Absorption in GI (±-20%)
1a	234	64.98 ± 0.07	−2.08± 0.06	−0.24± 0.02	0.0 ± 0.0	−4.39± 0.08	1151.21 ± 31.11	576.06 ± 16.83	88.94 ± 0.13
1b	28	62.58 ± 1.14	−2.48± 0.08	−0.18± 0.02	0.0 ± 0.0	−4.56± 0.11	1440.90 ± 103.35	734.36 ± 57.10	93.95 ± 0.63
1c	112	61.19 ± 1.98	−3.04± 0.12	−0.28± 0.06	0.0 ± 0.0	−5.03± 0.14	1624.08 ± 235.51	836.33 ± 131.32	99.89 ± 0.59
1d	76	60.56 ± 2.32	−3.40± 0.19	−0.27± 0.07	0.0 ± 0.0	−5.03± 0.18	1698.90 ± 272.32	878.23 ± 152.35	100.0 ± 0.0
1e	206	60.98 ± 2.12	−3.41± 0.21	−0.37± 0.06	0.0 ± 0.0	−5.24± 0.22	1589.05 ± 213.30	816.75 ± 118.77	100.0 ± 0.0
1f	92	59.75 ± 2.69	−4.16± 0.21	−0.30± 0.09	0.0 ± 0.0	−6.03± 0.24	1734.30 ± 339.99	898.49 ± 191.11	100.0 ± 0.0
1g	92	59.75 ± 2.69	−4.53± 0.20	−0.19± 0.09	0.04 ± 0.20	−5.92± 0.23	1728.05 ± 335.44	1611.22 ± 339.45	100.0 ± 0.0
1h	92	59.75 ± 2.69	−4.93± 0.20	−0.14± 0.09	0.04 ± 0.20	−5.98± 0.22	1728.74 ± 335.40	2207.66 ± 464.85	100.0 ± 0.0
1i	188	59.79 ± 2.67	−5.02± 0.23	−0.13± 0.09	0.04 ± 0.20	−6.00± 0.24	1729.42 ± 333.80	2335.95 ± 484.07	100.0 ± 0.0
1j	8	59.75 ± 2.69	−5.05± 0.20	−0.13± 0.09	0.04 ± 0.20	−6.01± 0.22	1729.75 ± 336.51	2371.64 ± 500.72	100.0 ± 0.0
1k	92	59.72 ± 2.62	−5.69± 0.21	−0.05± 0.09	0.34 ± 0.48	−6.07± 0.21	1732.06 ± 323.09	4015.15 ± 811.36	100.0 ± 0.0
1l	100	104.52 ± 2.58	−4.19± 0.20	−1.31± 0.10	−2.00 ± 0.00	−6.00± 0.21	207.00 ± 37.71	90.28 ± 17.85	84.15 ± 1.44
1m	104	93.27 ± 2.90	−4.58± 0.46	−1.06± 0.11	−1.72 ± 0.45	−7.15± 0.43	571.94 ± 136.47	272.83 ± 70.13	97.86 ± 2.73
1n	536	59.73 ± 2.59	−7.10± 0.31	0.20± 0.09	1.02 ± 0.12	−6.03± 0.26	1728.20 ± 343.13	10000.0 ± 0.0	100.0 ± 0.0
1o	128	59.74 ± 2.68	−5.31± 0.26	−0.34± 010	0.0 ± 0.0	−5.88± 0.26	1750.60 ± 352.45	907.68 ± 198.42	100.0 ± 0.0
1p	96	103.73 ± 3.05	−5.57± 0.21	−0.87± 0.12	−1.13 ± 0.51	−6.01± 0.18	326.48 ± 82.53	663.07 ± 181.74	94.78 ± 2.74
1q	160	59.74 ± 2.94	−5.62± 0.38	−0.03± 0.08	0.26 ± 0.44	−6.03± 0.25	1708.09 ± 311.92	4282.09 ± 1167.17	100.0 ± 0.0
1r	106	60.23 ± 2.26	−6.15± 0.30	0.07± 0.08	0.80 ± 0.40	−5.96± 0.27	1736.78 ± 304.49	7278.47 ± 1411.76	100.0 ± 0.0
Standard	0	(-6.5/ 0.5)	(-3.0/ 1.2)	−2 inactive; +2 active	(concern below −5)	(<25 poor, >500 great)	(<25 poor, >500 great)		

Note: **For 95% of known drugs based on Schrödinger, USA-Qikprop v3.2 (2015) software results. Every values were calculated from Qikprop.
[a] log S: log [Conformation-independent predicted aqueous solubility].
[b] log BB: log [predicted brain/blood partition coefficient].
[c] CNS activity Ajay et al. [96].
[d] log HERG: log [predicted IC50 value for blockage of HERG K± channels].

Among full panel of tested 369 kinases, the compound **1n** showed good selectivity and inhibition towards c-Jun NH2-terminal kinase1 (JNK1). It was reported that alteration in JNKs signalling pathway [100–102] has been shown to be critical in the development of neuronal cytotoxicity. Moreover the JNKs as good therapeutic target for neurodegenerative diseases. Interestingly, our full panel kinase screening with potent compound **1n** also showed inhibitory activity and selectivity towards JNK1.

Massive production of nitric oxide (NO) can exert its cytotoxic effects, this effect due to formation of highly reactive free radical peroxynitrite, which damages DNA, proteins, and lipids by oxidation, as a results alters in signal transduction pathways, which leads to neuronal toxicity. In particular, NO can stimulate the activity of transcription factors including c-Jun, a substrate of JNK. Interestingly, JNK can activate c-Jun through phosphorylation [103] on Ser-63 and Ser-73. JNK inhibition of the compound **1n** could be block the phosphorylation of c-Jun and repress the activity of c-Jun.

The compound **1n** showed excellent NO Inhibition activity in LPS-induced BV-2 cell lines with IC_{50} value 0.07 μM and in full panel kinase screening also the selectivity and inhibition towards JNK1 with 36% inhibition value, with these observed results we strongly believe that our potent compound **1n** could act as neuroprotective agent in neurodegenerative diseases.

2.5. Molecular docking studies

Among the tested kinases, compound **1n** revealed best potency and selectivity towards JNK1. To further elucidate the inhibitory activity at the atomic level, a docking simulation of compound **1n** was conducted. Among the 34 PDBs (Protein Data Bank) of JNK1, 4E73 was chosen as the best docking model based on the method described in the supplementary information. The best pose of compound **1n** presented a hydrogen bonding interaction between the carbonyl group of the oxaza ring and Met111, a hinge residue (Fig. 5). In spite of weak H-bonding with N–H in Met111 (length: 3.24 A°, angle of H-bond donor: 123.9°), the docking pose of compound **1n** was overlaid with poses of other ligands of JNK1 so that it could occupy the region surrounding the hydrophobic residues (Ile32, Ala53, Val40, Ile86, Met108, Leu110, Met111, Ala113, Val158, and Leu168). The gate-keeper residue Met108 and sterically hindered residues did not permit the phenyl ring of compound **1n** to have pi-cation interaction with Lys55.

2.6. Animal studies

To confirm the effect of compound **1n** on short-term working memory dysfunction in scopolamine-induced mice [104–106], the

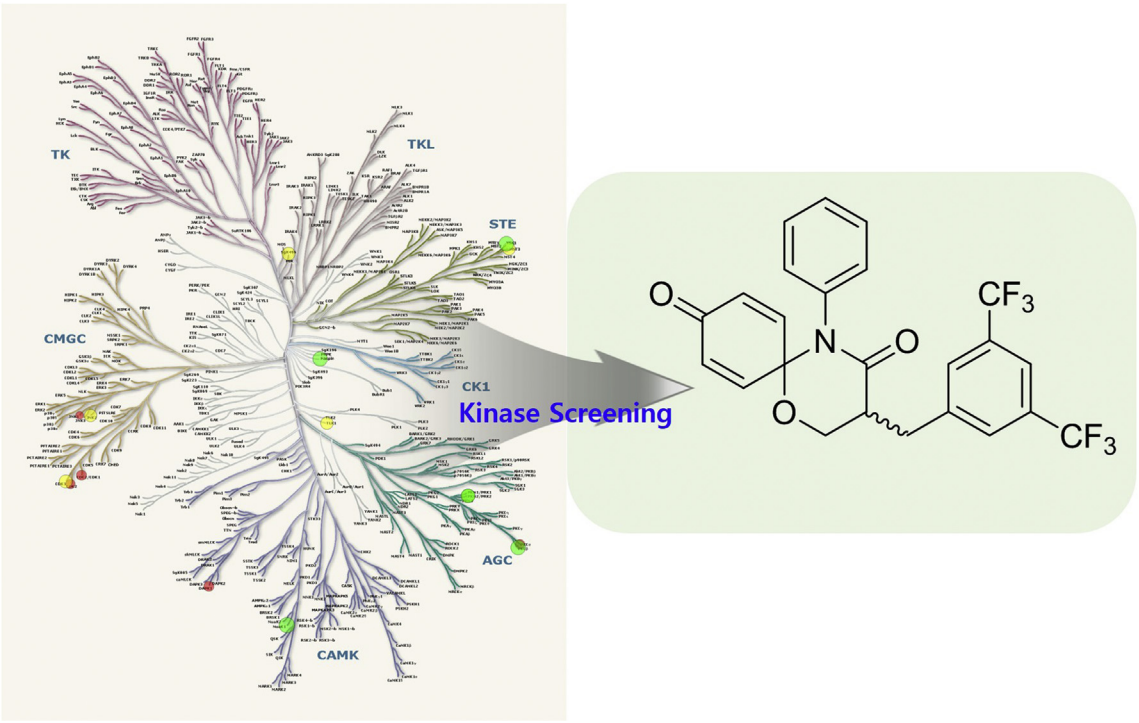

Fig. 4. The selectivity of compound **1n** is represented in a dendrogram.

Table 5
The % enzyme Activity Inhibition effect of compound **1n** on Kinases.[a,b]

Kinase:	% Enzyme Activity (relative to DMSO controls)		Control Compound IC_{50}(M):	Control Compound:
	data1	data2		
JNK1	36.03	35.58	5.70E-07	Staurosporine
CDK2/cyclin O	43.80	42.33	1.46E-09	Staurosporine
DAPK1	45.43	45.32	1.31E-08	Staurosporine
PKCa	46.47	44.81	4.74E-10	Staurosporine
CDK1/cyclin B	46.54	45.38	2.16E-09	Staurosporine
MST3/STK24	58.19	57.62	3.34E-09	Staurosporine
TLK1	58.62	57.28	3.04E-08	Staurosporine
JNK2	58.79	57.84	1.85E-06	Staurosporine
RIPK5	59.94	58.59	6.90E-08	Staurosporine
CDK3/cyclin E	60.20	58.48	2.08E-09	Staurosporine
PKN2/PRK2	64.75	62.16	1.97E-09	Staurosporine
Haspin	66.80	66.06	1.90E-08	Staurosporine
STK25/YSK1	66.95	66.88	1.90E-09	Staurosporine
ARK5/NUAK1	70.84	70.70	1.31E-09	Staurosporine
PKCb2	71.17	67.73	1.44E-09	Staurosporine
JNK3	73.42	70.58	7.70E-07	JNKi VIII

[a] 369 kinases (Reaction Biology Corp) were screened and assay method described in the experimental section.
[b] The presented kinases data was only upto 70% cut-off among the 369 kinases data.

Y-maze test was used to measure spontaneous alteration Fig. 6. Spontaneous alternation was significantly lowered in the normal group relative to the scopolamine treated group, and this reduced alternation was significantly increased by treatment with compound **1n** (10 mg/kg) and donepezil (5 mg/kg) (normal: 70.34%, control: 45.14%, donepezil: 62.30%, compound **1n**: 59.62%). Moreover, all the entries were not significant between the experimental groups. As a result, compound **1n** could prevent spatial short-term memory deficits induced by scopolamine.

3. Discussion

In this study, we developed new skeleton with easily assemble with diversification at different position (i. e. C-3, N-5 and on quinone ring) for rational drug design to neurodegenerative diseases with small molecules. We intended to elicit the targets for synthesised potent analogues, we followed deconvolution strategy [107,108], in which rational design of scaffold, SAR studies carried out with chemical optimization and target specific assays. In this regard, all synthesised derivaties (1n-1r) were screened Inhibitory effect of NO production in LPS-induced BV-2 cell lines and Structure–activity relationship (SAR) was developed for all synthesised analogues. The analogue 1n found as more potent with IC_{50} value was 0.07 μM among synthesised derivaties. In addition we conducted full panel kinase screening of potent compound 1n, it showed selectivity and inhibition towards neuroinflammation-

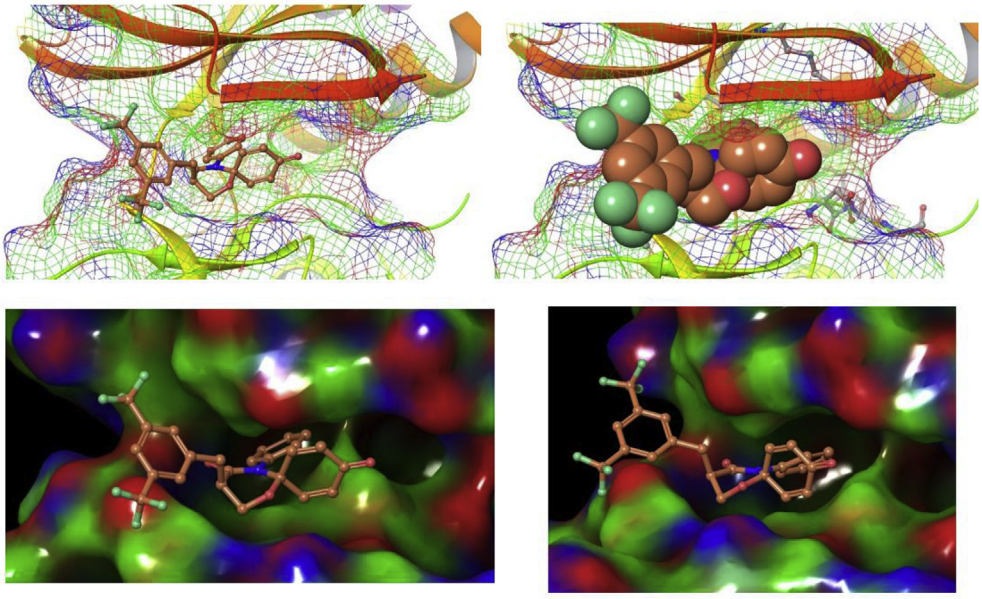

Fig. 5. A plausible binding pose of the compound **1n** to JNK1 (DFG-in).

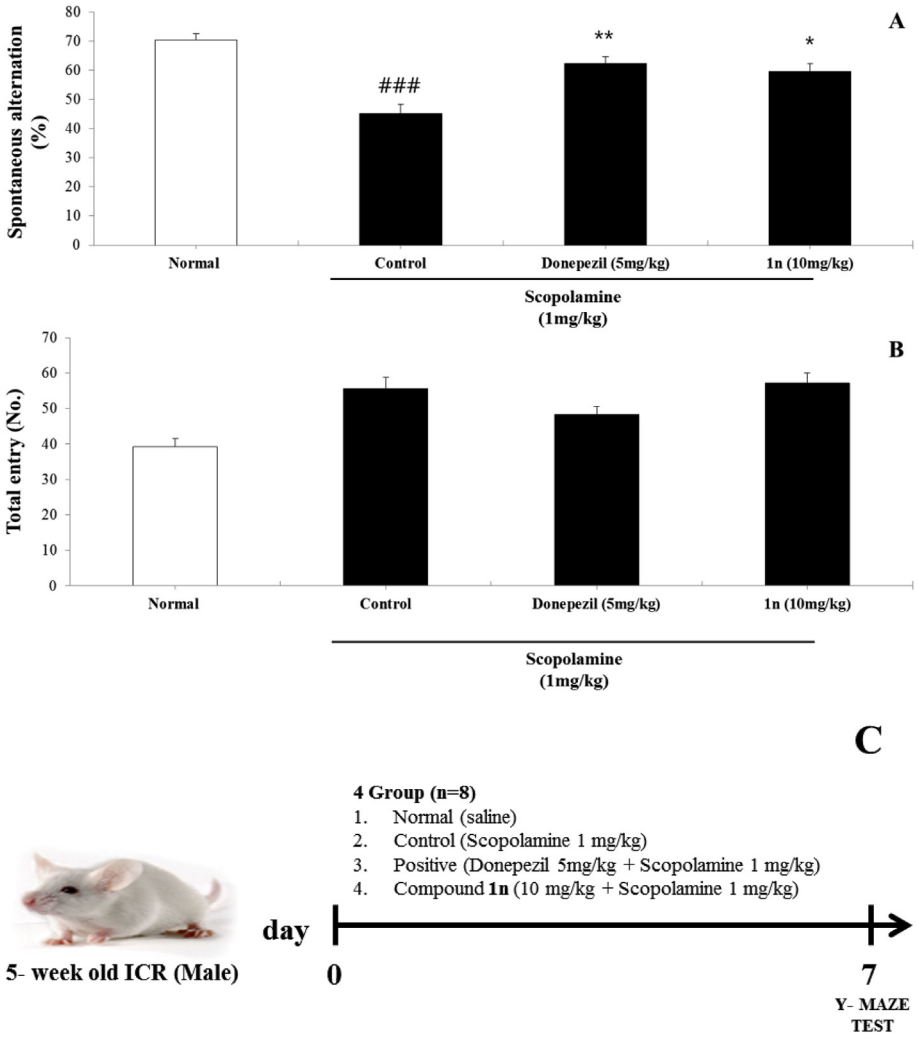

Fig. 6. Effect of compound **1n** on scopolamine-induced memory impairment in ICR mice on the Y-maze. Mice was orally administered donepezil (5 mg/kg) and compound **1n** (10 mg/kg), 60 min before the test. 30 min later, the mice were intraperitoneally treated with scopolamine at a concentration of 1 mg/kg of mice weight (**A**). The number of arm entries; (**B**) 8-min session was measured; (**C**) Schematic representation of Y-maze test. The data was represented as mean ± SEM (n = 8 per group) compared with the scopolamine treated group. The differences among the multiple groups were considered significant $p < 0.05$, $p < 0.01$, and $p < 0.001$.

related kinases JNK1, molecular docking studies were conducted. Finally *in vivo experiments were also* conducted on scopolamine-induced mice. Further extension of work with proposed skeleton is in progress to complete utilisation of designed skeleton for neurodegenerative diseases.

4. Conclusions

In summary, the unnatural and unprecedented new skeleton of 1, 5-oxaza spiroquinone have been developed and successfully achieved in a concise manner by utilising the Pd-mediated Buchwald-Hartwig, PTC reaction, and PIFA-mediated cyclisation as key reactions to produce 18 final compounds with diversification at C-3 with good yields (up to 91%). Most of compounds were showed good inhibitory effects on NO production in LPS-induced BV-2 cell lines. Furthermore compound **1n** was found as potent with IC_{50} value 0.07 μM. The most potent compound **1n** was further investigated for full panel kinase screening, and it showed selectivity and inhibition towards neuroinflammation-related kinases JNK1 and other kinases. Molecular docking of the compound on JNK1 provided atomic-level insight of compound **1n** as a kinase inhibitor and we also studied *in vivo* effect of **1n** on scopolamine-induced memory impairment. All these studies suggest that the new skeleton of 1, 5-oxaza spiroquinone could serve as protective therapeutics in neurodegenerative diseases and have significant value for future research. The future plan with proposed new skeleton of 1, 5-oxaza spiroquinone is, 1. Further diversification and the synthesis of the new scaffolds (e.g., C-3 and N-5 positions and on quinone moieties) with another moieties and evaluation of their neuroprotective activity for complete utilisation of proposed new1, 5-oxaza spiroquinone skeleton. 2. Finding the primary target identification studies of the potent compounds by comparing the various activities for neurodegenerative diseases, the polypharmacological profile of the scaffolds.

5. Experimental section

5.1. General chemistry

All of the reagents and solvents were reagent commercial grade and used without further purification unless specified otherwise. Tetrahydrofuran (THF) was freshly distilled from sodium benzophenone ketyl, dichloromethane, acetonitrile were distilled from CaH_2. For all moisture sensitive reactions, the glassware was dried in oven (>110 °C) or flame dried prior to use. K_2CO_3 was used in powered form and dried in desiccator. All reactions were performed under an atmosphere nitrogen, stirred magnetically with magnetic bar and reactions were monitored by analytical thin layer chromatography (TLC). Analytical thin layer chromatography (TLC) was performed on precoated silica gel 60 F254 plates. The TLC spots were visualized by UV light at 254 nm, Ninhydrine, PMA, solutions were used, for visualization the TLC was heating with a heat gun. Flash column chromatography was undertaken on silica gel (230–400 mesh). ^1H and ^{13}C NMR spectra were recorded on Brucker 600 MHz and chemical shifts were quoted in parts per million (ppm) and calibrated to the residual proton and carbon resonance of the solvent: for $CDCl_3$ δ_H 7.25, δ_C 77.0; for MeOD δ_H 3.31, δ_C 49.15; The NMR data was reported as follows: s = singlet, d = doublet, t = triplet, q = quartet, m = multiplet, dd = doublet of doublet, ddd = doublet of doublet of doublet, br = broad signal. J, were reported in hertz unit (Hz). ^{13}C NMR was recorded on Brucker 600 MHz, and was fully decoupled by broad band proton decoupling. Mass spectral data were obtained under the condition of Agilent LC/Q-TOP by using ESI positive method. UV–Visible data of compounds were measured with Bruker, Tensor27 series, for Melting points of solid compounds Optimelt, MPA100 series instruments were used.

5.2. Synthetic procedure and characterization of compounds

5.2.1. Bromo-4-(methoxymethoxy) benzene *(7)*

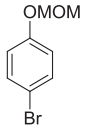

To suspension of sodium hydride (0.887 g, 23.12 mmol, 60% dispersion in paraffin oil) in dry THF (30 mL) at 0 °C was slowly added a solution of 4-bromophenol (**9**) (4.0 g, 60.78 mmol) in dry THF (20 mL) under nitrogen atmosphere and mixture was allowed to stir for 30 min at which point the hydrogen gas evolution had stopped. The resultant mixture was cooled to 0 °C and, bromomethyl methyl ether (27.74 mL, 66.87 mmol) was added dropwise and stirred for an additional 4 h at rt. After completion of reaction, the reaction mixture was quenched with Ice-cold water and extract with Ethyl acetate and the organic layer was washed with brine and dried over Na_2SO_4. The solvent was removed under reduced pressure, and the crude product was subjected to flash column chromatography (5% ethyl acetate-hexane) to give compound **7** (4.61 gr, 92%) as colour less oil; IR (neat): 2956, 2902, 2826, 1590, 1487, 1233, 1152, 997, 824 cm^{-1}; ^1H NMR (600 MHz, $CDCl_3$) δ 7.38 (d, $J = 9.0$ Hz, 1H), 6.93 (d, $J = 9.0$ Hz, 1H), 5.14 (s, 1H), 3.47 (s, 2H); ^{13}C NMR (150 MHz, $CDCl_3$) δ 156.13, 132.12 (2 C), 117.88 (2 C), 114.01, 94.30, 55.85 ppm; ESI-MS: $m/z = 217$ $[M]^+$.

5.2.2. 4-(Methoxymethoxy)–N-phenyl aniline *(5)*

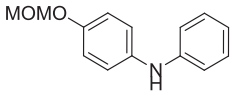

The oven dried resalable schlenk tube was charged with required amounts of $Pd_2(dba)_3$ (0.949 g, 1.03 mmol), BINAP (3.873 g, 6.22 mmol), NaO^tBu (2.849 g, 9.61 mmol) then add degassed anhydrous Toluene (40 mL), degas through pumping Argon, then add Aniline (**8**) (2.26 mL, 24.88 mmol) and compound **7** (4.5 gr, 20.73 mmol) the schlenk tube was capped with a septum and then evacuated and back filled with Argon, the resulting mixture stirred for 5–10 min at rt. The septum was replaced with a Teflon screwcap. The schlenk tube was sealed and the mixture was stirred at 80–100 for 12 h, monitored with TLC, after completion of compound **7** the reaction mixture was cooled to room temperature, diluted with DCM (50 mL), filtered through celite. Filtrate was washed with brine then concentrated under reduced pressure and the crude product was purified by column chromatography (10% ethyl acetate-hexane) to give compound **5** (5.828 g, 94%) as light brown liquid; IR (neat): 2962, 2954, 2900, 2818, 1597, 1511, 1304, 1149, 1077, 1015, 744 cm^{-1}; ^1H NMR (600 MHz, $CDCl_3$) δ 7.28–7.24 (m, 3H), 7.08 (t, $J = 9.0$ Hz, 1H), 7.02–6.98 (m, 2H), 6.92 (dd, $J = 10.6$, 4.1 Hz, 1H), 6.87 (dd, $J = 12.7$, 2.7 Hz, 1H), 6.74 (ddd, $J = 8.8$, 2.6, 1.4 Hz, 1H), 5.62–5.85 (bs, 1H), 5.14 (s, 2H), 3.54 (s, 3H); ^{13}C NMR (150 MHz, $CDCl_3$) δ 154.57, 152.95, 142.99, 138.64, 129.24, 120.88, 119.84, 117.24, 114.05, 114.03, 106.86, 106.72, 96.45, 56.15 ppm; ESI-MS: $m/z = 229$ $[M]^+$.

*5.2.3. Methyl 3-((4-(methoxymethoxy) phenyl) (phenyl) amino)-3-oxopropanoate **(4)***

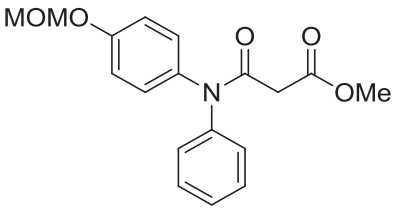

To a stirred solution of Methyl hydrogen malonate (**6**) (2.91 mL, 27.86 mmol) in anhydrous CH_2Cl_2 (30 mL) was treated with EDCI (5.826 gr, 30.39 mmol) and HOBt (4.650 gr, 30.39 mmol) at 0 °C, stirred this reaction mixture 30 min at same temperature and 30 min at rt. Again this reaction mixture taken to 0 °C then added compound **5** (5.8 gr, 25.32 mmol) in dry CH_2Cl_2 (40 mL) slowly drop wise and resulting mixture was stirred for 18 h. The reaction mixture was quenched with water and extracted with ethyl acetate (2 × 50 mL), the combined organic layer was washed with brine and dried over Mg_2SO_4. The solvent was removed under reduced pressure, and the crude product was subjected to column chromatography (10% ethyl acetate-hexane) to give compound **4** (6.499 gr, 78%) as light brown liquid; IR (neat): 2955, 2917, 2849, 2826, 2789, 1739, 1669, 1593, 1490, 1326, 1149, 731 cm^{-1}; ^1H NMR (600 MHz, $CDCl_3$) δ 7.46–7.28 (m, 5H), 7.25–7.15 (m, 2H), 7.09–6.96 (m, 2H), 5.16 (d, $J = 25.0$ Hz, 2H), 3.70 (s, 3H), 3.46 (d, $J = 21.6$ Hz, 3H), 3.41 (s, 2H); ^{13}C NMR (151 MHz, $CDCl_3$) δ 168.00, 166.18, 157.03, 142.28, 136.13, 129.94, 129.74, 128.91, 128.42, 127.56, 126.33, 126.06, 117.34, 116.61, 94.43, 56.20, 52.36, 42.45 ppm; ESI-MS: m/z = 330 $[M+1]^+$.

*5.2.4. Methyl 2-(4-bromobenzyl)-3-((4-(methoxymethoxy) phenyl) (phenyl) amino)-3-oxopropanoate **(10j)***

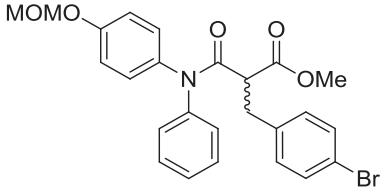

To a stirred solution of amide compound **4** (0.200 gr, 0.60 mmol) in Toluene (4 mL) at 5–10 °C 50% KOH solution (0.23 mL, 6.68 mmol) was added and stirring was continued for 10–15 min. The reaction mixture was turned to blue colour then reaction mixture was taken to 0 °C, 4-bromobenzyl bromide (0.165 gr, 0.66 mmol) in 1 mL toluene was added drop wise slowly followed by catalytic amount (19 mg) of TBAI was added, then the biphasic reaction mixture was allowed to rt and stirring was continued until completion starting material (amide compound 10), monitored by TLC. After completion of starting material the biphasic reaction mixture was diluted with water (5 mL) and extracted with ethyl acetate (2 × 20 mL), the combined organic layer was washed with brine and dried over anhydrous Na_2SO_4. The solvent was removed under reduced pressure, and the crude product was subjected to flash column chromatography (3–5% ethyl acetate-hexane) to give corresponding alkylated compound **10j** (0.268 gr, 89%) as colour less liquid; IR (neat): 2955, 2917, 2850, 2826, 2790, 1745, 1667, 1506, 1440, 1199, 1233, 1151, 1077, 732 cm^{-1}; ^1H NMR (400 MHz, $CDCl_3$) δ 7.43 (d, $J = 7.9$ Hz, 2H), 7.33–7.25 (m, 2H), 7.19–7.07 (m, 2H), 7.06–6.58 (m, 7H), 5.14 (d, $J = 17.4$ Hz, 2H), 3.81–3.71 (m, 4H), 3.46 (d, $J = 22.0$ Hz, 3H), 3.28 (t, $J = 12.0$ Hz, 1H), 3.13 (dd, $J = 13.5, 4.6$ Hz, 1H); ^{13}C NMR (150 MHz, $CDCl_3$) δ 169.60, 168.54, 156.91, 142.27, 137.30, 136.10, 131.53 (2 C), 131.24, 129.88, 129.69, 128.92, 128.59, 128.14, 127.47, 126.43, 126.11, 120.67, 117.06, 116.59, 94.43, 56.23, 52.64, 51.35, 34.74 ppm; ESI-MS: $m/z = 498$ $[M]^+$.

*5.2.5. 2-(4-Bromobenzyl)-3-hydroxy-N-(4-(methoxymethoxy) phenyl)–N-phenylpropanamide **(11j)***

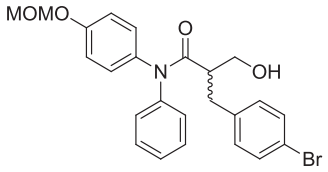

To a stirred solution of alkylated compound **10j** (0.240 gr, 0.48 mmol) in dry THF (5 mL) was added ca.30% Lithium Tri-tert-butoxyaluminium Hydride in THF (2.45 mL, 2.89 mmol) drop wise at −20 °C and mixture was stirred for 1 h same temperature then allowed to room temperature and stirring was continued 4 h. After completion of starting material the reaction mixture was quenched with saturated sodium potassium tartrate solution at 0 °C, then extracted with extracted with ethyl acetate (3 × 30 mL), the organic layer was dried over anhydrous Na_2SO_4. The solvent was removed under reduced pressure, and the crude product was subjected to flash column chromatography (40% ethyl acetate-hexane) to give corresponding reductive compound **11j** (0.207 gr, 92%) as colour dense liquid; IR (neat): 2958, 2927, 2850, 2826, 2788, 1663, 1507, 1489, 1265, 11151, 1105, 1011, 733 cm^{-1}; ^1H NMR (600 MHz, $CDCl_3$) δ 7.41 (t, $J = 7.2$ Hz, 2H), 7.33 (t, $J = 7.6$ Hz, 2H), 7.20 (t, $J = 7.4$ Hz, 1H), 7.14 (d, $J = 7.8$ Hz, 1H), 7.06 (d, $J = 8.8$ Hz, 1H), 7.01–6.97 (m, 2H), 6.94 (d, $J = 8.1$ Hz, 1H), 6.92–6.75 (m, 3H), 5.16 (d, $J = 26.9$ Hz, 2H), 3.80 (d, $J = 10.8$ Hz, 1H), 3.77–3.70 (bs, 1H), 3.48 (d, $J = 32.5$ Hz, 3H), 3.05–2.88 (m, 3H), 2.83–2.73 (m, 1H); ^{13}C NMR (150 MHz, $CDCl_3$) δ 175.19, 156.80, 142.37, 138.02, 135.95, 131.54 (2 C), 131.12, 131.08, 129.88, 129.76, 129.07, 128.63, 128.02, 127.71, 126.38, 120.43, 117.17, 116.73, 94.51, 63.41, 56.27, 46.25, 34.96 ppm; ESI-MS: $m/z = 470$ $[M]^+$.

*5.2.6. Reduction procedure for unsubstituted ester at α position **(11a)***

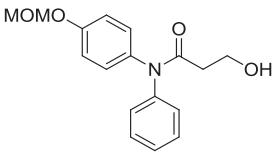

To a stirred solution of amide compound **4** (0.175 gr, 0.53 mmol) in dry THF (3 mL) $NaBH_4$ (0.022 gr, 0.58 mmol) was added at 0 °C the reaction mixture was slowly warmed to rt and stirring was continued overnight. After completion of starting material the reaction mixture was filtered and concentrated under reduced pressure to give crude product, the crude product was dissolved in DCM then washed with brine and the organic layer was dried over anhydrous Na_2SO_4. The solvent was removed under reduced pressure, and the crude product was subjected to flash column chromatography (50% ethyl acetate-hexane) to give mono reductive compound **11a** (0.124, 78%) as white dense liquid; ^1H NMR (600 MHz, $CDCl_3$) δ 7.37 (d, $J = 44.7$ Hz, 2H), 7.28 (d, $J = 7.5$ Hz, 2H), 7.20 (d, $J = 8.4$ Hz, 2H), 7.04 (d, $J = 28.2$ Hz, 2H), 5.16 (d, $J = 19.2$ Hz, 2H), 3.84 (dd, $J = 11.4$, 5.7 Hz, 2H), 3.47 (d, $J = 18.2$ Hz, 3H),

3.40–3.35 (bs, 1H), 2.49 (t, $J = 5.3$ Hz, 2H); ^{13}C NMR (150 MHz, $CDCl_3$) δ 173.10, 156.83, 142.20, 135.92, 129.84, 129.65, 128.90, 128.36, 127.58, 126.29, 126.10, 117.25, 116.60, 94.36, 58.71, 56.10, 37.16 ppm; ESI-MS: $m/z = 302$ $[M+H]^+$.

*5.2.7. 2-(4-Bromobenzyl)-3-hydroxy-N-(4-hydroxyphenyl)–N-phenylpropanamide **(2j)***

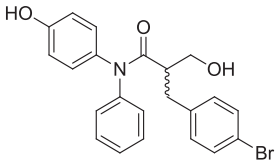

To stirred solution of above reductive compound **11j** (0.170 gr, 0.40 mmol) in 1:1 ACN and DCM (8 mL) was added NaI (0.600 gr, 4.10 mmol) followed by TMSCl (0.5 mL, 4.10 mmol) was added dropwise at 0 °C, the reaction mixture was stirred for additional 1 h at room temperature. The reaction was quenched with saturated $Na_2S_2O_3$ solution at 0 °C and the aqueous layer was extracted with DCM (2 × 25 mL), the combined organic layer was dried over anhydrous Mg_2SO_4. The solvent was removed under reduced pressure, and the crude product was subjected to flash column chromatography (60% ethyl acetate-hexane) to give MOM deprotected compound **2j** (0.146 gr, 95%) as white solid; M.P.:175.2–176.1 °C, IR (neat): bs 3500, 2962, 2936, 2905, 2847, 1709, 1640, 1592, 1450, 1265, 1030, 762 cm^{-1}, ^{1}H NMR (600 MHz, MeOD) δ 7.47 (d, $J = 7.0$ Hz, 2H), 7.32–7.23 (m, 3H), 7.17 (t, $J = 7.0$ Hz, 1H), 7.09 (d, $J = 7.5$ Hz, 1H), 7.00 (dd, $J = 21.1$, 7.4 Hz, 2H), 6.91 (d, $J = 7.8$ Hz, 1H), 6.77–6.56 (m, 3H), 3.86 (t, $J = 8.9$ Hz, 1H), 3.58 (t, $J = 8.9$ Hz, 1H), 3.13–2.99 (m, 1H), 2.83–2.74 (m, 1H), 2.74–2.65 (m, 1H); ^{13}C NMR (150 MHz, MeOD) δ 176.34, 158.48, 144.41, 139.92, 135.08, 132.58 (2 C), 132.43, 130.99, 130.51, 129.99, 129.71, 129.18, 128.87, 127.81, 127.65, 121.30, 116.95, 116.63, 64.87, 49.28, 36.24 ppm; HRMS-ESI (m/z): Calculated for $C_{22}H_{21}NO_3Br$ $(M+H)^+$: 426.0705, Found: 426.0708.

*5.3. MOM deprotection procedure for **11c**, **11d** and **11e** compounds*

To a stirred solution of compound **11c** (0.180 gr, 0.52 mmol) in Dimethyl sulphide (3 mL) BF_3Et_2O (0.42 mL, 1.58 mmol) was added dropwise at 0 °C then starring was allowed to additional 15–20 min at same temperature and monitored by TLC. After completion of starting material the reaction mixture was concentrated under reduced pressure (the water bath temperature was maintained below 15 °C) to give a residue, which was dissolved in DCM and washed with saturated $NaHCO_3$, the aqueous layer was extracted two time with DCM (2 × 20 mL) and the combined organic layer was dried over Mg_2SO_4. The removal of solvent to give crude product, which was subjected flash column chromatography to afford MOM deprotected compound **2c** (0.122, 78%) as white solid.

*5.3.1. 3-(4-Bromobenzyl)-5-phenyl-1-oxa-5-azaspiro [5.5] undeca-7, 10-diene-4, 9-dione **(1j)***

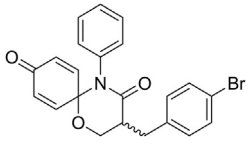

To stirred solution of MOM deprotected compound **2j** (0.030 gr, 0.07 mmol) in anhydrous ACN (10 mL) anhydrous powered K_2CO_3 was added at 0 °C then stirred the reaction mixture at same temperature for 30 min. The reaction mixture was allowed to stir at rt additional 45 min to 1 h, again the reaction mixture taken to 0 °C then added slowly drop wise the solution of [Bis (trifluoroacetoxy) iodo] benzene (PIFA) (0.0 gr, 0.07 mmol) in anhydrous ACN (2 mL), the light brown reaction mixture was allowed to rt and stirring was continued 3–4 h, monitored by TLC. After completion of starting material the reaction mixture was filtered through filter paper and concentrated under reduced pressure, the crude product was dissolved in DCM (15 mL) and quenched with ice-pieces extracted with DCM (2 × 15 mL) the combined organic layer was washed with brine solution and dried over anhydrous Na_2SO_4. The solvent was removed under reduced pressure, temperature was maintained below 20 °C, the crude product was subjected to column chromatography (10, 15 and 25% ethyl acetate-hexane) to afford cyclised spiro compound **1j** (0.022 gr, 75%) as light yellow dense liquid. White liquid, 74% yield; purity 98.6%; IR (neat): 2990, 2968, 2860, 1715, 1589, 1445, 1358, 1228, 1090, 747, cm^{-1}; ^{1}H NMR (600 MHz, $CDCl_3$) δ 7.61 (d, $J = 7.8$ Hz, 2H), 7.41 (d, $J = 7.8$ Hz, 2H), 7.37–7.29 (m, 3H), 7.05–6.98 (s, 2H), 6.93 (dd, $J = 10.1$, 2.3 Hz, 1H), 6.78–6.71 (m, 1H), 6.05 (d, $J = 10.4$ Hz, 2H), 4.19 (dd, $J = 12.2$, 4.9 Hz, 1H), 4.02 (dd, $J = 12.2$, 6.5 Hz, 1H), 3.37 (dd, $J = 13.4$, 2.9 Hz, 1H), 3.17–3.02 (m, 2H); ^{13}C NMR (150 MHz, $CDCl_3$) δ 183.79, 169.40, 143.57, 143.29, 142.34, 136.26, 129.91, 129.84, 129.70, 129.41, 129.35, 129.20, 129.16, 129.13, 128.98, 125.66, 125.63, 123.23, 83.33, 62.96, 43.36, 34.68 ppm; HRMS-ESI (m/z): Calculated for $C_{22}H_{19}NO_3Br$ $(M+H)^+$: 423.0587, Found: 423.0591.

*5.3.2. 3-hydroxy-N-(4-hydroxyphenyl)–N-phenylpropanamide **(2a)***

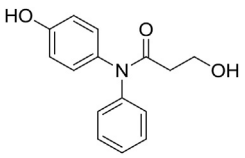

White solid; 89% yield; M.P.:110.2–110.9 °C; IR (neat): bs 3500, 2978, 2933, 2879, 1703, 1640, 1591, 1374, 1265, 1028, 862, 695 cm^{-1}, ^{1}H NMR (600 MHz, $CDCl_3$) δ 7.39 (d, $J = 49.2$ Hz, 2H), 7.29 (s, 1H), 7.11 (s, 2H), 6.84–6.57 (m, 3H), 3.88 (t, $J = 5.4$ Hz, 2H), 3.64–3.47 (bs 1H), 2.52 (t, $J = 5.3$ Hz, 2H); ^{13}C NMR (150 MHz, $CDCl_3$) δ 173.53, 156.11, 142.40, 134.40, 129.94, 129.69, 128.99, 128.15, 127.85, 126.41, 126.09, 116.65, 116.18, 58.79, 37.08 ppm; HRMS-ESI (m/z): Calculated for $C_{15}H_{15}NO_3$ $(M+H)^+$: 257.1126, Found: 257.1129.

*5.3.3. 5-Phenyl-1-oxa-5-azaspiro [5.5] undeca-7, 10-diene-4, 9-dione **(1a)***

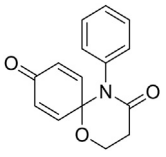

White liquid; 91% yield; purity 97.8%; IR (neat): 2975, 2969, 2849, 1730, 1452, 1418, 1260, 1055, 763, cm^{-1}; ^{1}H NMR (600 MHz, $CDCl_3$) δ 7.37–7.29 (m, 3H), 7.09–7.04 (m, 2H), 7.02–6.93 (m, 2H), 6.09 (d, $J = 10.2$ Hz, 2H), 4.33 (t, $J = 6.0$ Hz, 2H), 2.85 (t, $J = 6.0$ Hz, 2H); ^{13}C NMR (150 MHz, $CDCl_3$) δ 183.94, 167.19, 143.71 (2 C), 136.32, 129.87 (2 C), 129.81 (2 C), 129.14, 129.09, 129.02, 83.07,

60.26, 32.82 ppm; HRMS-ESI (*m/z*): Calculated for $C_{15}H_{14}NO_3$ $(M+H)^+$: 256.0974, Found: 256.0967.

5.3.4. Methyl 3-((4-(methoxymethoxy) phenyl) (phenyl) amino)-2-methyl-3-oxopropanoate ***(10b)***

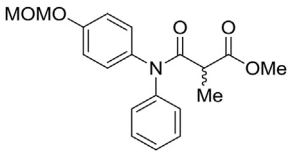

^{1}H NMR (600 MHz, $CDCl_3$) δ 7.47–7.27 (m, 4H), 7.26–6.93 (m, 5H), 5.16 (d, J = 29.5 Hz, 2H), 3.69 (s, 3H), 3.65–3.57 (m, 1H), 3.46 (d, J = 26.6 Hz, 3H), 1.41 (d, J = 7.1 Hz, 3H); ^{13}C NMR (150 MHz, $CDCl_3$) δ 170.94, 170.21, 156.76, 142.34, 135.96, 129.65, 128.67, 128.35, 127.96, 127.38, 125.96, 119.68, 117.12, 116.39, 94.24, 56.00, 52.19, 44.18, 13.97 ppm; ESI-MS: *m/z* = 344 $[M+H]^+$.

5.3.5. 3-Hydroxy-N-(4-(methoxymethoxy) phenyl)-2-methyl-N-phenylpropanamide ***(11b)***

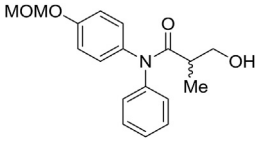

^{1}H NMR (600 MHz, $CDCl_3$) δ 7.47–7.29 (m, 4H), 7.24–6.96 (m, 5H), 5.16 (d, J = 23.1 Hz, 2H), 3.72 (dd, J = 8.5, 4.5 Hz, 2H), 3.47 (d, J = 23.0 Hz, 3H), 2.93–2.83 (bs, 2H), 1.13 (d, J = 7.0 Hz, 3H); ^{13}C NMR (151 MHz, $CDCl_3$) δ 176.91, 142.63, 136.22, 129.80 (2 C), 128.97 (2 C), 128.52, 127.77, 126.38, 119.91, 117.25, 116.66, 94.47, 65.14, 56.04, 39.00, 14.30 ppm; ESI-MS: *m/z* = 316 $[M+H]^+$.

5.3.6. 3-Hydroxy-N-(4-hydroxyphenyl)-2-methyl-N-phenylpropanamide ***(2b)***

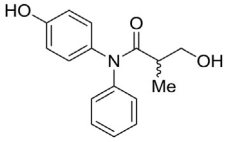

White solid; 85% yield; M.P.:163.7–164.8 °C; IR (neat): bs 3490, 2952, 2945, 2915, 2875, 1640, 1593, 1511, 1462, 1405, 1229, 1024, 833, 695 cm^{-1};^{1}H NMR (600 MHz, MeOD) δ 7.51–7.06 (m, 7H), 6.91–6.67 (m, 2H), 3.79 (dd, J = 10.4, 8.5 Hz, 1H), 3.44 (dd, J = 10.0, 5.5 Hz, 1H), 2.87 (dd, J = 16.7, 10.2 Hz, 1H), 1.05 (d, J = 6.9 Hz, 3H); ^{13}C NMR (150 MHz, MeOD) δ 178.16, 158.57, 144.51, 135.54, 130.83, 129.89, 129.51, 129.27, 128.88, 127.82, 127.40, 117.21, 116.54, 65.85, 41.23, 14.56 ppm; HRMS-ESI (*m/z*): Calculated for $C_{16}H_{18}NO_3$ $(M+H)^+$: 272.1287, Found: 272.1285.

5.3.7. 3-Methyl-5-phenyl-1-oxa-5-azaspiro [5.5] undeca-7, 10-diene-4, 9-dione ***(1b)***

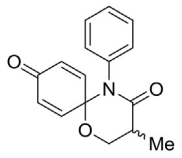

White liquid; 85% yield; purity 98.4%; IR (neat): 2958, 2920, 2856, 1679, 1630, 1585, 1490, 1396, 1350, 1072, 916, 760, 697 cm^{-1}; ^{1}H NMR (600 MHz, $CDCl_3$) δ 7.55 (d, J = 8.0 Hz, 1H), 7.40–7.30 (m, 3H), 7.11–7.05 (m, 2H), 6.94 (dd, J = 10.2, 3.2 Hz, 1H), 6.12 (dd, J = 10.2, 2.0 Hz, 1H), 6.08 (dd, J = 10.2, 2.0 Hz, 1H), 4.32 (dd, J = 11.9, 5.5 Hz, 1H), 4.06 (dd, J = 11.9, 7.8 Hz, 1H), 2.98–2.88 (m, 1H), 1.39 (d, J = 7.2 Hz, 3H); ^{13}C NMR (150 MHz, $CDCl_3$) δ 184.09, 171.21, 144.51, 143.52, 136.60, 130.05, 129.81, 129.79, 129.17, 129.11, 129.05, 120.02, 83.53, 66.14, 37.29, 13.72 ppm; HRMS-ESI (*m/z*): Calculated for $C_{16}H_{15}NO_3(M+H)^+$: 269.1065, Found: 269.1061.

5.3.8. Methyl 2-((4-(methoxymethoxy) phenyl) (phenyl) carbamoyl) pent-4-enoate ***(10c)***

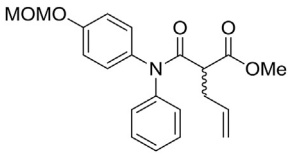

^{1}H NMR (600 MHz, $CDCl_3$) δ 7.44–7.25 (m, 4H), 7.23–7.11 (m, 3H), 7.04 (d, J = 8.1 Hz, 1H), 6.96 (d, J = 8.0 Hz, 1H), 5.78–5.68 (m, 1H), 5.20–5.09 (m, 3H), 5.06 (d, J = 10.1 Hz, 1H), 3.68 (s, 3H), 3.65–3.57 (m, 1H), 3.44 (d, J = 31.6 Hz, 3H), 2.79–2.69 (m, 1H), 2.61 (dd, J = 13.0, 6.3 Hz, 1H); ^{13}C NMR (151 MHz, $CDCl_3$) δ 169.78, 168.69, 156.76, 142.38, 135.86, 134.32, 129.95, 129.63, 128.67, 127.96, 127.41, 126.06, 126.01, 117.55, 117.02, 116.38, 94.26, 56.02, 52.24, 49.29, 33.61 ppm; ESI-MS: *m/z* = 370 $[M+H]^+$.

5.3.9. 2-(Hydroxymethyl)–N-(4-(methoxymethoxy) phenyl)–N-phenylpent-4-enamide ***(11c)***

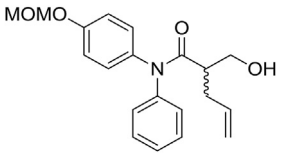

^{1}H NMR (600 MHz, $CDCl_3$) δ 7.47–7.40 (m, 1H), 7.39–7.29 (m, 3H), 7.28–7.15 (m, 3H), 7.08 (d, J = 8.1 Hz, 1H), 7.02 (d, J = 8.1 Hz, 1H), 5.75–5.62 (m, 1H), 5.25–5.04 (m, 4H), 3.84–3.75 (m, 2H), 3.49 (d, J = 29.0 Hz, 3H), 2.95–2.83 (m, 2H), 2.51–2.42 (m, 1H), 2.36–2.28 (m, 1H); ^{13}C NMR (150 MHz, $CDCl_3$) δ 175.63, 156.82, 142.68, 135.05, 130.10, 129.82, 129.01, 128.84, 127.96, 127.85, 126.49, 126.43, 117.41, 117.23, 116.71, 94.53, 63.45, 56.27, 43.90, 33.86 ppm; ESI-MS: *m/z* = 342 $[M+H]^+$.

*5.3.10. 2-(Hydroxymethyl)–N-(4-hydroxyphenyl)–N-phenylpent-4-enamide **(2c)***

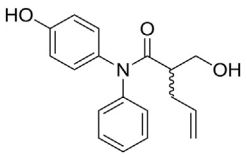

White solid; 74% yield; M.P.:140.2–141.1 °C; IR (neat): bs 3500, 2960, 2924, 2868, 1639, 1591, 1511, 1491, 1264, 1230, 834, 725 cm^{-1}; ^1H NMR (600 MHz, MeOD) δ 7.45–7.30 (m, 3H), 7.26 (s, 1H), 7.19 (d, $J = 7.4$ Hz, 2H), 7.07 (d, $J = 8.4$ Hz, 1H), 6.82 (d, $J = 8.5$ Hz, 1H), 6.74 (d, $J = 8.4$ Hz, 1H), 5.78–5.67 (m, 1H), 5.11–5.04 (t, $J = 12.4$ Hz, 2H), 3.80 (dd, $J = 10.5$, 8.5 Hz, 1H), 3.53 (dd, $J = 10.4$, 5.4 Hz, 1H), 3.02–2.86 (m, 1H), 2.38–2.26 (m, 1H), 2.21–2.13 (m, 1H); ^{13}C NMR (151 MHz, MeOD) δ 176.79, 158.51, 144.57, 136.51, 135.38, 131.25, 130.62, 129.88 (2 C), 129.27, 127.87 (2 C), 117.41, 117.06, 116.53, 64.49, 46.45, 35.14 ppm; HRMS-ESI (*m/z*): Calculated for $C_{19}H_{22}NO_3$ $(M+H)^+$: 312.1600, Found: 312.1600.

*5.3.11. 3-Allyl-5-phenyl-1-oxa-5-azaspiro [5.5] undeca-7, 10-diene-4, 9-dione **(1c)***

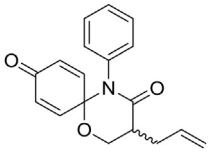

White liquid; 80% yield; purity 97.7%; IR (neat): 2956, 2920, 2850, 1678, 1634, 1492, 1391, 1354, 1093, 1071, 916, 760, 697 cm^{-1}; ^1H NMR (600 MHz, $CDCl_3$) δ 7.34–7.29 (m, 3H), 7.06–7.03 (m, 2H), 7.01 (dd, $J = 10.2$, 3.2 Hz, 1H), 6.95 (dd, $J = 10.2$, 3.2 Hz, 1H), 6.12–6.03 (m, 2H), 5.91–5.80 (m, 1H), 5.23–5.14 (m, 2H), 4.29 (dd, $J = 12.2$, 5.5 Hz, 1H), 4.13 (dd, $J = 12.2$, 7.0 Hz, 1H), 2.89–2.81 (m, 1H), 2.75–2.69 (m, 1H), 2.57–2.50 (m, 1H); ^{13}C NMR (150 MHz, $CDCl_3$) δ 183.84, 169.72, 143.89, 143.52, 136.34, 135.13, 134.44, 129.76, 129.64, 128.97, 128.87, 124.29, 119.91, 118.19, 117.60, 83.11, 63.33, 41.24, 33.09 ppm; HRMS-ESI (*m/z*): Calculated for $C_{24}H_{20}NO_3F_6$ $(M+H)^+$: 310.1443, Found: 310.1440.

*5.3.12. Methyl 2-((4-(methoxymethoxy) phenyl) (phenyl) carbamoyl)-4-methylpent-4-enoate **(10d)***

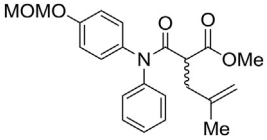

^1H NMR (600 MHz, $CDCl_3$) δ 7.45–6.95 (m, 9H), 5.15 (d, $J = 32.3$ Hz, 2H), 4.81 (d, $J = 22.3$ Hz, 2H), 3.79–3.65 (m, 4H), 3.46 (d, $J = 27.7$ Hz, 3H), 2.79 (s, 1H), 2.57 (d, $J = 13.7$ Hz, 1H), 1.59 (t, $J = 17.9$ Hz, 3H); ^{13}C NMR (150 MHz, $CDCl_3$) δ 170.28, 169.05, 156.92, 142.70, 141.89, 136.11, 130.07, 129.83, 128.88, 128.78, 128.11, 127.68, 126.27, 117.23, 116.59, 113.10, 94.48, 56.21, 52.50, 48.35, 37.46, 22.49 ppm; ESI-MS: $m/z = 384$ $[M+H]^+$.

*5.3.13. 2-(Hydroxymethyl)–N-(4-(methoxymethoxy) phenyl)-4-methyl-N-phenylpent-4-enamide **(11d)***

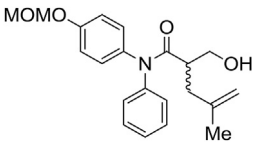

^1H NMR (600 MHz, $CDCl_3$) δ 7.51–6.88 (m, 9H), 5.15 (d, $J = 22.2$ Hz, 2H), 4.82–4.74 (m, 1H), 3.75 (s, 2H), 3.46 (d, $J = 12.8$ Hz, 3H), 3.02–2.94 (m, 1H), 2.91–282 (m, 1H), 2.48–2.40 (m, 1H), 2.28–2.19 (m, 1H), 1.40 (d, $J = 31.7$ Hz, 3H); ^{13}C NMR (150 MHz, $CDCl_3$) δ 175.95, 155.60, 142.68, 142.04, 136.52, 130.09 (2 C), 129.76, 128.98 (2 C), 128.82, 127.88, 127.84 (2 C), 126.48, 126.39, 117.20, 116.68, 113.34, 94.46, 63.39, 56.14, 42.29, 37.65, 21.99 ppm; ESI-MS: $m/z = 356$ $[M+H]^+$.

*5.3.14. 2-(Hydroxymethyl)–N-(4-hydroxyphenyl)-4-methyl-N-phenylpent-4-enamide **(2d)***

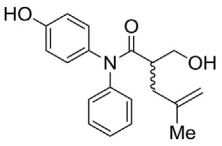

White solid; 74% yield; M.P.:149.2–150.4 °C; IR (neat): bs 3495, 2962, 2926, 1703, 1635, 1511, 1231, 1024, 833, 694 cm^{-1}; ^1H NMR (600 MHz, MeOD) δ 7.44–7.36 (m, 1H), 7.34–7.29 (m, 2H), 7.26–7.13 (m, 3H), 7.07 (d, $J = 8.5$ Hz, 1H), 6.83 (d, $J = 8.5$ Hz, 1H), 6.75 (d, $J = 8.5$ Hz, 1H), 4.82–4.78 (m, 1H), 4.75 (d, $J = 8.0$ Hz, 1H), 3.81 (t, $J = 9.5$ Hz, 1H), 3.52–3.48 (m, 1H), 3.11–3.01 (m, 1H), 2.42–3.24 (m, 1H), 2.12–2.02 (m, 1H), 1.49 (d, $J = 33.9$ Hz, 3H); ^{13}C NMR (150 MHz, MeOD) δ 177.32, 158.66, 144.81, 144.10, 135.54, 131.43, 130.81, 130.09, 129.50, 128.98, 128.10, 127.68, 117.27, 116.74, 113.58, 64.83, 45.09, 39.22, 22.63 ppm; HRMS-ESI (*m/z*): Calculated for $C_{19}H_{22}NO_3$ $(M+H)^+$: 312.1600, Found: 312.1604.

*5.3.15. 3-(2-Methylallyl)-5-phenyl-1-oxa-5-azaspiro [5.5] undeca-7, 10-diene-4,9-dione **(1d)***

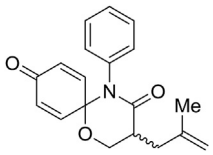

Light yellow liquid; 80% yield; purity 98.6%; IR (neat): 2950, 2921, 2856, 1679, 1674, 1443, 1390, 1353, 939, 760, 696 cm^{-1}; ^1H NMR (600 MHz, $CDCl_3$) δ 7.32–7.29 (m, 3H), 7.06–7.02 (m, 2H), 7.01 (dd, $J = 10.0$, 3.2 Hz, 1H), 6.97 (dd, $J = 10.0$, 3.1 Hz, 1H), 6.11–6.05 (m, 2H), 4.86 (d, $J = 44.8$ Hz, 2H), 4.25 (dd, $J = 12.2$, 5.2 Hz, 1H), 4.08 (dd, $J = 12.2$, 6.6 Hz, 1H), 2.95–2.88 (m, 1H), 2.78 (dd, $J = 14.1$, 3.7 Hz, 1H), 2.41 (dd, $J = 14.0$, 11.0 Hz, 1H), 1.79 (s, 3H); ^{13}C NMR (150 MHz, $CDCl_3$) δ 183.95, 170.25, 143.97, 143.73, 141.82, 136.49, 129.90, 129.75, 129.06, 128.94, 113.59, 83.23, 77.25, 77.04, 76.83, 63.35, 39.85, 37.10, 21.92 ppm; HRMS-ESI (*m/z*): Calculated for $C_{24}H_{20}NO_3F_6$ $(M+H)^+$: 310.1443, Found: 310.1449.

*5.3.16. Methyl 2-((4-(methoxymethoxy) phenyl) (phenyl) carbamoyl) hex-5-enoate **(10e)***

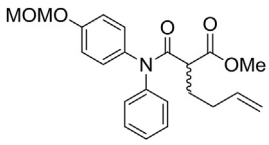

^{1}H NMR (600 MHz, $CDCl_3$) δ 7.44–7.26 (m, 4H), 7.24-7-15 (m, 3H), 7.06 (d, J = 8.0 Hz, 1H), 6.99 (d, J = 7.6 Hz, 1H), 5.72–5.62 (m, 1H), 5.22–5.09 (m, 2H), 5.04–4.87 (m, 2H), 3.70 (s, 3H), 3.59–3.52 (m, 1H), 3.46 (d, J = 29.3 Hz, 3H), 2.16–1.96 (m, 4H); ^{13}C NMR (150 MHz, $CDCl_3$) δ 170.40, 169.18, 156.89, 142.52, 137.24, 129.99, 129.77, 128.81, 128.71, 128.11, 127.51, 126.17, 126.10, 117.17, 116.52, 115.56, 94.38, 56.12, 52.31, 49.14, 31.38, 28.68 ppm; ESI-MS: m/z = 384 $[M+H]^+$.

*5.3.17. 2-(Hydroxymethyl)–N-(4-(methoxymethoxy) phenyl)–N-phenylhex-5-enamide **(11e)***

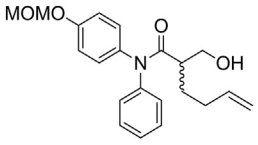

^{1}H NMR (600 MHz, $CDCl_3$) δ 7.40 (d, J = 7.1 Hz, 1H), 7.36–7.27 (m, 2H), 7.26–7.12 (m, 4H), 7.03 (dd, J = 36.7, 8.1 Hz, 2H), 5.64–5.50 (m, 1H), 5.15 (d, J = 28.8 Hz, 2H), 4.97–4.83 (m, 2H), 3.80–3.71 (m, 2H), 3.46 (d, J = 27.0 Hz, 3H), 2.93–2.75 (m, 2H), 2.05–1.95 (m, 1H), 1.78 (s, 1H), 1.74–1.63 (m, 1H); ^{13}C NMR (150 MHz, $CDCl_3$) δ 176.33, 156.78, 142.64, 137.60, 137.53, 136.46, 130.03, 129.82, 129.00, 128.77, 127.93, 127.79, 117.24, 116.70, 115.26, 94.48, 63.19, 56.20, 43.38, 31.18, 28.38 ppm; ESI-MS: m/z = 356 $[M+H]^+$.

*5.3.18. 2-(Hydroxymethyl)–N-(4-hydroxyphenyl)–N-phenylhex-5-enamide **(2e)***

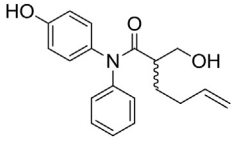

White solid; 74% yield; M.P.:140.2–141.1 °C; IR (neat): bs 3500, 2960, 2924, 2868, 1639, 1591, 1511, 1491, 1264, 1230, 834, 725 cm^{-1}; ^{1}H NMR (600 MHz, MeOD) δ 7.46–7.31 (m, 3H), 7.24–7.17 (d, J = 7.7 Hz, 1H), 7.24–7.17 (d, J = 7.3 Hz, 2H), 7.09 (d, J = 8.4 Hz, 1H), 6.83 (d, J = 8.5 Hz, 1H), 6.75 (d, J = 8.4 Hz, 1H), 5.75–5.65 (m, 1H), 4.97 (t, J = 15.1 Hz, 1H), 4.90 (d, J = 10.7 Hz, 1H), 3.79 (dd, J = 10.5, 8.3 Hz, 1H), 3.54 (dd, J = 10.3, 5.5 Hz, 1H), 2.95–2.82 (m, 1H), 2.13–1.96 (m, 2H), 1.74–1.68 (m, 1H), 1.55–1.45 (m, 1H); ^{13}C NMR (150 MHz, MeOD) δ 177.41, 158.54, 144.62, 139.04, 135.41, 135.34, 131.22, 130.67, 129.92, 129.26, 127.87, 127.46, 117.10, 116.57, 115.42, 64.70, 46.14, 32.51, 30.11 ppm; HRMS-ESI (m/z): Calculated for $C_{19}H_{22}NO_3$ $(M+H)^+$: 312.1600, Found: 312.1600.

*5.3.19. 3-(But-3-en-1-yl)-5-phenyl-1-oxa-5-azaspiro [5.5] undeca-7, 10-diene-4, 9-dione **(1e)***

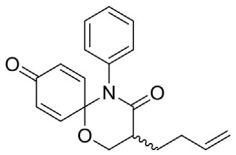

White liquid; 80% yield; purity 98.4%; IR (neat): 2956, 2920, 2850, 1678, 1634, 1492, 1391, 1354, 1093, 1071, 916, 760, 697 cm^{-1}; ^{1}H NMR (600 MHz, $CDCl_3$) δ 7.33–7.29 (m, 3H), 7.07–7.02 (m, 2H), 7.01 (dd, J = 10.2, 3.2 Hz, 1H), 6.95 (dd, J = 10.2, 3.2 Hz, 1H), 6.11–6.02 (m, 2H), 5.88–5.80 (m, 1H), 5.13–5.09 (m, 1H), 5.06–5.03 (m, 1H), 4.32 (dd, J = 12.0, 5.3 Hz, 1H), 4.11 (dd, J = 12.1, 6.9 Hz, 1H), 2.79 (m, 1H), 2.32–2.19 (m, 2H), 2.17–2.07 (m, 1H), 1.83–1.75 (m, 1H); ^{13}C NMR (150 MHz, $CDCl_3$) δ 183.76, 170.25, 143.88, 143.47, 137.22, 136.31, 129.74 (2 C), 129.55, 129.51, 128.87 (2 C), 128.74, 115.60, 82.97, 63.78, 41.13, 30.94, 27.80 ppm; HRMS-ESI (m/z): Calculated for $C_{24}H_{20}NO_3F_6$ $(M+H)^+$: 310.1443, Found: 310.1440.

*5.3.20. Methyl 2-benzyl-3-((4-(methoxymethoxy) phenyl) (phenyl) amino)-3-oxopropanoate **(10f)***

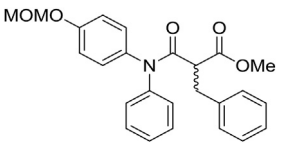

^{1}H NMR (600 MHz, $CDCl_3$) δ 7.34–7.22 (m, 6H), 7.18–7.07 (m, 4H), 7.00 (d, J = 8.8 Hz, 1H), 6.97–6.69 (m, 3H), 5.13 (d, J = 23.5 Hz, 2H), 3.83–3.71 (m, 4H), 3.45 (d, J = 31.8 Hz, 3H), 3.38–3.29 (m, 1H), 3.23–3.10 (m, 1H); ^{13}C NMR (150 MHz, $CDCl_3$) δ 169.65, 168.64, 156.60, 142.21, 138.05, 135.72, 131.34, 129.75, 129.33 (2 C), 128.65, 128.46, 128.28, 127.76, 127.36, 126.61, 126.12, 125.99, 116.71, 116.33, 94.22, 55.99, 52.36, 51.30, 35.22 ppm; ESI-MS: m/z = 420 $[M+H]^+$.

*5.3.21. 2-Benzyl-3-hydroxy-N-(4-(methoxymethoxy) phenyl)–N-phenylpropanamide **(11f)***

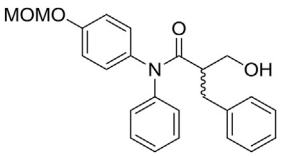

^{1}H NMR (600 MHz, $CDCl_3$) δ 7.33–7.24 (m, 5H), 7.20–7.10 (m, 2H), 7.09–7.00 (m, 3H), 6.95 (dd, J = 23.6, 8.6 Hz, 2H), 6.76 (d, J = 55.1 Hz, 2H), 5.14 (d, J = 23.5 Hz, 2H), 3.83–3.72 (m, 2H), 3.46 (d, J = 30.4 Hz, 3H), 3.12–3.04 (m, 1H), 3.01–2.95 (m, 1H), 2.94–2.90 (bs, 1H), 2.85–2.71 (m, 1H); ^{13}C NMR (151 MHz, $CDCl_3$) δ 175.38, 155.55, 142.40, 138.93, 129.84, 129.53, 129.31, 129.28, 128.98, 128.90, 128.59, 128.38 (2 C), 127.79, 127.67, 126.50, 126.39, 126.34, 116.95, 116.58, 94.39, 63.54, 56.11, 46.32, 35.60 ppm; ESI-MS: m/z = 392 $[M+H]^+$.

*5.3.22. 2-Benzyl-3-hydroxy-N-(4-hydroxyphenyl)–N-phenylpropanamide **(2f)***

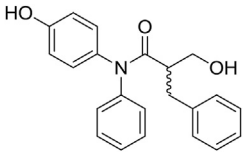

White solid; 74% yield; M.P.:148.5–149.4 °C; IR (neat): bs 3485, 2965, 3027, 2957, 2929, 2874, 2851, 1630, 1512, 1407, 1324, 1101, 966, 727 cm^{-1}; ^1H NMR (600 MHz, MeOD) δ 7.39–7.23 (m, 6H), 7.19 (t, $J = 7.3$ Hz, 1H), 7.15–7.06 (m, 4H), 6.92 (d, $J = 8.7$ Hz, 1H), 6.78–6.61 (m, 2H), 3.92–3.86 (m, 1H), 3.63–3.59 (m, 1H), 3.16–3.03 (m, 1H), 2.87–2.80 (m, 1H), 2.78–2.70 (m, 1H); ^{13}C NMR (151 MHz, MeOD) δ 175.24, 156.99, 143.11, 139.21, 133.77, 129.68, 129.11, 129.09, 129.00, 128.53, 128.41, 128.12, 127.81, 127.36, 126.47, 126.23, 126.20, 115.43, 115.15, 63.61, 48.10, 35.57 ppm; HRMS-ESI (m/z): Calculated for $C_{22}H_{22}NO_3$ $(M+H)^+$: 348.1600, Found: 348.1595.

*5.3.23. 3-Benzyl-5-phenyl-1-oxa-5-azaspiro [5.5] undeca-7, 10-diene-4, 9-dione **(1f)***

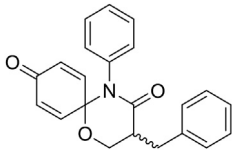

White liquid; 80% yield; purity 97.9%; IR (neat): 2989, 2969, 2862, 1715, 1590, 1438, 1348, 1220, 1086, 747, cm^{-1}; ^1H NMR (600 MHz, $CDCl_3$) δ 7.39–7.26 (m, 8H), 7.05–7.01 (m, 2H), 6.92 (dd, $J = 10.4$, 3.2 Hz, 1H), 6.66 (dd, $J = 10.4$, 3.2 Hz, 1H), 6.05–5.99 (m, 1H), 4.18 (dd, $J = 12.2$, 5.2 Hz, 1H), 4.06 (dd, $J = 12.2$, 6.4 Hz, 1H), 3.29 (dd, $J = 13.2$, 3.5 Hz, 1H), 3.16–3.01 (m, 2H); ^{13}C NMR (151 MHz, $CDCl_3$) δ 183.87, 169.67, 143.76, 143.57, 138.02, 136.42, 129.84, 129.72, 129.68, 129.40, 129.06, 128.97, 128.93, 128.90, 128.78, 128.67, 126.87, 120.08, 83.16, 63.10, 43.37, 34.94 ppm; HRMS-ESI (m/z): Calculated for $C_{22}H_{20}NO_3$ $(M+H)^+$: 346.1425, Found: 346.1420.

*5.3.24. Methyl 2-(4-fluorobenzyl)-3-((4-(methoxymethoxy) phenyl)(phenyl)amino)-3-oxopropanoate **(10g)***

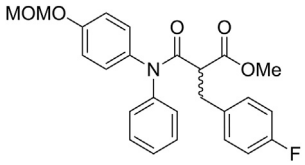

^1H NMR (400 MHz, cdcl$_3$) δ 7.32–7.26 (m, 2H), 7.20–7.06 (m, 4H), 7.05–6.67 (m, 7H), 5.13 (d, $J = 16.7$ Hz, 2H), 3.80–3.70 (m, 4H), 3.46 (d, $J = 21.6$ Hz, 3H), 3.31 (t, $J = 12.0$ Hz, 1H), 3.19–3.10 (m, 1H); ^{13}C NMR (150 MHz, $CDCl_3$) δ 169.71, 168.66, 161.09, 156.92, 142.33, 133.98, 131.05, 131.00, 129.91, 129.66, 128.93, 128.63, 128.13, 127.51, 126.43, 126.15, 117.03, 116.60, 115.33, 115.19, 94.45, 56.24, 52.62, 51.57, 34.55 ppm; ESI-MS: $m/z = 438$ $[M+H]^+$.

*5.3.25. 2-(4-Fluorobenzyl)-3-hydroxy-N-(4-(methoxymethoxy) phenyl)–N-phenylpropanamide **(11g)***

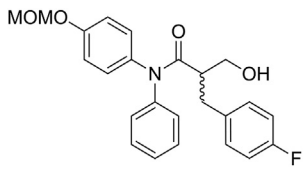

^1H NMR (600 MHz, $CDCl_3$) δ 7.30 (t, $J = 7.3$ Hz, 3H), 7.17 (t, $J = 7.4$ Hz, 1H), 7.11 (d, $J = 7.7$ Hz, 1H), 7.02 (dd, $J = 17.3$, 7.2 Hz, 2H), 6.99–6.77 (m, 6H), 5.14 (d, $J = 26.4$ Hz, 2H), 3.79 (d, $J = 9.8$ Hz, 1H), 3.76–3.70 (bs, 1H), 3.46 (d, $J = 31.9$ Hz, 3H), 3.08–2.87 (m, 3H), 2.83–2.70 (m, 1H); ^{13}C NMR (150 MHz, $CDCl_3$) δ 175.23, 162.54, 156.75, 142.36, 135.96, 134.65, 130.80, 130.75, 129.84, 129.66, 128.99, 128.59, 127.67, 126.51, 126.33, 117.08, 116.66, 115.25, 115.11, 94.45, 63.36, 56.19, 46.40, 34.71 ppm; ESI-MS: $m/z = 410$ $[M+H]^+$.

*5.3.26. 2-(4-Fluorobenzyl)-3-hydroxy-N-(4-hydroxyphenyl)–N-phenylpropanamide **(2g)***

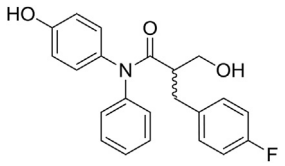

White solid; 77% yield; M.P.:140.2–141.5 °C; IR (neat): bs 3495, 3057, 2967, 2855, 1751, 1663, 1360, 1221, 726 cm^{-1}; ^1H NMR (600 MHz, MeOD) δ 7.32–7.24 (m, 3H), 7.17 (t, $J = 7.2$ Hz, 1H), 7.13–6.98 (m, 6H), 6.91 (d, $J = 8.3$ Hz, 1H), 6.75–6.58 (m, 2H), 3.86 (t, $J = 8.9$ Hz, 1H), 3.58 (t, $J = 8.9$ Hz, 1H), 3.12–2.99 (m, 1H), 2.85–2.77 (m, 1H), 2.74–7.68 (m, 1H); ^{13}C NMR (150 MHz, MeOD) δ 176.40, 163.96, 158.40, 144.36, 136.50, 136.43, 135.74, 135.06, 132.04, 131.99, 130.41, 129.89, 129.11, 127.75, 127.55, 116.84, 116.52, 116.06, 115.92, 64.80, 49.39, 35.94 ppm; HRMS-ESI (m/z): Calculated for $C_{22}H_{22}NO_3F$ $(M+H)^+$: 366.1505, Found: 366.1497.

*5.3.27. 3-(4-Fluorobenzyl)-5-phenyl-1-oxa-5-azaspiro [5.5] undeca-7, 10-diene-4, 9-dione **(1g)***

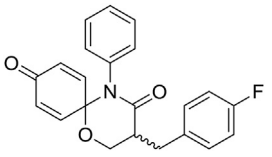

White liquid; 78% yield; purity 98.2%; IR (neat): 2970, 2965, 2950, 2850, 1715, 1680, 1450, 1298, 1320, 790 cm^{-1}; ^1H NMR (600 MHz, $CDCl_3$) δ 7.34–7.29 (m, 3H), 7.27–7.21 (m, 2H), 7.08–6.97 (m, 4H), 6.92 (dd, $J = 10.3$, 2.9 Hz, 1H), 6.73–6.68 (m, 1H), 6.04 (d, $J = 10.2$ Hz, 2H), 4.18 (dd, $J = 12.2$, 5.2 Hz, 1H), 4.04 (dd, $J = 12.2$, 6.5 Hz, 1H), 3.25 (dd, $J = 13.7$, 3.8 Hz, 1H), 3.11–3.05 (m, 1H), 3.04–2.98 (m, 1H); ^{13}C NMR (150 MHz, $CDCl_3$) δ 183.65, 169.37, 162.46, 160.84, 143.51, 143.24, 136.16, 133.49, 130.72, 130.67, 129.66 (2 C), 129.60, 128.93 (2 C), 128.87, 115.42, 115.28, 83.05, 62.81, 43.28, 33.89 ppm; HRMS-ESI (m/z): Calculated for $C_{22}H_{19}NO_3F$ $(M+H)^+$:

363.1185, Found: 363.1190.

5.3.28. Methyl 2-(4-chlorobenzyl)-3-((4-(methoxymethoxy) phenyl) (phenyl) amino)-3-oxopropanoate ***(10h)***

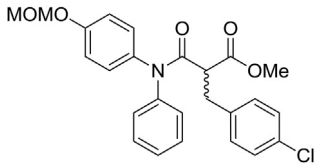

^{1}H NMR (600 MHz, $CDCl_3$) δ 7.32–7.26 (m, 5H), 7.15 (t, J = 7.2 Hz, 1H), 7.13–7.01 (m, 4H), 6.98–6.74 (m, 3H), 5.14 (d, J = 26.4 Hz, 2H), 3.80–3.71 (m, 4H), 3.46 (d, J = 33.1 Hz, 3H), 3.30 (t, J = 11.9 Hz, 1H), 3.15 (dd, J = 12.8, 5.2 Hz, 1H); ^{13}C NMR (150 MHz, $CDCl_3$) δ 169.50, 168.43, 156.80, 142.18, 136.67, 135.69, 132.54, 130.75, 129.78, 129.57, 128.80, 128.49, 128.45 (2 C), 128.02, 127.36, 126.30, 125.99, 116.94, 116.47, 94.31, 56.11, 52.51, 51.28, 34.56 ppm; ESI-MS: m/z = 454 $[M+H]^+$.

5.3.29. 2-(4-Chlorobenzyl)-3-hydroxy-N-(4-(methoxymethoxy) phenyl)–N-phenylpropanamide ***(11h)***

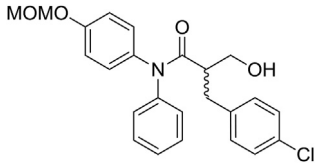

^{1}H NMR (600 MHz, $CDCl_3$) δ 7.26–7.18 (m, 5H), 7.08 (d, J = 50.7 Hz, 2H), 7.01–6.69 (m, 6H), 5.15 (d, J = 26.7 Hz, 2H), 3.76 (d, J = 34.1 Hz, 2H), 3.46 (d, J = 32.2 Hz, 3H), 3.09–2.88 (m, 3H), 2.79 (s, 1H); ^{13}C NMR (150 MHz, $CDCl_3$) δ 175.06, 174.99, 155.56, 142.22, 137.35, 136.04, 135.80, 132.27, 130.57, 130.54, 129.73, 129.59, 128.90, 128.48, 128.41 (2 C), 127.55, 126.22, 117.01, 116.57, 94.34, 63.25, 56.10, 46.12, 34.73 ppm; ESI-MS: m/z = 426 $[M+H]^+$.

5.3.30. 2-(4-Chlorobenzyl)-3-hydroxy-N-(4-hydroxyphenyl)–N-phenylpropanamide ***(2h)***

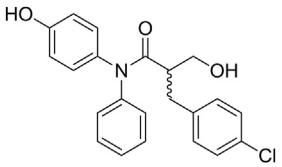

White solid; 89% yield; M.P.:159.2–160.3 °C; IR (neat): bs 3510, 3025, 2957, 1751, 1715, 1519, 1350, 1225, 837, 696 cm^{-1}; ^{1}H NMR (600 MHz, MeOD) δ 7.36–7.26 (m, 4H), 7.18 (t, J = 7.3 Hz, 1H), 7.13–7.02 (m, 4H), 6.90 (d, J = 8.5 Hz, 1H), 6.76–6.57 (m, 3H), 3.86 (t, J = 9.2 Hz, 1H), 3.62–3.53 (m, 1H), 3.14–3.01 (m, 1H), 2.84–2.76 (m, 1H), 2.75–2.67 (m, 1H); ^{13}C NMR (150 MHz, MeOD) δ 176.35, 158.50, 144.42, 139.45, 135.09, 133.46, 132.05 (2 C), 131.00, 130.50, 129.98, 129.54 (2 C), 129.17, 128.86, 127.81, 127.63, 116.93, 116.60, 49.31, 36.15, 20.84 ppm; HRMS-ESI (m/z): Calculated for $C_{22}H_{21}NO_3Cl$ $(M+H)^+$: 382.1210, Found: 382.1216.

5.3.31. 3-(4-Chlorobenzyl)-5-phenyl-1-oxa-5-azaspiro [5.5] undeca-7, 10-diene-4, 9-dione ***(1h)***

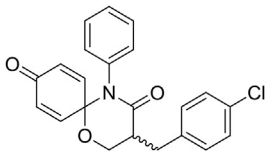

Yellow liquid; 76% yield; purity 97.5%; IR (neat): 2923, 2852, 1679, 1634, 1492, 1391, 1355, 1093, 940, 739, 696 cm^{-1}; ^{1}H NMR (600 MHz, $CDCl_3$) δ 7.38–7.29 (bs, 5H), 7.22 (d, J = 7.8 Hz, 2H), 7.04–6.94 (bs, 2H), 6.92 (d, J = 9.8 Hz, 1H), 6.73 (d, J = 9.0 Hz, 1H), 6.05 (d, J = 10.1 Hz, 2H), 4.18 (dd, J = 12.2, 4.2 Hz, 1H), 4.02 (dd, J = 11.8, 6.3 Hz, 1H), 3.25 (d, J = 13.2 Hz, 1H), 3.08–2.97 (m, 2H); ^{13}C NMR (150 MHz, $CDCl_3$) δ 183.86, 169.54, 143.70, 143.41, 136.55, 136.34, 132.80, 130.76 (2 C), 129.90, 129.87 (2 C), 129.84, 129.16 (2 C), 129.11, 128.87 (2 C), 83.30, 62.99, 43.39, 34.23 ppm; HRMS-ESI (m/z): Calculated for $C_{22}H_{29}NO_3Cl$ $(M+H)^+$: 379.0986, Found: 379.0988.

5.3.32. Methyl 2-(3-bromobenzyl)-3-((4-(methoxymethoxy) phenyl) (phenyl) amino)-3-oxopropanoate ***(10i)***

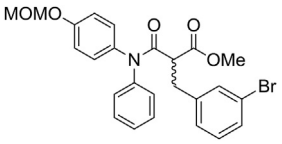

^{1}H NMR (600 MHz, $CDCl_3$) δ 7.45 (d, J = 7.8 Hz, 1H), 7.36–7.27 (m, 5H), 7.25–7.10 (m, 4H), 7.07–6.94 (m, 3H), 5.24–5.09 (m, 2H), 3.79 (s, 3H), 3.48 (d, J = 34.9 Hz, 3H), 3.32 (t, J = 12.2 Hz, 1H), 3.22–3.11 (m, 1H); ^{13}C NMR (150 MHz, $CDCl_3$) δ 169.53, 168.53, 156.93, 142.24, 140.63, 132.36, 130.10, 129.95 (2C), 129.86, 128.91, 128.58, 128.36 (2C), 127.58, 126.20, 122.55, 117.04, 116.59, 94.46, 56.22, 52.67, 51.15, 35.03 ppm; ESI-MS: m/z = 498 $[M]^+$.

5.3.33. 2-(3-Bromobenzyl)-3-hydroxy-N-(4-(methoxymethoxy) phenyl)–N-phenylpropanamide ***(11i)***

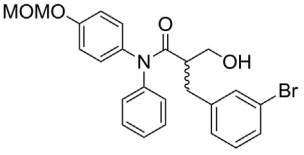

^{1}H NMR (600 MHz, $CDCl_3$) δ 7.42 (dd, J = 8.0, 0.8 Hz, 1H), 7.33 (dd, J = 15.0, 7.3 Hz, 3H), 7.23–7.12 (m, 4H), 7.10–6.95 (m, 4H), 6.83 (s, 1H), 5.51–4.98 (m, 2H), 4.00–3.69 (m, 2H), 3.48 (d, J = 32.9 Hz, 3H), 3.17–2.88 (m, 3H), 2.79 (m, 1H); ^{13}C NMR (150 MHz, $CDCl_3$) δ 174.99, 156.80, 142.31, 141.44, 132.28, 130.02, 129.80 (2C), 129.69 (2C), 129.00, 128.56, 128.13, 127.73, 126.54, 126.39, 122.56, 117.08, 116.67, 94.49, 63.60, 56.21, 46.17, 35.34 ppm; ESI-MS: m/z = 470 $[M]^+$.

*5.3.34. 2-(3-Bromobenzyl)-3-hydroxy-N-(4-hydroxyphenyl)–N-phenylpropanamide **(2i)***

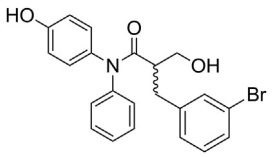

White solid; 82% yield; M.P.:191.2–191.9 °C; IR (neat): bs 3500, 2963, 2924, 2852, 17021633, 1591, 1265, 1224, 1071, 725, 693 cm^{-1}; ^1H NMR (600 MHz, MeOD) δ 7.53–7.47 (m, 1H), 7.34–7.24 (m, 5H), 7.20 (t, $J = 7.4$ Hz, 1H), 7.14–7.06 (m, 3H), 6.94–6.88 (m, 1H), 6.75–6.71 (m, 2H), 3.93–3.86 (m, 1H), 3.62 (dd, $J = 10.6$, 6.0 Hz, 1H), 3.16–3.01 (m, 1H), 2.83–2.70 (m, 2H); ^{13}C NMR (150 MHz, MeOD) δ 176.26, 158.52, 144.43, 143.34, 135.07, 133.53, 131.40, 130.74, 130.53, 130.02 (2C), 129.75, 129.45, 129.27, 127.93 (2C), 123.52, 116.97, 116.63, 64.93, 49.29, 36.58 ppm; HRMS-ESI (m/z): Calculated for $C_{20}H_{20}NO_3Br$ $(M+H)^+$: 426.0705, Found: 426.0709.

*5.3.35. 3-(3-Bromobenzyl)-5-phenyl-1-oxa-5-azaspiro [5.5] undeca-7, 10-diene-4, 9-dione **(1i)***

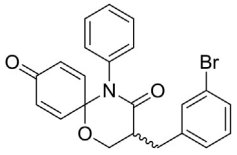

White liquid; 91% yield; purity 98.8%; IR (neat): 2995, 2967, 2858, 1711, 1441, 1419, 1358, 1221, 1092, 747, cm^{-1}; ^1H NMR (600 MHz, $CDCl_3$) δ 7.44 (d, $J = 8.2$ Hz, 1H), 7.44–7.40 (m, 1H), 7.33–7.29 (m, 3H), 7.24–7.19 (m, 2H), 7.04–7.01 (m, 2H), 6.93 (dd, $J = 10.4$, 3.2 Hz, 1H), 6.69 (dd, $J = 10.4$, 3.2 Hz, 1H), 4.19 (dd, $J = 12.3$, 5.1 Hz, 1H), 4.03 (dd, $J = 12.3$, 6.3 Hz, 1H), 3.25 (dd, $J = 12.7$, 3.0 Hz, 1H), 3.09–2.99 (m, 2H); ^{13}C NMR (150 MHz, $CDCl_3$) δ 183.81, 169.37, 143.62, 143.37, 140.47, 136.29, 132.28, 130.25, 130.06, 129.88 (2C), 129.85, 129.80, 129.11 (2C), 129.06, 128.06, 122.75, 83.25, 63.00, 43.21, 34.58 ppm; HRMS-ESI (m/z): Calculated for $C_{22}H_{19}NO_3Br$ $(M+H)^+$: 423.0587, Found: 423.0591.

*5.3.36. Methyl 3-((4-(methoxymethoxy) phenyl) (phenyl) amino)-3-oxo-2-(4-(trifluoromethyl) benzyl) propanoate **(10k)***

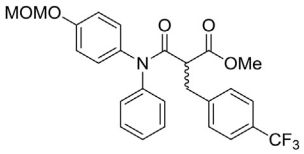

^1H NMR (400 MHz, cdcl$_3$) δ 7.56 (d, $J = 7.8$ Hz, 2H), 7.32–7.22 (m, 5H), 7.16 (t, $J = 7.5$ Hz, 1H), 7.09 (d, $J = 7.8$ Hz, 1H), 7.04–6.72 (m, 4H), 5.14 (d, $J = 16.1$ Hz, 2H), 3.84–3.74 (m, 4H), 3.46 (d, $J = 21.0$ Hz, 3H), 3.38 (t, $J = 11.9$ Hz, 1H), 3.28–3.29 (m, 1H); ^{13}C NMR (150 MHz, $CDCl_3$) δ 169.49, 168.40, 156.93, 142.55, 135.70, 129.81 (2 C), 129.71, 129.12, 128.94, 128.48, 128.18, 127.42, 126.48, 126.06, 125.39, 125.36, 125.11, 123.31, 117.09, 116.61, 94.42, 56.22, 52.70, 51.29, 35.12 ppm; ESI-MS: $m/z = 488$ $[M+H]^+$.

*5.3.37. 3-hydroxy-N-(4-(methoxymethoxy) phenyl)–N-phenyl-2-(4-(trifluoromethyl) benzyl) propanamide **(11k)***

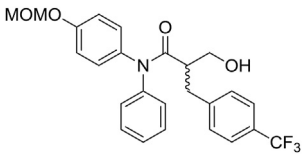

^1H NMR (600 MHz, $CDCl_3$) δ 7.52 (t, $J = 7.1$ Hz, 2H), 7.35–7.28 (m, 2H), 7.21–7.08 (m, 4H), 7.03 (d, $J = 8.9$ Hz, 1H), 7.00–6.74 (m, 4H), 5.14 (d, $J = 25.0$ Hz, 2H), 3.81 (d, $J = 10.5$ Hz, 1H), 3.77–3.69 (bs, 1H), 3.46 (d, $J = 31.1$ Hz, 3H), 3.15–3.05 (m, 1H), 3.04–2.94 (m, 2H), 2.90–2.83 (m, 1H); ^{13}C NMR (150 MHz, $CDCl_3$) δ 174.51, 156.30, 142.77, 135.36, 129.26 (2 C), 129.18, 128.57, 128.42, 128.02, 127.54, 127.16, 126.14, 125.83, 124.89, 124.87, 124.67, 122.87, 116.69, 116.23, 93.99, 62.87, 55.74, 45.70, 34.82 ppm; ESI-MS: $m/z = 460$ $[M+H]^+$.

*5.3.38. 3-Hydroxy-N-(4-hydroxyphenyl)–N-phenyl-2-(4 (trifluoromethyl) benzyl) propanamide **(2k)***

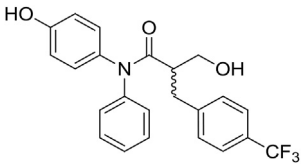

White solid; 87% yield; M.P.:175.2–176.1 °C; IR (neat): bs 3490, 3056, 2918, 2850, 1680, 1636, 1391, 1324, 1066, 736 cm^{-1}; ^1H NMR (600 MHz, MeOD) δ 7.65 (d, $J = 6.9$ Hz, 2H), 7.38–7.24 (m, 5H), 7.19 (t, $J = 7.1$ Hz, 1H), 7.10 (d, $J = 7.7$ Hz, 1H), 6.91 (d, $J = 8.3$ Hz, 1H), 6.76–6.60 (m, 3H), 3.91 (t, $J = 9.0$ Hz, 1H), 3.66–3.61 (m, 1H), 3.19–3.06 (m, 1H), 2.98–2.80 (m, 2H); ^{13}C NMR (150 MHz, MeOD) δ 176.09, 158.44, 145.38, 144.31, 135.68, 134.95, 131.02, 130.82, 130.44, 129.93, 129.55, 129.07, 128.82, 127.70, 127.60, 126.34, 126.31, 124.89, 116.88, 116.55, 64.79, 49.22, 36.57 ppm; HRMS-ESI (m/z): Calculated for $C_{23}H_{21}NO_3F_3$ $(M+H)^+$: 416.1474, Found: 416.1478.

*5.3.39. 5-Phenyl-3-(4-(trifluoromethyl) benzyl)-1-oxa-5-azaspiro [5.5] undeca-7, 10-diene-4, 9-dione **(1k)***

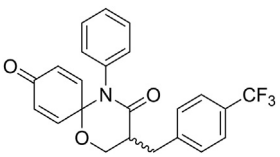

White liquid; 75% yield; purity 96.9%; IR (neat): 2960, 2922, 2848, 1680, 1638, 1587, 1460, 1385, 1314, 1120, 768, 697 cm^{-1}; ^1H NMR (600 MHz, $CDCl_3$) δ 7.48 (d, $J = 7.3$ Hz, 2H), 7.32 (bs, 3H), 7.16 (d, $J = 7.5$ Hz, 2H), 7.02 (bs, 2H), 6.92 (d, $J = 10.4$ Hz, 1H), 6.74 (d, $J = 10.0$ Hz, 1H), 6.05 (d, $J = 10.1$ Hz, 2H), 4.17 (d, $J = 11.0$ Hz, 1H), 4.05–3.99 (m, 1H), 3.24 (d, $J = 12.2$ Hz, 1H), 3.09–2.97 (m, 2H); ^{13}C NMR (150 MHz, $CDCl_3$) δ 183.84, 169.49, 143.68, 143.38, 137.07, 136.63, 136.32, 131.82 (2 C), 131.12 (2 C), 129.89, 129.86 (2 C), 129.84, 129.15 (2 C), 129.10, 120.82, 83.29, 62.98, 43.33, 34.27 ppm; HRMS-ESI (m/z): Calculated for $C_{23}H_{19}NO_3F_3$ $(M+H)^+$: 413.1258, Found:

413.1262.

*5.3.40. Methyl 3-((4-(methoxymethoxy) phenyl) (phenyl) amino)-2-(4-nitrobenzyl)-3-oxopropanoate **(10l)***

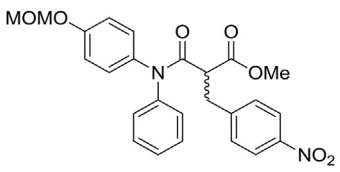

^{1}H NMR (600 MHz, $CDCl_3$) δ 8.17 (d, J = 5.5 Hz, 2H), 7.36–7.27 (m, 5H), 7.17 (t, J = 7.0 Hz, 1H), 7.10 (d, J = 7.7 Hz, 1H), 7.02 (d, J = 8.5 Hz, 1H), 6.91–6.81 (t, J = 30.8 Hz, 3H), 5.14 (d, J = 30.3 Hz, 2H), 3.85–3.78 (m, 1H), 3.75 (s, 3H), 3.46 (d, J = 36.2 Hz, 4H), 3.29 (dd, J = 12.6, 5.7 Hz, 1H); ^{13}C NMR (150 MHz, $CDCl_3$) δ 169.26, 168.05, 157.09, 146.98, 146.18, 142.11, 135.58, 130.37, 130.17, 129.86, 129.78, 129.00, 128.49, 127.36, 125.99, 123.65 (2 C), 120.64, 117.23, 116.66, 94.44, 60.40, 56.27, 52.79, 35.03 ppm; ESI-MS: m/z = 465 $[M+H]^+$.

*5.3.41. 3-Hydroxy-N-(4-(methoxymethoxy) phenyl)-2-(4-nitrobenzyl)–N-phenylpropanamide **(11l)***

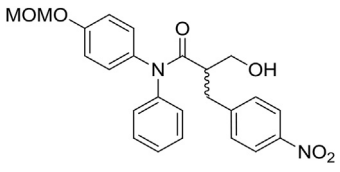

^{1}H NMR (600 MHz, $CDCl_3$) δ 8.20–8.10 (bs, 2H), 7.40–7.30 (bs, 2H), 7.26–7.16 (m, 3H), 7.13 (d, J = 6.3 Hz, 1H), 7.08–6.98 (m, 3H), 6.96–6.79 (m, 2H), 5.17 (d, J = 31.4 Hz, 2H), 3.84 (d, J = 10.4 Hz, 1H), 3.78–3.70 (bs, 1H), 3.49 (d, J = 37.3 Hz, 3H), 3.15 (d, J = 8.9 Hz, 1H), 3.10–2.92 (m, 3H); ^{13}C NMR (150 MHz, $CDCl_3$) δ 174.45, 156.79, 146.70, 142.01, 135.60, 130.06, 130.02, 129.73, 129.59, 128.96, 128.34, 128.08, 127.43, 126.56, 126.09, 123.52 (2 C), 117.15, 116.61, 94.35, 63.03, 56.14, 45.80, 35.01 ppm; ESI-MS: m/z = 437 $[M+H]^+$.

*5.3.42. 3-Hydroxy-N-(4-hydroxyphenyl)-2-(4-nitrobenzyl)–N-phenylpropanamide **(2l)***

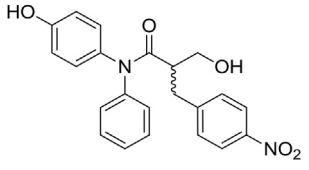

Light yellow solid; 86% yield; M.P.:175.8–176.6 °C; IR (neat): bs 3490, 2982, 2926, 2850, 1743, 1662, 1512, 1348, 1226, 1033, 853, 692 cm^{-1}; ^{1}H NMR (600 MHz, MeOD) δ 8.20 (d, J = 8.3 Hz, 2H), 7.39–7.25 (m, 5H), 7.17 (t, J = 7.3 Hz, 1H), 7.10 (d, J = 7.8 Hz, 1H), 6.91 (d, J = 8.4 Hz, 1H), 6.78–6.62 (m, 3H), 3.89 (t, J = 9.1 Hz, 1H), 3.65–3.57 (m, 1H), 3.20–3.07 (m, 1H), 3.00–2.93 (m, 1H), 2.92–2.82 (m, 1H); ^{13}C NMR (150 MHz, MeOD) δ 175.89, 158.64, 148.81, 148.31, 144.33, 134.99, 131.54, 130.95, 130.66, 130.04, 129.67, 129.16, 129.03, 127.78, 127.71, 124.62 (2 C), 117.08, 116.66, 64.80, 48.75, 36.56 ppm; HRMS-ESI (m/z): Calculated for $C_{22}H_{21}N_2O_5$ $(M+H)^+$: 392.1282, Found: 392.1279.

*5.3.43. 3-(4-Nitrobenzyl)-5-phenyl-1-oxa-5-azaspiro [5.5] undeca-7, 10-diene-4, 9-dione **(1l)***

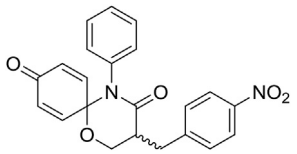

Yellow liquid; 66% yield; purity 97.8%; IR (neat): 2922, 2851, 1678, 1634, 1517, 1392, 1345, 1096, 942, 735, 698 cm^{-1}; ^{1}H NMR (600 MHz, $CDCl_3$) δ 8.22 (d, J = 8.4 Hz, 2H), 7.47 (d, J = 8.3 Hz, 2H), 7.40–7.29 (m, 3H), 7.02 (d, J = 3.4 Hz, 2H), 6.93 (d, J = 8.3 Hz, 1H), 6.79 (d, J = 9.7 Hz, 1H), 6.07 (d, J = 10.1 Hz, 2H), 4.21 (dd, J = 12.1, 5.0 Hz, 1H), 4.02 (dd, J = 12.1, 6.8 Hz, 1H), 3.41 (dd, J = 13.6, 3.9 Hz, 1H), 3.17 (dd, J = 13.4, 9.3 Hz, 1H), 3.14–3.07 (m, 1H); ^{13}C NMR (151 MHz, $CDCl_3$) δ 183.73, 169.13, 146.05, 143.50, 143.05, 136.16, 130.24 (2 C), 130.07, 130.03, 129.94, 129.84 (2 C), 129.25, 129.24, 129.09, 123.97 (2 C), 83.44, 63.00, 43.30, 34.65 ppm; HRMS-ESI (m/z): Calculated for $C_{22}H_{19}N_2O_5$ $(M+H)^+$: 391.1294, Found: 391.1303.

*5.3.44. Methyl 3-((4-(methoxymethoxy) phenyl) (phenyl) amino)-3-oxo-2-(2-((phenylsulfonyl) methyl) benzyl) propanoate **(10m)***

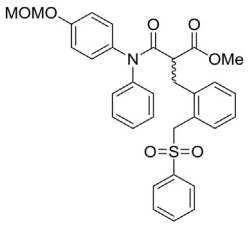

^{1}H NMR (600 MHz, $CDCl_3$) δ 7.66 (d, J = 7.6 Hz, 2H), 7.61 (t, J = 7.4 Hz, 1H), 7.46 (t, J = 7.7 Hz, 2H), 7.35–7.20 (m, 6H), 7.07–6.98 (m, 1H), 6.97–6.67 (m, 2H), 6.96–6.67 (m, 4H), 5.12 (d, J = 37.1 Hz, 2H), 4.51 (t, J = 13.0 Hz, 1H), 4.22–4.15 (m, 1H), 3.80–3.66 (m, 4H), 3.44 (d, J = 39.6 Hz, 3H), 3.14 (dd, J = 14.2, 11.0 Hz, 1H), 2.85 (d, J = 14.4 Hz, 1H); ^{13}C NMR (150 MHz, $CDCl_3$) δ 169.22, 168.31, 156.65, 142.00, 138.41, 138.15, 135.42, 133.55, 132.47, 130.54, 129.57, 129.42, 128.86, 128.79 (2 C), 128.68, 128.33 (2 C), 128.27, 127.96, 127.20, 126.95, 126.89, 125.82, 116.79, 116.34, 94.15, 77.03, 59.09, 52.43, 50.55, 30.85 ppm; ESI-MS: m/z = 574 $[M+H]^+$.

*5.3.45. 3-Hydroxy-N-(4-(methoxymethoxy) phenyl)–N-phenyl-2-(2-((phenyl sulfonyl) methyl) benzyl) propanamide **(11m)***

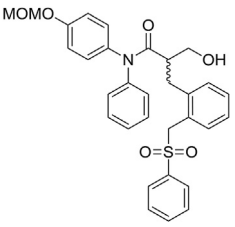

^{1}H NMR (600 MHz, $CDCl_3$) δ 7.65 (d, J = 7.5 Hz, 2H), 7.61 (t, J = 7.4 Hz, 1H), 7.45 (t, J = 7.7 Hz, 2H), 7.32–7.22 (m, 4H), 7.17 (q, J = 8.0 Hz, 2H), 7.11–7.01 (m, 2H), 6.99–6.74 (m, 5H), 5.14 (d, J = 35.5 Hz, 2H), 4.34–4.16 (m, 2H), 3.74–3.67 (bs, 1H), 3.61–3.54 (bs, 1H), 3.45 (d, J = 34.5 Hz, 3H), 3.12 (dd, J = 17.0, 5.6 Hz, 1H), 2.95–2.82 (bs, 1H), 2.88–2.78 (m, 1H), 2.69 (dd, J = 13.5, 6.1 Hz, 1H); ^{13}C NMR (150 MHz, $CDCl_3$) δ 175.04, 156.69, 155.68, 142.28, 142.21,

139.35, 139.33, 138.37, 135.77, 133.78, 132.54, 130.97, 129.73, 129.09, 129.01 (2 C), 128.54 (2 C), 128.02, 127.66, 126.92, 126.57, 126.32, 117.18, 116.66, 94.41, 63.20, 59.24, 56.20, 45.62, 31.39 ppm; ESI-MS: $m/z = 546$ $[M+H]^+$.

5.3.46. 3-Hydroxy-N-(4-hydroxyphenyl)–N-phenyl-2-(2-((phenyl sulfonyl) methyl) benzyl) propanamide ***(2m)***

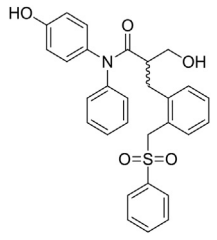

Light yellow solid; 86% yield; M.P.:110.2–110.8 °C; IR (neat): bs 3510, 2986, 2934, 2838, 2850, 1701, 1630, 1511, 1448, 1309, 1148, 831 cm^{-1}; ^1H NMR (600 MHz, MeOD) δ 7.89 (s, 1H), 7.75–7.58 (m, 3H), 7.52 (t, $J = 7.6$ Hz, 2H), 7.34 (t, $J = 7.2$ Hz, 1H), 7.29–7.20 (m, 4H), 7.15 (d, $J = 7.2$ Hz, 2H), 7.08 (dd, $J = 20.8$, 7.5 Hz, 1H), 6.99 (d, $J = 7.8$ Hz, 1H), 6.80 (d, $J = 8.6$ Hz, 1H), 6.71–6.55 (m, 3H), 4.59 (s, 1H), 4.44 (dd, $J = 30.1$, 14.2 Hz, 1H), 4.28 (dd, $J = 32.0$, 14.2 Hz, 1H), 3.79 (t, $J = 8.9$ Hz, 1H), 3.52 (dd, $J = 9.8$, 6.8 Hz, 1H), 3.04–2.90 (m, 1H), 2.76–2.59 (m, 2H); ^{13}C NMR (150 MHz, MeOD) δ 176.21, 158.43, 144.23, 141.19, 139.66, 135.12, 134.94, 133.98, 132.21, 130.87, 130.48, 130.23 (2 C), 129.98, 129.64 (2 C), 129.58, 129.05, 128.87, 128.38, 127.90, 127.71, 127.67, 116.90, 116.59, 64.81, 59.88, 48.84, 33.20 ppm; HRMS-ESI (m/z): Calculated for $C_{29}H_{28}NO_3S$ $(M+H)^+$: 502.1688, Found: 502.1687.

5.3.47. 5-Phenyl-3-(2-((phenylsulfonyl) methyl) benzyl)-1-oxa-5-azaspiro [5.5] undeca-7, 10-diene-4, 9-dione ***(1m)***

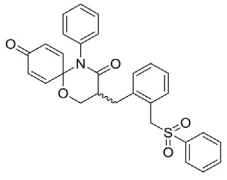

White liquid; 70% yield; purity 98.2%; IR (neat): 2960, 2952, 2853, 1743, 1678, 1446, 1318, 1085, 790 cm^{-1}; ^1H NMR (600 MHz, $CDCl_3$) δ 7.78 (d, $J = 7.0$ Hz, 2H), 7.63 (t, $J = 6.5$ Hz, 1H), 7.50 (d, $J = 7.4$ Hz, 2H), 7.41–7.27 (m, 5H), 7.25–7.16 (m, 2H), 7.05 (s, 2H), 6.98 (d, $J = 10.1$ Hz, 1H), 6.91 (d, $J = 10.0$ Hz, 1H), 6.10–6.06 (m, 2H), 4.53 (s, 2H), 4.20 (d, $J = 11.9$ Hz, 1H), 4.03 (d, $J = 11.5$ Hz, 1H), 3.31 (d, $J = 12.4$ Hz, 1H), 3.04–2.92 (m, 2H); ^{13}C NMR (150 MHz, $CDCl_3$) δ 183.88, 169.82, 143.87, 143.35, 138.89, 138.63, 136.32, 133.88, 132.93, 130.58, 129.95 (3 C), 129.85, 129.31, 129.14 (2 C), 129.10 (2 C), 128.54 (2 C), 127.20 (2 C), 126.82, 83.37, 62.91, 59.33, 43.46, 31.61 ppm; HRMS-ESI (m/z): Calculated for $C_{29}H_{26}NO_5S$ $(M+H)^+$: 500.1532, Found: 500.1518.

5.3.48. Methyl 2-(3, 5-bis (trifluoromethyl) benzyl)-3-((4-(methoxymethoxy) phenyl) (phenyl) amino)-3-oxopropanoate ***(10n)***

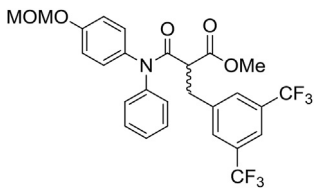

^1H NMR (600 MHz, $CDCl_3$) δ 7.82 (s, 1H), 7.60 (d, $J = 18.8$ Hz, 2H), 7.34–7.27 (m, 3H), 7.16 (t, $J = 7.3$ Hz, 1H), 7.07 (d, $J = 7.8$ Hz, 1H), 7.01–6.77 (m, 4H), 5.19–5.10 (m, 2H), 3.83 (dd, $J = 10.3$, 4.8 Hz, 1H), 3.78 (s, 3H), 3.51–3.40 (m, 4H), 3.37–3.28 (m, 1H); ^{13}C NMR (150 MHz, $CDCl_3$) δ 169.08, 167.96, 157.16, 141.94, 140.97, 135.55, 131.94, 131.72, 129.90, 129.66, 128.96 (2 C), 128.29, 127.36, 126.62, 126.00 (2 C), 124.14, 122.33, 120.86, 117.23, 116.61, 94.41, 56.17, 52.84, 50.98, 34.99 ppm; ESI-MS: $m/z = 556$ $[M+H]^+$.

5.3.49. 2-(3, 5-Bis (trifluoromethyl) benzyl)-3-hydroxy-N-(4-(methoxymethoxy) phenyl)–N-phenylpropanamide ***(11n)***

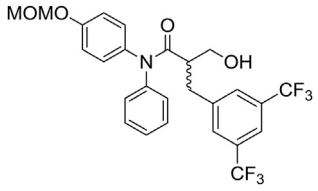

^1H NMR (600 MHz, $CDCl_3$) δ 7.79 (s, 1H), 7.50 (d, $J = 28.7$ Hz, 2H), 7.30 (dd, $J = 12.5$, 4.8 Hz, 2H), 7.18 (t, $J = 7.4$ Hz, 1H), 7.07 (d, $J = 7.7$ Hz, 1H), 7.02–6.68 (m, 5H), 5.20–5.10 (m, 2H), 3.87 (d, $J = 10.9$ Hz, 1H), 3.82–3.72 (m, 1H), 3.46 (d, $J = 26.4$ Hz, 3H), 3.24–3.17 (m, 1H), 3.09–2.99 (m, 1H), 3.00–2.91 (m, 1H), 2.86 (t, $J = 7.4$ Hz, 1H); ^{13}C NMR (150 MHz, $CDCl_3$) δ 174.30, 157.05, 141.99, 141.71, 135.56, 131.88, 131.66, 129.88, 129.48 (2 C), 129.03 (2 C), 128.28, 127.51, 126.70, 126.17 (2 C), 124.15, 120.62, 117.20, 116.68, 94.43, 63.28, 56.15, 46.02, 35.21 ppm; ESI-MS: $m/z = 428$ $[M+H]^+$.

5.3.50. 2-(3, 5-Bis (trifluoromethyl) benzyl)-3-hydroxy-N-(4-hydroxyphenyl)–N-phenylpropanamide ***(2n)***

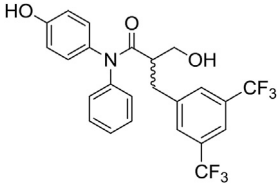

White solid; 89% yield; M.P.:177.1–177.8 °C; IR (neat): bs 3520, 2987, 2946, 2838, 2826, 1704, 1639, 1593, 1361, 1129, 762 cm^{-1}; ^1H NMR (600 MHz, MeOD) δ 7.93 (s, 1H), 7.73 (s, 1H), 7.69 (s, 1H), 7.27 (dd, $J = 10.7$, 4.9 Hz, 3H), 7.17 (t, $J = 7.4$ Hz, 1H), 7.05–6.95 (m, 1H), 6.82 (d, $J = 8.8$ Hz, 1H), 6.73–6.57 (m, 3H), 3.94–3.88 (m, 1H), 3.64 (dd, $J = 10.6$, 6.1 Hz, 1H), 3.21–3.06 (m, 1H), 3.03–2.90 (m, 2H); ^{13}C

NMR (150 MHz, MeOD) δ 175.64, 158.76, 144.18, 144.16, 134.87, 132.99, 132.77, 131.07, 130.71, 130.00 (2 C), 129.47, 129.05, 127.80, 127.69 (2 C), 125.82, 124.02, 121.55, 117.13, 116.61, 64.78, 49.18, 36.39 ppm; HRMS-ESI (*m/z*): Calculated for $C_{24}H_{20}NO_3F_6$ $(M+H)^+$: 484.1347, Found: 484.1348.

5.3.51. 3-(3, 5-Bis (trifluoromethyl) benzyl)-5-phenyl-1-oxa-5-azaspiro [5.5] undeca-7,10-diene-4,9-dione ***(1n)***

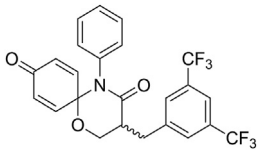

White liquid; 78% yield; purity 98.2%; IR (neat): 2955, 2918, 2856, 1702, 1636, 1390, 1354, 1072, 918, 760, 734 cm^{-1}; ^1H NMR (600 MHz, $CDCl_3$) δ 7.82 (s, 1H), 7.76 (s, 2H), 7.36–7.29 (m, 3H), 7.05–6.98 (m, 2H), 6.94 (dd, *J* = 10.0, 3.1 Hz, 1H), 6.74 (dd, *J* = 10.0, 2.8 Hz, 1H), 6.07 (t, *J* = 10.3 Hz, 2H), 4.23 (dd, *J* = 12.3, 5.1 Hz, 1H), 4.03 (dd, *J* = 12.2, 6.7 Hz, 1H), 3.43 (dd, *J* = 14.0, 4.3 Hz, 1H), 3.21 (dd, *J* = 14.0, 8.8 Hz, 1H), 3.15–3.07 (m, 1H); ^{13}C NMR (150 MHz, $CDCl_3$) δ 183.68, 168.93, 143.36, 142.95, 140.91, 136.08, 132.38, 132.16, 131.94, 131.72, 130.05, 129.81, 129.48, 129.46, 129.23, 129.21, 125.92, 124.11, 122.30, 121.03, 83.43, 62.93, 43.23, 34.55 ppm; HRMS-ESI (*m/z*): Calculated for $C_{24}H_{18}NO_3F_6$ $(M+H)^+$: 482.1191, Found: 482.1188.

5.3.52. Methyl 2-(3, 5-dimethylbenzyl)-3-((4-(methoxymethoxy) phenyl) (phenyl) amino)-3-oxopropanoate ***(10o)***

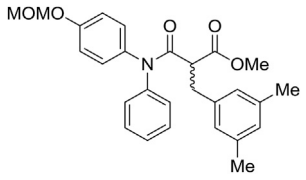

^1H NMR (600 MHz, $CDCl_3$) δ 7.30–7.19 (m, 3H), 7.16–7.06 (m, 2H), 6.99 (d, *J* = 8.3 Hz, 1H), 6.95–6.85 (m, 3 H), 6.74 (d, *J* = 19.5 Hz, 3H), 5.12 (d, *J* = 24.2 Hz, 2H), 3.75 (d, *J* = 17.5 Hz, 4H), 3.45 (d, *J* = 31.5 Hz, 3H), 3.25 (t, *J* = 7.4 Hz, 1H), 3.11 (d, *J* = 8.5 Hz, 1H), 2.30 (s, 6H); ^{13}C NMR (150 MHz, $CDCl_3$) δ 169.94, 169.08, 156.75, 142.45, 137.93, 136.32, 136.00, 130.02, 129.31, 128.80, 128.74, 128.27 (2 C), 127.86, 127.63, 127.34 (2 C), 126.25, 116.68, 116.49, 94.42, 56.15, 52.52, 51.39, 35.39, 21.20 (2 C) ppm; ESI-MS: *m/z* = 448 $[M+H]^+$.

5.3.53. 2-(3, 5-Dimethylbenzyl)-3-hydroxy-N-(4-(methoxymethoxy) phenyl)–N-phenylpropanamide ***(11o)***

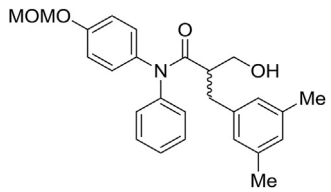

^1H NMR (600 MHz, $CDCl_3$) δ 7.33–7.24 (m, 3H), 7.16 (s, 1H), 7.05–6.84 (m, 4H), 6.83–6.72 (m, 1H), 6.64 (d, *J* = 27.0 Hz, 3H), 5.14 (d, *J* = 21.4 Hz, 2H), 3.79 (s, 2H), 3.46 (d, *J* = 27.4 Hz, 3H), 2.98 (bs, 3H), 2.70 (s, 1H), 2.28 (s, 6H); ^{13}C NMR (150 MHz, $CDCl_3$) δ 175.82, 156.83, 142.72, 138.99, 138.04, 136.55, 130.18, 129.56, 129.09, 128.94, 128.21 (2 C), 127.97, 127.88, 127.39, 127.37, 126.63, 116.95, 116.77, 94.63, 63.92, 56.32, 46.59, 35.86, 21.38 (2 C) ppm; ESI-MS: *m/z* = 420 $[M+H]^+$.

5.3.54. 2-(3, 5-Dimethylbenzyl)-3-hydroxy-N-(4-hydroxyphenyl) –N-phenylpropanamide ***(2o)***

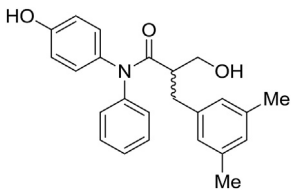

White solid; 92% yield; M.P.:208.4–208.9 °C; IR (neat): bs 3495, 2975, 2918, 2852, 1631, 1511, 1235, 1056, 707 cm^{-1}; ^1H NMR (600 MHz, MeOD) δ 7.31–7.20 (m, 3H), 7.16 (t, *J* = 7.3 Hz, 1H), 7.06 (d, *J* = 7.9 Hz, 2H), 6.94 (s, 1H), 6.86 (d, *J* = 8.5 Hz, 1H), 6.71–6.57 (m, 4H), 3.90–3.82 (m, 1H), 3.65–3.54 (m, 1H), 3.13–2.93 (m, 1H), 2.75–2.59 (m, 2H), 2.31 (s, 6H); ^{13}C NMR (150 MHz, MeOD) δ 176.84, 158.38, 144.60, 140.30, 139.09, 135.98, 135.22, 131.20, 130.23, 129.94 (2 C), 129.28, 128.98, 128.70, 128.43, 127.95, 127.63, 116.68, 116.55, 65.06, 49.53, 37.02, 21.45 (2 C) ppm; HRMS-ESI (*m/z*): Calculated for $C_{24}H_{26}NO_3$ $(M+H)^+$: 376.1913, Found: 376.1912.

5.3.55. 3-(3, 5-Dimethylbenzyl)-5-phenyl-1-oxa-5-azaspiro [5.5] undeca-7, 10-diene-4, 9-dione ***(1o)***

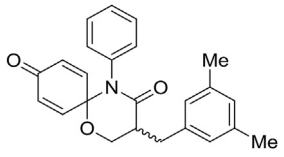

White liquid; 82% yield; purity 98.0%; IR (neat): 2921, 2848, 2918, 1689, 16431406, 1379, 1116, 868, 758, 713 cm^{-1}; ^1H NMR (600 MHz, $CDCl_3$) δ 7.35–7.28 (m, 3H), 7.03 (d, *J* = 1.6 Hz, 2H), 6.97–6.87 (m, 4H), 6.72 (d, *J* = 10.3 Hz, 1H), 6.04 (d, *J* = 9.9 Hz, 2H), 4.16 (d, *J* = 12.2 Hz, 1H), 4.09–4.01 (m, 1H), 3.23 (d, *J* = 11.5 Hz, 1H), 3.07–2.95 (m, 2H), 2.32 (s, 6H); ^{13}C NMR (151 MHz, $CDCl_3$) δ 183.88, 169.86, 143.79, 143.67, 138.16 (2 C), 137.84, 136.43, 129.83, 129.65, 129.60, 129.00 (2 C), 128.91 (2 C), 128.37, 127.09 (2 C), 83.10, 63.02, 43.36, 34.70, 21.20 (2 C); HRMS-ESI (*m/z*): Calculated for $C_{24}H_{24}NO_3$ $(M+H)^+$: 374.1756, Found: 376.1764.

5.3.56. Methyl 3-((4-(methoxymethoxy) phenyl) (phenyl) amino)-2-(2-nitro-4-(trifluoromethyl) benzyl)-3-oxopropanoate ***(10p)***

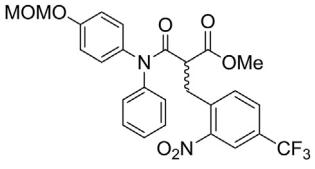

^1H NMR (600 MHz, $CDCl_3$) δ 8.27 (d, *J* = 4.2 Hz, 1H), 7.84 (dd, *J* = 8.0, 1.0 Hz, 1H), 7.71 (d, *J* = 8.0 Hz, 1H), 7.29 (m, 3H), 7.17 (t, *J* = 7.4 Hz, 1H), 7.12 (d, *J* = 7.8 Hz, 1H), 7.03 (d, *J* = 8.8 Hz, 1H), 6.99–6.80 (m, 3H), 5.17–5.10 (m, 2H), 4.14–4.10 (m, 1H), 3.75 (s, 3H), 3.70–3.62 (m, 1H), 3.56–3.51 (m, 1H), 3.45 (d, *J* = 20.5 Hz, 4H); ^{13}C NMR (150 MHz, $CDCl_3$) δ 169.11, 168.13, 157.07, 149.14, 142.10, 137.70, 135.15, 129.86, 129.50, 129.00 (2 C), 128.19, 127.32, 125.94

(2 C), 123.67, 122.35, 121.87, 117.23, 116.65, 94.38, 56.16, 52.83, 49.52, 49.46, 32.86 ppm; ESI-MS: m/z = 533 $[M+H]^+$.

5.3.57. 3-Hydroxy-N-(4-(methoxymethoxy) phenyl)-2-(2-nitro-4-(trifluoromethyl) benzyl)–N-phenylpropanamide ***(11p)***

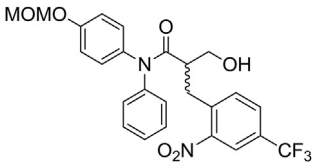

^{1}H NMR (600 MHz, $CDCl_3$) δ 8.22 (d, J = 3.1 Hz, 1H), 7.84 (dd, J = 8.0, 1.3 Hz, 1H), 7.69 (t, J = 7.4 Hz, 1H), 7.34–7.26 (m, 2H), 7.19 (t, J = 7.4 Hz, 1H), 7.12 (d, J = 7.8 Hz, 1H), 7.00 (d, J = 19.5 Hz, 2H), 6.85 (m, 3H), 5.14 (d, J = 15.4 Hz, 2H), 3.87 (d, J = 10.9 Hz, 1H), 3.79–3.72 (m, 1H), 3.45 (d, J = 22.4 Hz, 4H), 3.36–3.28 (m, 1H), 3.27–3.21 (m, 1H), 2.88 (t, J = 8.5 Hz, 1H); ^{13}C NMR (150 MHz, $CDCl_3$) δ 174.47, 156.89, 155.74, 149.11, 141.83, 138.42, 134.65 (2 C), 129.86, 129.37, 128.22, 128.03, 127.49, 126.68, 126.15, 123.70, 122.40, 121.90, 117.28, 116.70, 94.41, 63.64, 56.13, 44.19, 32.85 ppm; ESI-MS: m/z = 505 $[M+H]^+$.

5.3.58. 3-Hydroxy-N-(4-hydroxyphenyl)-2-(2-nitro-4-(trifluoromethyl) benzyl)–N-phenylpropanamide ***(2p)***

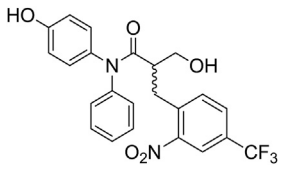

Yellow solid; 78% yield; M.P.:180.0–180.9 °C; IR (neat): bs 3515, 2960, 2927, 2854, 1678, 1637, 1538, 1392, 1355, 1325, 1136, 733 cm^{-1}; ^{1}H NMR (600 MHz, MeOD) δ 8.31 (d, J = 7.1 Hz, 1H), 8.05–8.01 (m, 1H), 7.66 (t, J = 7.6 Hz, 1H), 7.30 (t, J = 7.9 Hz, 1H), 7.24 (m, 2H), 7.18 (t, J = 7.4 Hz, 1H), 7.10 (d, J = 7.5 Hz, 1H), 6.91 (d, J = 8.8 Hz, 1H), 6.76–6.53 (m, 3H), 3.89 (dd, J = 10.6, 8.2 Hz, 1H), 3.66 (dd, J = 10.6, 5.6 Hz, 1H), 3.37–3.31 (m, 1H), 3.30–3.24 (m, 1H), 3.08 (dd, J = 12.7, 10.4 Hz, 1H); ^{13}C NMR (150 MHz, MeOD) δ 175.71, 158.61, 150.82, 144.26, 140.07, 135.77, 134.84, 130.67, 130.04, 129.11, 129.03, 127.74 (2 C), 125.46, 123.66, 123.42, 117.11, 116.66, 65.11, 48.76, 48.61, 47.50, 33.83 ppm; HRMS-ESI (m/z): Calculated for $C_{23}H_{19}N_2O_5F_3$ $(M+H)^+$: 461.1324, Found: 461.1318.

5.3.59. 3-(2-Nitro-4-(trifluoromethyl) benzyl)-5-phenyl-1-oxa-5-azaspiro [5.5] undeca-7, 10-diene-4, 9-dione ***(1p)***

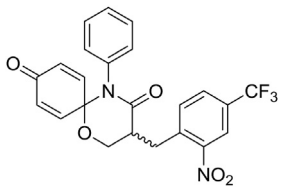

Yellow liquid; purity 96.5%; 64% yield; IR (neat): 3331, 2946, 2834, 1647, 1450, 1327, 1020, 916, 762, 696 cm^{-1}; ^{1}H NMR (600 MHz, $CDCl_3$) δ 8.30 (d, J = 0.9 Hz, 1H), 7.82 (dd, J = 8.1, 1.5 Hz, 1H), 7.77 (d, J = 8.1 Hz, 1H), 7.37–7.31 (m, 3H), 7.09 (dd, J = 10.3, 3.2 Hz, 1H), 7.06–70.2 (m, 2H), 6.94 (d, J = 3.2 Hz, 1H), 6.15 (dd, J = 10.3, 2.0 Hz, 1H), 6.09 (dd, J = 10.2, 2.0 Hz, 1H), 4.43 (dd, J = 12.1, 5.1 Hz, 1H), 4.21 (dd, J = 12.1, 6.9 Hz, 1H), 3.74 (dd, J = 13.5, 8.0 Hz, 1H), 3.26 (dd, J = 13.5, 5.9 Hz, 1H), 3.23–3.13 (m, 1H); ^{13}C NMR (150 MHz, $CDCl_3$) δ 183.78, 169.20, 149.09, 143.51, 143.22, 138.41, 136.00, 134.36, 130.79, 130.57, 130.07, 130.05, 129.90, 129.61, 129.58, 129.20, 129.17, 122.46, 122.44, 83.53, 64.10, 43.41, 32.16 ppm; HRMS-ESI (m/z): Calculated for $C_{23}H_{18}N_2O_5F_3$ $(M+H)^+$: 459.1168, Found: 459.1165.

5.3.60. Methyl 2-(2-fluoro-6-(trifluoromethyl) benzyl)-3-((4-(methoxymethyl) phenyl) (phenyl) amino)-3-oxopropanoate ***(10q)***

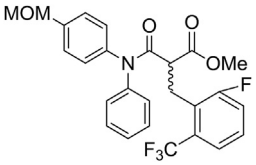

^{1}H NMR (600 MHz, $CDCl_3$) δ 7.42 (t, J = 7.7 Hz, 1H), 7.32 (dd, J = 34.3, 6.7 Hz, 2H), 7.20 (m, 5H), 6.97 (d, J = 8.6 Hz, 1H), 6.92–6.73 (m, 3H), 5.13 (s, 2H), 3.91 (t, J = 7.2 Hz, 1H), 3.41 (d, J = 6.2 Hz, 1H) 3.67 (s, 3H), 3.61–3.54 (m, 1H), 3.44 (d, J = 7.7 Hz, 4H), 3.41 (d, J = 6.2 Hz, 1H); ^{13}C NMR (150 MHz, $CDCl_3$) δ 169.58, 168.44, 162.85, 142.40, 142.08, 135.59, 129.79, 129.66, 128.84 (2 C), 128.52 (2 C), 128.46, 127.36, 126.17, 125.93 (2 C), 122.17, 119.15, 119.00, 117.07, 94.32, 60.43, 52.59, 49.94, 25.34 ppm; ESI-MS: m/z = 506 $[M+H]^+$.

5.3.61. 2-(2-Fluoro-6-(trifluoromethyl) benzyl)-3-hydroxy-N-(4-(methoxymethyl) phenyl)–N-phenylpropanamide ***(11q)***

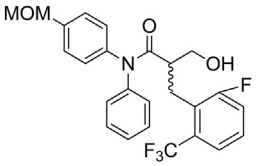

^{1}H NMR (600 MHz, $CDCl_3$) δ 7.40 (t, J = 8.1 Hz, 1H), 7.33 (m, 3H), 7.26–7.06 (m, 5H), 6.98 (d, J = 8.7 Hz, 1H), 6.79 (d, J = 44.8 Hz, 2H), 5.13 (q, J = 6.9 Hz, 2H), 3.89 (m, 1H), 3.77 (d, J = 10.8 Hz, 1H), 3.45 (d, J = 11.9 Hz, 3H), 3.43–3.35 (m, 1H), 3.22 (bs, 1H), 2.90 (d, J = 14.3 Hz, 2H); ^{13}C NMR (150 MHz, $CDCl_3$) δ 174.60, 162.47, 142.17, 141.91, 135.50, 129.38, 129.22 (2 C), 128.62 (2 C), 128.16, 127.99, 172.241, 127.93, 125.87, 121.92, 118.89, 118.74, 116.67, 116.31, 94.03, 64.25, 55.70, 43.81, 25.55 ppm; ESI-MS: m/z = 478 $[M+H]^+$.

5.3.62. 2-(2-Fluoro-6-(trifluoromethyl) benzyl)-3-hydroxy-N-(4-hydroxyphenyl)–N-phenylpropanamide ***(2q)***

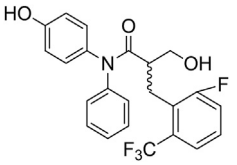

White solid; 78% yield; M.P.:143.3–143.9 °C; IR (neat): bs 3495, 2962, 2928, 2850, 1640, 1592, 1512, 1316, 1168, 1114, 833, 965 cm^{-1}; ^{1}H NMR (600 MHz, MeOD) δ 7.89 (s, 1H), 7.53–7.47 (m, 2H), 7.43–7.39 (m, 1H), 7.31 (t, J = 7.9 Hz, 2H), 7.24–7.14 (m, 4H), 7.03 (d, J = 8.8 Hz, 1H), 6.73 (d, J = 8.8 Hz, 1H), 6.59 (s, 1H), 3.93 (m, 1H), 3.54 (m, 1H), 3.27–3.21 (m, 1H), 3.20–3.13 (m, 1H), 2.83 (t, J = 10.9 Hz, 1H); ^{13}C NMR (150 MHz, MeOD) δ 175.88, 163.88, 158.01, 157.04, 144.17, 134.77, 130.13, 129.71, 129.58 (2 C), 128.76, 128.35, 127.38

(2 C), 127.18, 123.09, 120.33, 120.17, 116.58, 116.22, 64.80, 46.55, 26.15 ppm; HRMS-ESI (*m/z*): Calculated for $C_{23}H_{20}NO_3F_4$ $(M+H)^+$: 434.1379, Found: 434.1378.

5.3.63. 3-(2-Fluoro-6-(trifluoromethyl) benzyl)-5-phenyl-1-oxa-5-azaspiro [5.5] undeca-7, 10-diene-4, 9-dione ***(1q)***

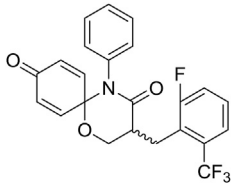

White liquid; 64% yield; purity 97.2%; IR (neat): 2958, 2917, 2849, 1678, 1635, 1467, 1392, 1316, 1115, 768, 697 cm^{-1};^{1}H NMR (600 MHz, $CDCl_3$) δ 7.48 (d, $J = 7.8$ Hz, 1H), 7.35 (m, 1H), 7.31–7.26 (m, 4H), 7.11–7.03 (m, 3H), 6.95 (dd, $J = 10.2$, 3.2 Hz, 1H), 6.10 (dd, $J = 10.2$, 2.0 Hz, 1H), 6.06 (dd, $J = 10.2$, 2.0 Hz, 1H), 4.15 (m, 2H), 3.74 (m, 1H), 3.22–3.15 (m, 1H), 3.07 (m, 1H); ^{13}C NMR (150 MHz, $CDCl_3$) δ 183.96, 168.85, 161.22, 143.79, 136.30, 130.09 (2 C), 129.88 (2 C), 129.04 (3 C), 129.00, 128.65, 128.59, 124.70, 122.19, 119.23, 119.07, 83.44, 63.97, 42.36, 25.26 ppm; HRMS-ESI (*m/z*): Calculated for $C_{23}H_{18}NO_3F_4$ $(M+H)^+$: 432.1223, Found: 432.1234.

5.3.64. Methyl 2-(2-chloro-5-(trifluoromethyl) benzyl)-3-((4-(methoxymethoxy) phenyl) (phenyl) amino)-3-oxopropanoate ***(10r)***

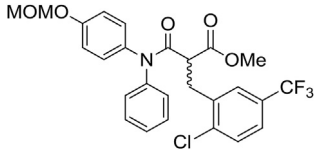

^{1}H NMR (600 MHz, $CDCl_3$) δ 7.68 (s, 1H), 7.53 (d, $J = 7.4$ Hz, 1H), 7.46 (t, $J = 7.4$ Hz, 3H, 1H, 1H), 7.30 (m, 3H), 7.17 (t, $J = 7.4$ Hz, 1H), 7.10 (d, $J = 7.8$ Hz, 1H), 6.98 (m, 3H), 5.16 (d, $J = 30.2$ Hz, 2H), 4.09–4.02 (m, 1H), 3.79 (s, 3H), 3.52–3.36 (m, 5H); ^{13}C NMR (150 MHz, $CDCl_3$) δ 169.37, 168.34, 156.89, 155.62, 142.05, 138.46, 136.89, 135.66, 130.01, 129.71, 129.56, 128.87 (2 C), 128.29, 127.48, 126.50, 126.11 (2 C), 125.20, 117.10, 116.55, 94.36, 56.10, 52.73, 48.01, 33.51 ppm; ESI-MS: $m/z = 522$ $[M+H]^+$.

5.3.65. 2-(2-Chloro-5-(trifluoromethyl) benzyl)-3-hydroxy-N-(4-(methoxymethoxy) phenyl)–N-phenylpropanamide ***(11r)***

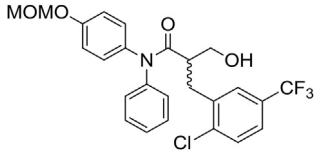

^{1}H NMR (600 MHz, $CDCl_3$) δ 7.57 (d, $J = 10.3$ Hz, 1H), 7.48 (dd, $J = 8.3$, 2.0 Hz, 1H), 7.44–7.37 (m, 1H), 7.33–7.26 (m, 3H), 7.17 (t, $J = 7.4$ Hz, 1H), 7.10 (d, $J = 7.7$ Hz, 1H), 7.06–6.67 (m, 4H), 5.14 (d, $J = 23.4$ Hz, 2H), 3.88–3.81 (m, 1H), 3.79 (m, 1H), 3.45 (d, $J = 26.9$ Hz, 3H), 3.26 (ddd, $J = 10.0$, 8.3, 3.6 Hz, 1H), 3.20–3.13 (m, 1H), 3.07–3.01 (m, 1H), 2.98 (bs, 1H); ^{13}C NMR (150 MHz, $CDCl_3$) δ 174.75, 156.67, 155.66, 142.09, 138.36, 137.66, 135.90, 130.00, 129.64, 128.91 (2 C), 128.48, 128.26, 127.58, 126.25 (2 C), 124.86, 124.51, 117.06, 116.58, 94.30, 63.65, 56.01, 42.98, 33.66 ppm; ESI-MS: $m/z = 494$ $[M+H]^+$.

5.3.66. 2-(2-Chloro-5-(trifluoromethyl) benzyl)-3-hydroxy-N-(4-hydroxyphenyl)–N-phenylpropanamide ***(2r)***

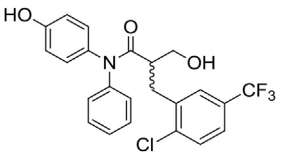

Yellow solid; 85% yield; M.P.:188.5–189.4 °C; IR (neat): bs 3485, 2968, 2917, 2849, 1711, 1703, 1591, 1491, 1322, 1122, 1081, 1054, 827, 728 cm^{-1}; ^{1}H NMR (600 MHz, MeOD) δ 7.61–7.58 (m, 3H), 7.32–7.26 (m, 3H), 7.17 (dd, $J = 9.3$, 1H), 7.09–7.04 (m, 2H), 6.86 (d, $J = 8.8$ Hz, 1H), 6.68 (d, $J = 8.8$ Hz, 2H), 3.97–3.85 (m, 1H), 3.73–3.51 (m, 1H), 3.39–3.31 (m, 1H), 3.04 (m, 1H), 2.97–2.86 (m, 1H); ^{13}C NMR (150 MHz, MeOD) δ 174.52, 157.17, 156.12, 142.84, 138.12, 133.48, 130.30, 129.22, 128.87, 128.52 (2 C), 128.11, 127.68, 127.51, 126.34 (2 C), 126.31, 124.88, 115.65, 115.12, 63.49, 44.81, 33.30 ppm; HRMS-ESI (*m/z*): Calculated for $C_{23}H_{20}NO_3ClF_3$ $(M+H)^+$: 450.1084, Found: 450.1075.

5.3.67. 3-(2-chloro-5-(trifluoromethyl) benzyl)-5-phenyl-1-oxa-5-azaspiro [5.5] undeca-7, 10-diene-4, 9-dione ***(1r)***

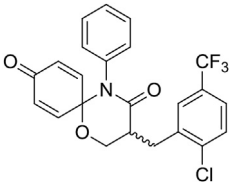

White liquid; 72% yield; purity 96.8%; IR (neat): 2918, 2850, 1678, 1635, 1545, 1494, 1392, 1326, 1168, 1125, 1082, 733 cm^{-1}, ^{1}H NMR (600 MHz, $CDCl_3$) δ 7.65 (d, $J = 1.7$ Hz, 1H), 7.56 (d, $J = 8.4$ Hz, 1H), 7.53–7.49 (m, 1H), 7.37–7.31 (m, 3H), 7.08–7.05 (m, 2H), 6.94 (dd, $J = 10.3$, 3.2 Hz, 1H), 6.89 (dd, $J = 10.4$, 3.2 Hz, 1H), 6.12–6.07 (m, 2H), 4.23 (dd, $J = 12.2$, 5.0 Hz, 1H), 4.13 (dd, $J = 12.2$, 6.9 Hz, 1H), 3.62 (dd, $J = 12.7$, 3.7 Hz, 1H), 3.24–3.15 (m, 2H); ^{13}C NMR (150 MHz, $CDCl_3$) δ 183.95, 169.35, 143.91, 143.30, 138.37, 137.55, 136.36, 130.53, 130.09, 130.09, 130.06 (2 C), 129.29 (2 C), 129.14, 128.39, 125.34, 124.87, 120.38, 83.56, 63.37, 42.67, 32.21 ppm; HRMS-ESI (*m/z*): Calculated for $C_{23}H_{18}NO_3F_3Cl$ $(M+H)^+$: 447.0858, Found: 447.0862.

5.4. Biology

5.4.1. General

Dulbecco's modified Eagle medium (DMEM), penicillin streptomycin (PS) and fetal bovine serum (FBS) were purchased from Invitrogen (Carlsbad, CA, USA). Griess reagent, 3-(4,5-dimethylthiazol-2-yl)-2,5-diphenyltetrazolium bromide (MTT) reagent and dimethyl sulfoxide (DMSO), Lipopolysaccharide (LPS), Donepezil, (−) scopolamine hydro bromide and All other chemicals and reagents were purchased from Sigma Chemical (St. Louis, MO, USA). All other materials were obtained from normal commercial sources and were of the highest grade available.

5.4.2. Mice experiments and maintenance

Male ICR mice (Orient Bio, Seoul, Korea), weighing 25–30 g and aged 6 weeks, were used. Animals were housed 4 or 5 per cage, had free access to food and water, and maintained at temperature (23 ± 1 °C) and humidity (60 ± 10%) environment under 12 h of

darkness (from 19:00 to 7:00) and 12 h of light (7:00 to 19:00). Animal care in accordance with the Principle of Laboratory Animal Care (GIACUC-R2017016) and the Animal Care and Use Guidelines of Gachon University, Korea.

5.4.3. Ethical regulation of laboratory animals

This study was conducted with the approval of the institution animal care committee, this work was done in the Gachon University, Centre of Animal Care and Use (CACU), Lee Gil Ya Cancer and Diabetes Institute, Korea.

5.4.4. Y-maze test

The Y-maze test was administered to assess spatial perception. A 20-cm-long, 5-cm-wide, 10-cm-high Y-shaped maze was prepared. The three arms of the maze were designated A, B, and C. The mouse was dropped at the centre of the Y-maze for 2 min for habituation after which it was observed for 8 min during which the number of times it made a full entry (from nose to tail) into each arm was recorded. If the mouse entered three different arms consecutively, 1 point was given for each arm entered. If the entries were not consecutive, no points were given. Alternation behaviour was defined as three consecutive entries into three different arms of the maze. Spatial perception ability was calculated according to the formula below [109].

$$\text{Voluntary alternation behaviour rate } (\%) = [(N_{alternation})/(N_{entries} - 2)] \times 100$$

where $N_{alternations}$ is the number of times the alternation behaviour was observed (scored by points), and $N_{entries}$ is the total number of arm entries.

5.4.5. Cell culture

BV-2 microglial cells were purchased from the Korean Cell Line Bank, Seoul, Korea. BV-2 cells were cultured in Dulbecco's modified Eagle's medium (DMEM) containing 10% fetal bovine serum (FBS), 1% penicillin (1×10^5 U/L) and streptomycin (100 mg/mL) at a temperature of 37 °C in a humidified incubator with 5% CO_2, according to the method described by Hwang et al.

5.4.6. Cell viability assay

A Tetrazolium bromide reduction MTT assay was used to measure cell viability according to the method described by Hwang et al. (Hwang et al., 2016). 96-well plate was used to culture the cell with different concentration of samples with lipopolysaccharide (LPS). After 24 h, media were removed from each well. Cells were incubated for 1 h after adding MTT solution to each well. After incubation, the MTT solution was removed, and dimethyl sulfoxide (DMSO, 150 μL) was added. The absorbance was measured spectrophotometrically at 570 nm.

5.4.7. Measurement of NO production induced by LPS in BV-2 cells

The inhibitory effect of compounds on LPS-induced BV-2 cells NO was evaluated in according to the method described by Han et al. (Han et al., 2016), with some modification. In 96-well plate, cells at a density of 4×10^4 were seeded and pre-treated of samples, followed by LPS activation for 24 h. The NO level was measured in culture media using Gries reagent. 50 μL of conditioned medium was mixed with 50 μL of Gries reagent and absorbance was detected at 540 nm.

5.4.8. Statistical analysis

SPSS statistics software was used for statistical analysis and the data was expressed as a mean ± standard error of the mean (SEM). For comparison of differences among multiple groups, one-way analysis of variance (ANOVA) followed by Tukey's honest significance test was used. The differences among the multiple groups were considered significant at $p < 0.05$, $p < 0.01$, and $p < 0.001$.

5.5. Biochemical kinase assays

The selectivity of compound **1n** was investigated against a panel of **369** kinases (Reaction Biology Corp). The radiolabelled ATP ([γ-^{33}P] ATP) replaced a substrate with ^{33}P-phosphorylated substrate so that the activity of a kinase was measured from the radiolabelled phosphorylated substrate. Compound **1n** was tested at 30 μM, against an ATP concentration of 10 μM and a substrate concentration of 10 μM. Control Compound Staurosporine was tested in 10-dose IC_{50} mode with 4-fold serial dilution starting at 20 or 100 μM. Alternate Control Compounds were tested in 10-dose IC_{50} mode with 3 or 4-fold serial dilution starting at 10, 20, or 100 μM. Curve fits of control compounds were performed where the enzyme activities at the highest concentration of compounds were less than 65%. The concentration of DMSO was controlled and raw data, % Enzyme activity was calculated relative to DMSO controls.

5.6. Molecular docking studies

3D conformation of the compound **1n** was generated using Open eye OMEGA and representative conformers of the compound **1n** were sampled through in-house code to get efficient query [110]. Every ligand of deposited 34 JNK1PDBs was downloaded and 3D-shape of the X-ray conformers were compared with the shape of the compound **1n** using Open eye ROCS. After the calculation, two low similar PDBs (4E73 and 4WHZ), three moderate similar PDBs (4IZY, 2H96 and 1UKI) and highest similar (2G01, sim = 0.456) were selected according to 3D similarity of X-ray ligands against the query compound. The selected PDBs were prepared using protein preparation for docking simulations. After the preparation, grid of 6 PDBs were generated under default condition except for H-bond constraint of hinge residue using Glide and then docking of every available x-ray ligand and our test compound were conducted under the condition of SP docking scoring, flexible docking, H-bond constraint (within only post-minimization) with writing residue contribution within 12 Å from grid centers. The best docking result of the test compound was chosen able to show the least deviation between redocking score of a used PDB ligand and docking score of our test compound.

Conflicts of interest

The authors declare no conflict of interest.

Authors' contributions

Mi-hyun Kim and Arramshetti Venkanna designed the study; Arramshetti Venkanna, Lama Prema Dhorma, Duddukuri Nandan Kumar performed the synthetic experiments and analysed data; Kyo Hee Cho performed the biology study and animal experiments; Arramshetti Venkanna, Mi-hyun Kim, Sun Yeou Kim, Jung Mi Hah, Hyeung-geun Park wrote the paper. All authors read and approved the final manuscript.

Acknowledgement

This study was supported by the Basic Science Research Program of the National Research Foundation of Korea (NRF), funded by the Ministry of Education, Science, and Technology (No.: 2017R1E1A1A01076642). In addition, a grant was also provided by

the Korea Health Technology R&D Project through the Korea Health Industry Development Institute (KHIDI), funded by the Ministry for Health and Welfare, Korea (No.: HI14C1135).

Appendix A. Supplementary data

Supplementary data related to this article can be found at https://doi.org/10.1016/j.ejmech.2018.11.037.

References

[1] P. Vallance, J. Leiper, Blocking NO synthesis: how, where and why? J. Nat. Rev. Drug Discovery 1 (2002) 939–950.
[2] A.J. Duncan, S.J.R. Heales, Nitric oxide and neurological disorders, Mol. Aspect. Med. 26 (2005) 67–96.
[3] U. Forstermann, W.C. Sessa, Nitric oxide synthases: regulation and function, Eur. Heart J. 33 (2012) 829–837.
[4] H.H. Schmidt, U. Walter, NO at work, Cell 78 (1994) 919–925.
[5] L.S. Krimer, P.S. Goldman-Rakic, Prefrontalmicrocir-cuits: membrane properties and excitatory input focal, medium, andwidearborinterneurons, J. Neurosci. 21 (2001) 3788–3796.
[6] L.S. Krimer, P.S. Goldman-Rakic, Prefrontalmicrocir-cuits: membrane properties and excitatory input focal, medium, andwidearborinterneurons, J. Neurosci. 21 (2001) 3788–3796.
[7] C. Nathan, Inducible nitric oxide synthase: what difference does it make? J. Clin. Invest. 100 (1997) 2417–2423.
[8] S. Moncada, E.A. Riggs, Molecular mechanisms and therapeutic strategies related to nitric oxide, FASEB (Fed. Am. Soc. Exp. Biol.) J. 9 (1995) 1319–1330.
[9] L. Zhou, D.-Y. Zhu, Neuronal nitric oxide synthase: structure, subcellular localization, regulation, and clinical implications, Nitric Oxide 20 (2009) 223–230.
[10] A. Goedert, M.G. Spillantini, A century of Alzheimer's disease, Science 314 (2006) 777–781.
[11] A. Gustavssona, P. Brinck, N. Bergvall, K. Kolasa, A. Wimo, B. Winblad, J. Jonssonb, Predictors of costs of care in Alzheimer's disease: a multinational sample of 1222 patients, Alzheimer's Dementia 7 (2011) 318–327.
[12] L. Zhang, V.L. Dawson, T.M. Dawson, Role of nitric oxide in Parkinson's disease, Pharmacol. Ther. 109 (2006) 33–41.
[13] J.L. Rubenstein, M.M. Merzenich, Model of autism: increased ratioofexcitation/inhibitioninkey neuralsystems, Gene Brain Behav. 2 (2003) 255–267.
[14] H. Gonzalez, D. Elgueta, A. Montoya, R. Pacheco, Neuroimmune regulation of microglial activity involved in neuroinflammation and neurodegenerative diseases, J. Neuroimmunol. 274 (2014) 1–13.
[15] Y. Yang, T. Yu, Y-j. Lian, R. Ma, S. Yang, J.Y. Cho, Nitric oxide synthase inhibitors: a review of patents from 2011 to the present, Expert Opin. Ther. Pat. 25 (2015) 49–68.
[16] Q. Jing, H. Li, L.J. Roman, P. Martasek, T.L. Poulos, R.B. Silverman, Accessible chiral linker to enhance potency and selectivity of neuronal nitric oxide synthase inhibitors, ACS Med. Chem. Lett. 5 (2014) 56–60.
[17] J. Patman, N. Bhardwaj, J. Ramnauth, S.C. Annedi, A. Paul Renton, S.P. Maddaford, S. Rakhit, J.S. Andrews, Novel 2-aminobenzothiazoles as selective neuronal nitric oxide synthase inhibitors, Bioorg. Med. Chem. Lett 17 (2007) 2540–2544.
[18] P. Renton, J. Speed, S. Maddaford, S.C. Annedi, J. Ramnauth, S. Rakhit, J. Andrew, 1,5-Disubstituted indole derivatives as selective human neuronal nitric oxide synthase inhibitors, Bioorg. Med. Chem. Lett 21 (2011) 5301–5304.
[19] S.C. Annedi, S.P. Maddaford, J. Ramnauth, P. Renton, T.S. Rybak, S. Silverman, S. Rakhit, G. Mladenovic, P. Dove, J.S. Andrews, D. Zhang, F. Porreca, Discovery of a potent, orally bioavailable and highly selective human neuronal nitric oxide synthase (nNOS) inhibitor, N-(1-(piperidin-4-yl)indolin-5-yl) thiophene-2-carboximidamide as a pre-clinical development candidate for the treatment of migraine, Eur. J. Med. Chem. 55 (2012) 94–107.
[20] F. Xue, H. Li, S.L. Delker, J. Fang, P. Martasek, L.J. Roman, T.L. Poulos, R.B. Silverman, Potent, highly selective, and orally bioavailable gem-difluorinated monocationic inhibitors of neuronal nitric oxide synthase, J. Am. Chem. Soc. 132 (2010) 14229–14238.
[21] H. Chen, B.-Y. Chen, C.-T. Liu, Z. Zhao, W.-H. Shao, H. Yuan, K.-J. Bi, J.-Y. Liu, Q.-Y. Sun, W.-D. Zhang, Synthesis and structure activity relationships of guanine-type sesquiterpenes lactone derivatives with respect to inhibiting NO production in lipopolysaccharide-induced RAW 264.7 macrophages, Eur. J. Med. Chem. 83 (83) (2014) 307–316.
[22] I. Hueso-Falcón, I. Cuadrado, F. Cidre, J.M. Amaro-Luis, A.G. Ravelo, A. Estevez-Braun, B. d. Heras, S. Hortelano, Synthesis and anti-inflammatory activity of ent-kaurene derivatives, Eur. J. Med. Chem. 46 (2011) 1291–1305.
[23] N.I. Martin, J.J. Woodward, M.B. Winter, W.T. Beeson, M.A. Marletta, Design and synthesis of C5 methylated L-arginine analogues as active site probes for nitric oxide synthase, J. Am. Chem. Soc. 129 (2007) 12563–12570.
[24] J. López, Angel Lorente, J. Steingrub, J. Bakker, A. McLuckie, S. Willatts, M. Brockway, A. Anzueto, L. Holzapfel, D. Breen, M.S. Silverman, J. Takala, J. Donaldson, C. Arneson, G. Grove, S. Grossman, R. Grover, Multiple-center, randomized, placebo-controlled, double-blind study of the nitric oxide synthase inhibitor 546C88: effect on survival in patients with septic shock, Crit. Care Med. 32 (2004) 21–30.
[25] P. Mukherjee, M.A. Cinelli, S. Kang, R.B. Silverman, Development of nitric oxide synthase inhibitors for neurodegeneration and neuropathic pain, Chem. Soc. Rev. 43 (2014) 6814–6834.
[26] A.J. Duncan, S.J.R. Heales, Nitric oxide and neurological disorders, Mol. Aspect. Med. 26 (2005) 67–96.
[27] C. Villanueva, C. Giulivi, Subcellular and cellular locations of nitric oxide synthase isoforms as determinants of health and disease, Free Radical Biol. Med. 49 (2010) 307–316.
[28] J. Olesen, Nitric oxide-related drug targets in headache, Neurotherapeutics 7 (2010) 183–190.
[29] L. Zhang, V.L. Dawson, T.M. Dawson, Role of nitric oxide in Parkinson's disease, Pharmacol. Therapeut. 109 (2006) 33–41.
[30] N.R. Sims, M.F. Anderson, Mitochondrial contributions to tissue damage in stroke, Neurochem. Int. 40 (2002) 511–526.
[31] A. Venkanna, O.W. Kwon, S. Afzal1, C. Jang, K.H. Cho, D.K. Yadav, K. Kim, H-g. Park, K.-H. Chun, S.-Y. Kim, M-h. Kim, Pharmacological use of a novel scaffold, anomeric N, N-diarylamino tetrahydropyran: molecular similarity search, chemocentric target profiling, and experimental evidence, Sci. Rep. 7 (2017) 12535.
[32] S.-G. Ma, R.-M. Gao, Y.-H. Li, J.-D. Jiang, N.-B. Gong, L. Li, Y. Lu, W.-Z. Tang, Y.-B. Liu, J. Qu, H.-N. Lu, Y. Li, S.-S. Yu, Antiviral spirooliganones A and B with unprecedented skeletons from the roots of illicium oligandrum, Org. Lett. 15 (2013) 4450–4453.
[33] Y. Nagayama, H. Kato, H. Rotinsulu, R.E.P. Mangindaan, N. J. de Voogd, S. Tsukamoto, Spironaamidine, a new spiroquinone-containing alkaloid from the marine sponge Leucetta microraphis, Tetrahedron Lett. 52 (2011) 5342–5344.
[34] M. Liu, S. Lin, M. Gan, M. Chen, L. Li, S. Wang, J. Zi, X. Fan, Y. Liu, Y. Si, Y. Yang, X. Chen, J. Shi, Yaoshanenolides a and B: new spirolactones from the bark of machilus yaoshansis, Org. Lett. 14 (2012) 1004–1007.
[35] X.-W. Xian-Wen Yang, S.-M. Li, Y.-L. Li, J.-H. Xia, L. Wu, Y.-H. Shen, J.-M. Tian, N. Wang, Y. Liu, W.-D. Zhang, Abiespiroside A, an unprecedented sesquiterpenoid spirolactone with a 6/6/5 ring system from *Abies delavayi*, Eur. J. Org Chem. (2010) 6531–6534.
[36] F. Perron, K.F. Albiati, Chemistry of spiroketals, Chem. Rev. 89 (1989) 1617–1661.
[37] C.M. Marson, New and unusual scaffolds in medicinal chemistry, Chem. Soc. Rev. 40 (2011) 5514–5533.
[38] S. Pabbaraja, S.G. Kernie, G. Mehta, A. Kumar, A novel natural product inspired scaffold with robust neurotrophic, neurogenic and neuroprotective action, Sci. Rep. 5 (2015) 14134.
[39] P. Sandstrom, M.E. Brooke-Smith, A.C. Thomas, M.B. Grivell, G.T.P. Saccone, J. Toouli, J. Svanvik, Highly selective inhibition of inducible nitric oxide synthase ameliorates experimental acute pancreatitis, Pancreas 30 (2005) 10–15.
[40] A.C. Tinker, H.G. Beaton, N. Boughton-Smith, T.R. Cook, S.L. Cooper, L. Fraser-Rae, K. Hallam, P. Hamley, T. McInally, D.J. Nicholls, A.D. Pimm, A.V. Wallace, 1, 2-Dihydro-4-quinazolinamines: potent, highly selective inhibitors of inducible nitric oxide synthase which show anti-inflammatory activity in vivo, J. Med. Chem. 46 (2003) 913–916.
[41] Y. Zheng, C.M. Tice, S.B. Singh, The use of spirocyclic scaffolds in drug discovery, Bioorg. Med. Chem. Lett 24 (2014) 3673–3682.
[42] R.B. Weiss, The anthracyclines: will we ever find a better doxorubicin? Semin. Oncol. 19 (1992) 670–686.
[43] K. Jones, Pau D'arco: Immune Power from the Rain Forest, Healing Arts Press, Rochester, VT, 1995.
[44] J.R.G. Castellanos, J.M.P. Michael Heinrich, Red lapacho (Tabebuia impetiginosa)-A global ethnopharmacological commodity? J. Ethnopharmacol. 121 (2009) 1–13.
[45] G.R. Pettit, J.C. Collins, J.C. Knight, D.L.H. Ronald A, N.M.D. Williams, R.K. Pettit, Antineoplastic agents. 485. Isolation and structure of cribrostatin 6, a dark blue cancer cell growth inhibitor from the marine sponge *Cribrochalina sp*. J. Nat. Prod. 66 (2003) 544–547.
[46] H. Wang, S.L. Yeo, J. Xu, X. Xu, H. He, F. Ronca, A.E. Ting, T. Wang, V.C. Yu, M.M. Sim, Isolation of streptonigrin and its novel derivative from micromonospora as inducing agents of p53-dependent cell apoptosis, J. Nat. Prod. 65 (2002) 721–724.
[47] M. Minotti, P. Menna, E. Salvatorelli, G. Cairo, L. Gianni, Anthracyclines: molecular advances and pharmacologic developments in antitumor activity and cardiotoxicity, Pharmacol. Rev. 56 (2004) 185–229.
[48] J.H. Doroshow, Anthracyclines and anthracenediones, in: B.A. Chabner, D.L. Longo (Eds.), Cancer Chemotherapy and Biotherapy: Principles and Practice, Lippincott, Williams and Wilkins, Philadelphia, PA, 2001.
[49] R. Martinez, L. Chacon-Garcia, The search of DNA-intercalators as antitumoral drugs: what it worked and what did not work, Curr. Med. Chem. 12 (2005) 127–151.
[50] K. Muller, A. Sellmer, W. Wiegrebe, Potential antipsoriatic agents: lapacho compounds as potent inhibitors of HaCaT cell growth, J. Nat. Prod. 62 (1999) 1134–1136.
[51] J.P. Shrestha, Y.P. Subedi, L. Chen, C.-W. Tom Chang, A mode of action study of cationic anthraquinone analogs: a new class of highly potent anticancer agents, Med. Chem. Commun. 6 (2015) 2012–2022.

[52] J.W. Lown, Anthracycline and Anthraquinone anticancer agents: current status and recent developments, Pharmacol. Ther. 60 (1993) 185–214.
[53] A.B. Pardee, Y.Z. Li, C.J. Li, Cancer therapy with ß-lapachone, Curr. Cancer Drug Targets 2 (2002) 227–242.
[54] S. Afzal, A. Venkanna, H-g. Park, M-h. Kim, Metal-free α-C(sp3)-H functionalized oxidative cyclization of tertiary N, N-diaryl amino alcohols: construction of N, N-diarylaminotetrahydropyran scaffolds, Asian J. Org. Chem. 5 (2016) 232–239.
[55] M-h. Kim, J. Lee, K. Jung, M. Kim, Y.-J. Park, H. Ahn, Y.H. Kwon, J.-M. Hah, Syntheses and biological evaluation of 1-heteroaryl-2-aryl-1H-benzimidazole derivatives as c-Jun N-terminal kinase inhibitors with neuroprotective effects, Bioorg. Med. Chem. 21 (2013) 2271–2285.
[56] A. Venkanna, C.P. Kumar, B. Poornima, B. Siva, N. Jain, K.S. Babu, Design, synthesis and anti-proliferative activities of novel 7′-O-substituted schisantherin A derivatives, Med. Chem. Commun. 7 (2016) 1159–1170.
[57] A. Venkanna, B. Siva, B. Poornima, K.S. Babu, J.M. Rao, The first stereoselective synthesis of dendrodolide A, Tetrahedron Lett. 55 (2014) 403–406.
[58] B. Poornima, A. Venkanna, B. Swetha, K.R. Kamireddy, B. Siva, V.S.P. Babu, R. Ummanni, K.S. Babu, Total synthesis, biological evaluation of dendrodolides A-D and their analogues, Tetrahedron 72 (2016) 4789–4797.
[59] B. Poornima, B. Siva a, A. Venkanna, G. Shankaraiah, N. Jain, D.K. Yadav, S. Misra, K.S. Babu, Novel Gomisin B analogues as potential cytotoxic agents: design, synthesis, biological evaluation and docking studies, Eur. J. Med. Chem. 139 (2017) 441–453.
[60] M.E. Hart, K.L. Suchland, M. Miyakawa, J.R. Bunzow, D.K. Grandy, T.S. Scanlan, Trace amine-associated receptor agonists: synthesis and evaluation of thyronamines and related analogues, J. Med. Chem. 49 (2006) 1101–1112.
[61] F. Kaiser, L. Schwink, J. Veldera, H.-G. Schmalz, Studies towards the total synthesis of mumbaistatin: synthesis of highly substituted benzophenone and anthraquinone building blocks, Tetrahedron 59 (2003) 3201–3217.
[62] T. Ooi, H. Ichikawa, K. Maruoka, Practical approach to the meerwein ponndorf verley reduction of carbonyl substrates with new aluminum catalysts, Angew. Chem. Int. Ed. 40 (2001) 3610–3612.
[63] T. Choshi, S. Yamada, E. Sugino, T. Kuwada, S. Hibino, Total synthesis of grossularines -1 and -2, J. Org. Chem. 60 (1995) 5899–5904.
[64] S. Ueda, M. Su, S.L. Buchwald, Completely N^1-selective palladium-catalyzed arylation of unsymmetric imidazoles: application to the synthesis of nilotinib, J. Am. Chem. Soc. 134 (2012) 700–706.
[65] Y. Zhang, X. Yang, Q. Yao, D. Ma, CuI/DMPAO-Catalyzed N-arylation of acyclic secondary amines, Org. Lett. 14 (2012) 3056–3059.
[66] M.D. Charles, P. Schultz, S.L. Buchwald, Efficient Pd-catalyzed amination of heteroaryl halides, Org. Lett. 7 (2005) 3965–3968.
[67] Q. Shen, T. Ogata, J.F. Hartwig, Highly reactive, general and long-lived catalysts for palladium-catalyzed amination of heteroaryl and aryl chlorides, bromides, and iodides: scope and structure–activity relationships, J. Am. Chem. Soc. 130 (2008) 6586–6596.
[68] J.J. Hanthorn, L. Valgimigli, D.A. Pratt, Preparation of highly reactive pyridine- and pyrimidine-containing diarylamine antioxidants, J. Org. Chem. 77 (2012) 6908–6916.
[69] Z.-J. Wu, H.-C. Xu, Synthesis of C3-fluorinated oxindoles through reagent-free cross-dehydrogenative coupling, Angew. Chem. Int. Ed. 56 (2017) 4734–4738.
[70] M.S. Kim, Y. Ki, S.Y. Ahn, S. Yoon, S.-E. Kim, H-g Park, W. Sun, K. Son, M. Cui, S. Choi, L.V. Pearce, T.E. Esch, I.A. DeAndrea-Lazarus, P.M. Blumberg, J. Lee, Asymmetric synthesis and receptor activity of chiral simplified resiniferatoxin (sRTX) analogues as transient receptor potential vanilloid 1 (TRPV1) ligands, Bioorg. Med. Chem. Lett 24 (2014) 382–385.
[71] Mi-h. Kim, S-h. Choi, Y.-J. Lee, J. Lee, K. Nahm, B.-S. Jeong, H-g. Park, S-s Jew, The highly enantioselective phase-transfer catalytic mono-alkylation of malonamic esters, Chem. Commun. (2009) 782–784.
[72] D.S. Pugh, J.E.M.N. Klein, A. Perry, Preparation of 3-alkyl-oxindoles by copper (II)-mediated C-H, Ar-H coupling followed by decarboxyalkylation, Synlett 6 (2010) 934–938.
[73] R.T. Ruck, M.A. Huffman, M.A. Kim, M. Shevlin, W.V. Kandur, I.W. Davies, Palladium-catalyzed tandem heck reaction/C-H functionalization-preparation of spiro-indane-oxindoles, Angew. Chem. Int. Ed. 47 (2008) 4710–4714.
[74] T.A. Averes, New methods for the selective reduction of disibstitued malonates to the corresponding hydroxy-ester derivatives, Tetrahedron Lett. 40 (1999) 5467–5470.
[75] D.S. Reddy, N. Shibata, J. Nagai, S. Nakamura, T. Toru, S. Kanemasa, Desymmetrization-like catalytic enantioselective fluorination of malonates and its application to pharmaceutically attractive molecules, Angew. Chem. Int. Ed. 47 (2008) 164–168.
[76] J. Wilent, K.S. Petersen, Enantioselective desymmetrization of diesters, J. Org. Chem. 79 (2014) 2303–2307.
[77] D. Vina, L. Santana, E. Uriartea, C. Teran, 1, 2-Disubstituted cyclohexane nucleosides: comparative study for the synthesis of cis and trans adenosine analogues, Tetrahedron 61 (2005) 473–478.
[78] P. Haldar, J.K. Ray, $NaBH_4$-$InCl_3$-Mediated one-pot chemo and stereoselective decarboxylative reduction of r-aza gem-dicarboxylic esters to monoalcohols, Org. Lett. 7 (2005) 4341–4343.
[79] N.D. Patil, N. Yan, Study of the nitroxyl radical catalyst in aerobic oxidative cleavage and functionalization of lignin model compounds, Catal. Commun. 84 (2016) 155–158.
[80] M. Dawange, M.V. Galkin, J.S.M. Samec, Selective aerobic benzylic alcohol oxidation of lignin model compounds: route to aryl ketones, ChemCatChem 7 (2015) 401–404.
[81] M.B. Andrus, E.J. Hicken, E.L. Meredith, B.L. Simmons, J.F. Cannon, Selective synthesis of the para-quinone region of geldanamycin, Org. Lett. 5 (2003) 3859–3862.
[82] M.K. Hadden, B.S.J. Blagg, Synthesis and evaluation of radamide analogues, a chimera of radicicol and geldanamycin, J. Org. Chem. 74 (2009) 4697–4704.
[83] X. Chen, J. Chen, M. De Paolis, J. Zhu, Synthetic studies toward ecteinascidin 743, J. Org. Chem. 70 (2005) 4397–4408.
[84] D.J. Dixon, A.C. Foster, S.V. Ley, Short and efficient stereoselective synthesis of the polyhydroxylated macrolactone (+)-Aspicilin, Org. Lett. 2 (2000) 123–125.
[85] J. Murga, E. Falomir, J. Garcia-Fortanet, M. Carda, J.A. Marco, Stereoselective synthesis of microcarpalide, Org. Lett. 4 (2002) 3447–3449.
[86] V.V. Zhdankin, Chemistry of polyvalent iodine, Chem. Rev. 108 (2008) 5299–5358.
[87] Y. Zhou, X. Zhang, Y. Zhang, L. Ruan, J. Zhang, D. Zhang-Negrerie, Y. Du, Iodocyclization of N-arylpropynamides mediated by hypervalent iodine reagent: divergent synthesis of iodinated quinolin-2-ones and spiro[4,5]trienones, Org. Lett. 19 (2017) 150–153.
[88] L. Wei, M. Xiao, Z. Xie, Total syntheses of (-)-Spirooliganones a and B, Org. Lett. 16 (2014) 2784–2786.
[89] H. Liang, M.A. Ciufolini, Oxidative spirocyclization of phenolic sulfonamides: scope and applications, Chem. Eur J. 16 (2010) 13262–13270.
[90] L. Pouysegu, D. Deffieux, S. Quideau, Hypervalent iodine-mediated phenol dearomatization in natural product synthesis, Tetrahedron 66 (2010) 2235–2261.
[91] M. Uyanik, T. Yasui, T. Ishihara, Enantioselective kita oxidative spirolactonization catalyzed by in situ generated chiral hypervalent iodine(III) species, Angew. Chem. Int. Ed. 49 (2010) 2175–2177.
[92] S. Quideau, M. Lebon, A.M. Lamidey, Enantiospecific synthesis of the antituberculosis marine sponge metabolite (+)-Puupehenone. The arenol oxidative activation route, Org. Lett. 2 (2000) 123–125.
[93] A. Bartoli, F. Rodier, L. Commeiras, J.-C. Parrain, G. Chouraqui, Construction of spirolactones with concomitant formation of the fused quaternary centre-application to the synthesis of natural products, Nat. Prod. Rep. 28 (2011) 763–782.
[94] K.-A. Hwang, Y.J. Hwang, J. Song, Antioxidant activities and oxidative stress inhibitory effects of ethanol extracts from Cornus officinalis on raw 264.7 cells, BMC Complement Altern. Med. 16 (2016) 196.
[95] Y.-K. Han, Y.-S. Kim, S.B. Natarajan, W.-S. Kim, J.-W. Hwang, N.-J. Jeon, J.-H. Jeong, S.-H. Moon, B.-T. Jeon, P.-J. Park, Antioxidant and anti-inflammatory effects of chaenomeles sinensis leaf extracts on LPS-stimulated RAW 264.7 cells, Molecules 21 (2016) 422.
[96] Ajay, G.W. Bemis, M.A. Murkco, Designing libraries with CNS activity, J. Med. Chem. 42 (1999) 4942–4951.
[97] M.M. Mohyeldin, M.R. Akl, A.B. Siddique, H.M. Hassan, K.A.E. Sayed, The marine-derived pachycladin diterpenoids as novel inhibitors of wild-type and mutant EGFR. The marine-derived pachycladin diterpenoids as novel inhibitors of wild-type and mutant EGFR, Biochem. Pharmacol. 126 (2017) 51–68.
[98] L. Zhang, I.P. Holmes, F. Hochgräfe, S.R. Walker, N.A. Ali, E.S. Humphrey, J. Wu, M de Silva, W.J.A. Kersten, T. Connor, H. Falk, L. Allan, I.P. Street, J.D. Bentley, P.A. Pilling, B.J. Monahan, T.S. Peat, R.J. Daly, Characterization of the novel broad-spectrum kinase inhibitor CTx-0294885 as an affinity reagent for mass spectrometry-based kinome profiling, J. Proteome Res. 12 (2013) 3104–3116.
[99] J.W. Tyner, Kinase inhibitor screening in myeloid malignancies, Hematol. Oncol. Clin. N. Am. 31 (2017) 705–719.
[100] E.T. Coffey, Nuclear and cytosolic JNK signaling in neurons, Nat. Rev. Neurosci. 15 (2014) 285–299.
[101] C. Centeno, M. Repici1, J.-Y. Chatton, B.M. Riederer, C. Bonny, P. Nicod, M. Price, P.G.H. Clarke, S. Papa, G. Franzoso, T. Borsello, Role of the JNK pathway in NMDA-mediated excitotoxicity of cortical neurons, Cell Death Differ. (2006) 1–14.
[102] G. Spigolon, C. Veronesi, C. Bonny, A. Vercelli1, c-Jun N-terminal kinase signaling pathway in excitotoxic cell death following kainic acid-induced status epilepticus, Eur. J. Neurosci. 31 (2010) 1261–1272.
[103] H. Le Niculescu, E. Bonfoco, Y. Kasuya, F.X. Claret, D.R. Green, M. Karin, Withdrawal of survival factors results in activation of the JNK pathway in neuronal cells leading to fas ligand induction and cell death, Mol. Cell. Biol. Mol. Cell. Biol. 19 (1999) 751–763.
[104] R. Pariyara, C.-S. Yoona, T. Svaya, D.-S. Kim, H.-K. Cho, S.Y. Kim, H. Oha, Y.-C. Kim, J. Kim, Ho-S. Lee, J. Seo, Vitis labruscana leaf extract ameliorates scopolamine-induced impairments with activation of Akt, ERK and CREB in mice, Phytomedicine 36 (2017) 8–17.
[105] S.M. Hong, K.H. Soe, T.H. Lee, I.S. Kim, Y.M. Lee, B.O. Lim, Cognitive improving effects by highbush blueberry (vaccinium crymbosum L.) vinegar on scopolamine-induced amnesia mice model, J. Agric. Food Chem. 66 (2018) 99–107.
[106] S. Lee, Ho J. Park, Se J. Jeon, E. Kim, H.E. Lee, H. Kim, Y. Kwon, J. Zhang, I.H. Jung, J.H. Ryu, Cognitive ameliorating effect of acanthopanax koreanum against scopolamine-induced memory impairment in mice, Phytother Res. 31 (2017) 425–432.
[107] T. Singh Gujral, L. Peshkin, M.W. Kirschner, Exploiting polypharmacological

for drug target deconvolution, PANS 111 (2014) 5048–5053.
[108] G.C. Terstappen, C. Schlüpen, R. Raggiaschi, G. Gaviraghi, Target deconvolution strategies in drug discovery, Nat. Rev. Drug Discov. 6 (2007) 891–903.
[109] H.E. Lee, Se J. Jeon, B. Ryu, Se J. Park, S.Y. Ko, Y. Lee, E. Kim, S. Lee, H. Kim, D.S. Jang, J.H. Ryu, Swertisin, "a C-glucosylflavone, ameliorates scopolamine-induced memory impairment in mice with its adenosine A1 receptor antagonistic property", Behav. Brain Res. 306 (2016) 137–145.
[110] H. Kim, C. Jang, D.K. Yadav, M-h Kim, The comparison of automated clustering algorithms for resampling representative conformer ensembles with RMSD matrix, J. Cheminf. 9 (2017) 21.